Charles University

Faculty of Science

Study programme: Applied geology

Mgr. Petr Dědeček

Transient temperature field of the shallow subsurface and its sources

Nestacionární teplotní pole pod zemským povrchem a jeho zdroje

Doctoral thesis

Supervisor: RNDr. Jan Šafanda CSc.

July 2019

Content

Preface

The aim of my thesis is to assess various factors effecting the transient component of the subsurface temperature field. The thesis is based on three published articles and its content is a follow-up to my diploma thesis, in which I dealt with the processing of long-term temperature series measured in a borehole at the campus of the Geophysical Institute in Prague. In PhD thesis I tried to move the knowledge of mechanisms forming the transient component of subsurface temperature field and especially I wanted to separate the influence of climate and "disturbing" signals caused by human activities.

The initial impulse was monitoring of long-term warming of subsurface in several observatories operated by GFU, while the greatest warming in the borehole situated at the campus of the Institute did not correspond with regional climate change. Since this borehole is situated inside the built-up area, it was clear that the Urban Heat Island effect takes a role.

The next step was the development of several algorithms allowing the calculation of thermal diffusivity from long-term temperature series up to the depth of annual temperature variations. I have already dealt with this in my diploma thesis, but now the effect of possible convective heat transfer was included. It was thus possible to prove that heat transfer by conduction dominates in the vadose zone.

The findings mentioned above were used in the 3D numerical modeling enabling detection and quantification of the impact of local anthropogenic structures and regional climatic changes on subsurface temperature field in cases of Spořilov and Šempeter boreholes, were the strong influence of human activity on subsurface temperature field was discovered.

Abstrakt

Z důvodu rozlišení a popisu možných zdrojů nestacionární složky teplotního pole pod zemským povrchem byly zpracovány dlouhodobé teplotní řady a opakované teplotní karotáže zaznamenané v několika vrtech v České republice, Slovinsku a Portugalsku. Z dlouhodobých teplotních záznamů byl pak pomocí dvou různých metod proveden výpočet tepelné difuzivity půdy a skalního podloží. Na základě těchto výpočtů byl prokázán zanedbatelný vliv konvektivního přenosu tepla v půdě a horninovém masivu do hloubky 10 m a také, že vliv změny půdní vlhkosti na teplotní pole je významný pouze ve svrchních 5 cm půdního horizontu. Využitím 3D numerického modelování byl prokázán přímý vliv činnosti člověka na nárůst teploty pod zemským povrchem a byly rozlišeny příspěvky jednotlivých antropogenních struktur k tomuto oteplování. Díky tomu bylo možné rozdělit a popsat vliv změny klimatu a vliv člověka na nestacionární složku teplotního pole.

Abstract

Long-term air and ground temperature series and repeated temperature logs from several boreholes in Czech Republic, Slovenia and Portugal were processed to distinguish and describe possible sources of transient signals in subsurface temperature field. Two methods for estimation of the soil and bedrock thermal diffusivity from long-term temperature records are presented and compared. Results proved that on the annual time scale the convective heat transfer did not contribute significantly to the temperature-time variations monitored in the uppermost 10-m depth zone and that the influence of moisture changes on subsurface temperature field noticeably appears only in upper 5 cm of soil. Using 3D numerical modelling a direct human impact on the subsurface temperature warming was proved and contributions of individual anthropogenic structures to this change were evaluated. It made it possible to split the transient component of the present-day temperature depth profiles into the climatic and anthropogenic signals.

Introduction

There is clear evidence that the world climate has been undergoing a general warming. This warming was typical for the most of the last century, following the previous relatively colder nineteenth century, and continues in the 21st century. An important question to answer is whether this warming is just a manifestation of natural climate variability and a certain "return" to previous conditions or an indication of a new (and permanent) trend. What is alarming, is the matter of fact, that the warming rate has been accelerating in the last decades. The 1990s was the warmest decade of the last century (IPCC 2001) and the WMO Statement on the State of the Global Climate in 2018 (WMO 2019) states that past four years – 2015 to 2018 – were the top four warmest years in the global temperature record between 1.1 – 1.2 °C above the pre-industrial mean. It represents acceleration of the warming when the average global temperature for the decade 2006–2015 was 0.86 °C above the pre-industrial baseline.

Geothermal research based primarily on the temperature-depth logs measured in several hundred meters to several kilometres deep boreholes provides information on the energetic balance of the Earth (Pollack et al. 1993). However, the information stored in the transient component of the temperature-depth profiles, which is considered as a noise in the terrestrial heat flow determinations, can be used as a valuable archive of the past climatic changes (Harris and Chapman 1997; Beltrami 2002; Šafanda et al. 199199 4). The steady-state part of the subsurface temperature corresponds to the long-term annual mean of the ground surface temperature. The seasonal and inter-annual surface temperature variations propagate downward and disappear at the depth of 15–25 m. In case of a climatic change, however, the long-term annual mean of the surface temperature changes and this transient signal propagates much deeper— to hundreds of meters for the centennial and millennial climatic changes and to first kilometers for the glacial—interglacial cycles. By solving the inverse problem, the history of the ground surface temperature (GST) variations can be reconstructed from this transient component obtained by a precise temperature logging and by removing the steady-state part of the temperature-depth profile. For the climatic interpretation of the reconstructed ground surface temperature history, it is necessary to know how the long-term difference between the mean annual ground and surface air temperatures (SAT) behaves. The extent to which the SAT change will be reflected in the GST change depends especially on the albedo of the ground, intensity of solar radiation and

magnitude of the ground isolation that can be formed for instance by a vegetation or snow cover (Lewis and Wang 1992; Majorowicz and Skinner 1997a, b; Smerdon et al. 2003; Majorowicz and Safanda 2005). Transfer of heat from the surface into the ground (soil) and into the bedrock takes place mainly by the heat conduction, but precipitation affects the thermal properties of the soil. In winter, when air temperatures decrease below zero, the latent heat released or consumed during phase changes of water within the active layer can influence appreciably the heat transfer (Beltrami and Kellman 2003; Smerdon et al. 2003; Woodbury et al. 2009) leading to a certain decoupling between SAT and GST.

Beside the natural causes, the activities of people have been involving more and more in forming the Earth's surface. Human impact is either passive, when human activity changes the albedo or isolation of the Earth's surface, thereby altering the SAT–GST relation, or active, when heat is supplied into or extracted from the ground with the use of geothermal (ground source) heat pumps, for example. Humans began to radically alter temperature relations on the earth surface with the arrival of agriculture, when they started to deforest landscape and cultivate soil. Extensive deforestation of landscape and/or conversion into the arable land that took place in the past and continue in many regions of the world today, altered completely SAT–GST relations in that areas (Majorowicz and Skinner 1997a, 1997b; Nitoiu and Beltrami 2005; Bense and Beltrami 2007). Another substantial change has been brought by urbanization. Urban agglomerations, apart from extensive paved surfaces with a low albedo (asphalt, concrete) that absorb sunshine, bring also an active energy exchange due to heated or cooled buildings.

Heat transfer from the Earth surface downward is driven by thermal diffusivity of soil and bedrock. Knowledge of thermal diffusivity is therefore a prerequisite for modelling of time-dependent changes of subsurface temperature field in order to access a role of the individual factors affecting the non-stationary component. Estimates of thermal diffusivity from in-situ measured temperature series can be used as an input parameter of numerical models and also enable to assess the effect of convective heat transfer to the depth of penetration of periodic temperature variations.

Data set

Prague

As a part of the "Borehole and Climate" program of the International Geological Correlation Program (IGCP 428) 40 m and 150 m deep boreholes were drilled in October 1992 on the campus of the Geophysical Institute in Praha Spořilov (50º02'27" N, 14º28'39" E, 275 m a.s.l.). The holes are located on a low E-W trending ridge. The upper four meters of the lithological column represent soil and a man-made loose material backfill of low conductivity (1.7–2.0 W/mK), underlain by silt to clayey shale of gradually increasing conductivity, below 10 m the conductivity is practically constant (3.2 ± 0.2 W/mK) (Šafanda 1994; Štulc, 1995). The corresponding diffusivity of the upper strata is only 0.4 × 10−6 m2s−1, lower strata is characterized by values of 0.73–0.9 × 10−6 m2s−1.

Malence and Šempeter (Slovenia)

In order to study the coupling between the air, soil and bedrock temperatures, the Malence Borehole Climate Observatory (MBCO) was established at the borehole V-8/86 at Malence, SE Slovenia (45◦52.1´N, 15◦24.5´E, 152 m a.s.l.) in November 2003. The borehole is located on the alluvial plain of the Krka river on a rim of a meadow in the rural area of the Krško basin. The basin is filled with Tertiary and Quaternary sediments and belongs to the large Pannonian basin. The hole was drilled in October 1986 with a diameter of 90–120 mm through 16 m of Quaternary clay, sand and gravel, down to the bottom at 100 m through Miocene marl strata, sandier in its upper part and more clayey in its deeper part. The groundwater level in the borehole was 2.5m below the surface in 1987 and rose to approx. 1.5m after 2003. During a nine-month period of continuous monitoring in 2006/2007, the groundwater level slightly varied between 1.5 and 1.6 m. It is possible that during high stands of the Krka river, the groundwater can be even closer to the surface. The site was flooded for several days in 2010. The borehole was cased with a zinc-coated steel tube 1.6 in of inner diameter. Thermal conductivity was measured on the only two available rock samples collected from two different depth sections, 1.7 $W.m^{-1}.K^{-1}$ in 0.7 m depth and 1.45 $W.m^{-1}.K^{-1}$ in 99 m depth. As a part of the MBCO instrumentation a chain of platinum sensors (Pt1000, class A, sensitivity of first mK) for temperature monitoring was installed in 2003 and kept in the hole in the depth interval of 1 to 40 m for a permanent recording experiment

(Rajver et al 2006). The data logger system (16 channels, 24 bits A/D converter, 16 bits resolution) records air temperatures at 2 m and 0.05 m above the ground level, soil temperatures at 0.02, 0.05, 0.1, 0.2, 0.5 and 1 m below the surface and bedrock temperatures in the borehole at the depths of 2.5, 5, 10, 20, 30 and 40 m. The soil temperature sensors were buried about 1 m beside the borehole. All information was collected in preselected 30 min time intervals and for further interpretation the observed temperature data were averaged to furnish series of daily means. The experiment started on 13 November 2003.

The second Slovenian locality is the borehole Še-1 in Šempeter (45°55.28′N, 13°37.95′E, 68 m a.s.l) located in the southwestern part of Slovenia in a flat terrain of an industrial zone. The borehole is 1541 m deep, was drilled in 1994 and encountered Quaternary sediments (alternation of sandy and clayey layers) in the upper 90 m, which are followed by fine grained sedimentary rocks (marly shales, silty marls, siltstones, sandstones) of mostly Middle Eocene age with approximately horizontal position of bedding along its entire length. The thermal conductivity was measured only in lower part of the borehole and the mean value from several samples in section 500–1000 m was 2.4 $W.m^{-1}.K^{-1}$ along the bedding and 1.9 $W.m^{-1}.K^{-1}$ perpendicular to it. The borehole is cased and filled by groundwater, the level of which varies in the depth interval 13–16 m.

Evora (Portugal)

Geothermal Paleoclimatology Platform (http://www.cge.uevora.pt/index.php) is located 5 km apart of Evora in south-central Portugal. Long-term monitoring, with 30 minute sampling interval, of soil temperatures (at depths of 0.02, 0.05, 0.1, 0.2, 0.5 and 1 m), and bedrock temperatures (at depths of 1, 2.5, 5, 10, 20, 30 and 40 m), complemented by air temperature measurements at 2 and 0.05 m above the ground, has been started in May 2005. The close vicinity of the borehole is completely without vegetation cover and soil in the first 50 cm has character of clayey sand with gravelly layers.

1. Transient temperature signal in shallow subsurface

The observed increase of air temperature is linked to the increase of the surface (soil) temperature. The response to changes in the surface conditions slowly penetrates downwards into the shallow subsurface. Subsurface temperature field at depth of several tens to several hundreds of meters contains a record of what has happened on the surface in the past, i.e. the long-term ground surface (soil) temperature history (GSTH). Regular temperature variations at the surface occur at temporal scales, such as diurnal or seasonal/annual. The typical magnitude of the daily variations amounts 10-15 ºC, the amplitude of the seasonal variations may amount to 20-30 ºC and more. Inter-annual and long-term temperature change patterns are irregular. As the surface temperature signal propagates downward, its amplitude decreases exponentially with depth due to the diffusive process of heat conduction, each variation vanishes over a vertical distance related to the period of change and to the thermal diffusivity of the ground. The shorter period fluctuations attenuate more rapidly.

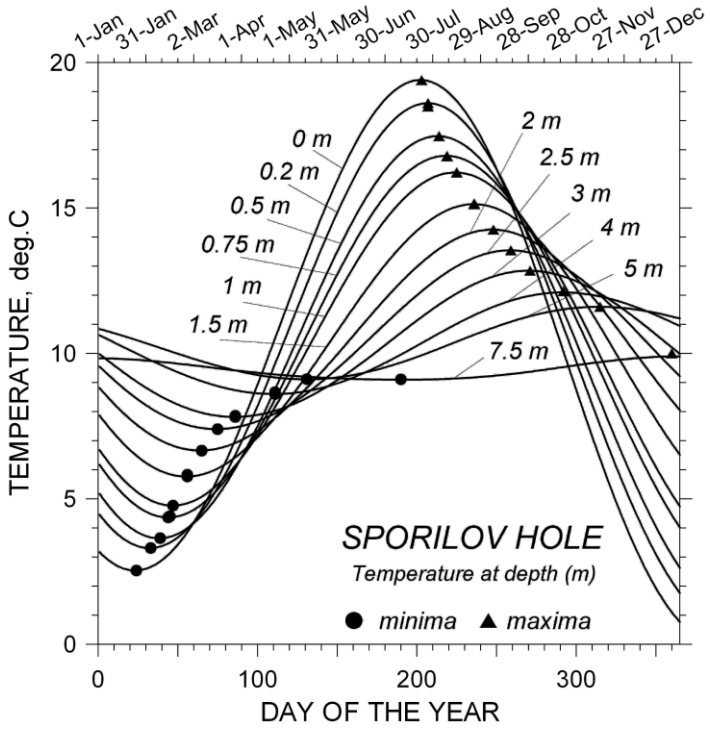

Figure 1. Characteristic temperature distribution in the shallow subsurface corresponding to the annual temperature variations on the surface.

Figure 1 demonstrates the amplitude attenuation of the temperature signal propagating downwards and the delay of its phase by presenting the results of the 12-year temperature monitoring in the Spořilov hole. Contrary to the annual temperature wave, the daily wave is practically not observable below 1 m depth. On the other hand, the temperature at 1 m depth represents integrated average of the daily signal of the previous day(s). Similarly, annual GST oscillations practically vanish at about 15-20 m depth, the temperature field below 20-30 m depth is free of any response to the annual or shorter temperature variations and contains exclusively the fingerprints of longer time scale evens with characteristic time of several last years.

The 15-year (1994-2008) record of temperature observed at 38.3 m depth in the Spořilov hole (**Figure 2**) clearly demonstrates the steady increase of temperature with slightly varying rate. The maximal warming rate, 0.038 °C/year, was observed during the period 2001 - 2005.

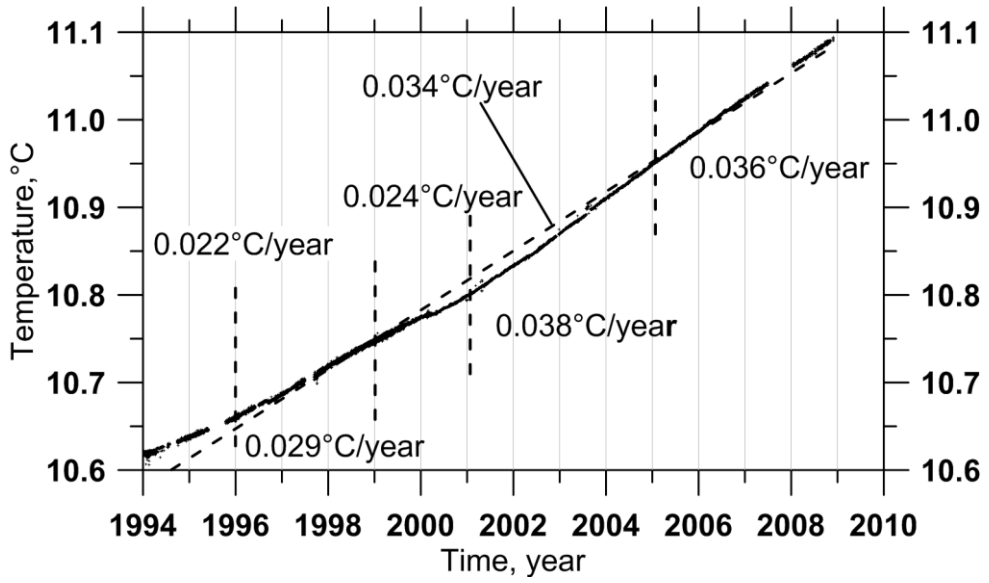

Figure 2. The observed time – temperature series at 38.3 m in the GFU-2 borehole divided into periods of approximately constant warming rate. The warming trend of the whole observational period 1994 – 2008 is 0.034 °C/ year.

The similar experiments were performed in the borehole located in a rural area on a meadow close to the meteorological station Kocelovice (49º28'02.2" N, 13º50'18.7" E, 519 m a.s.l.). **Figure 3** presents temperatures observed at depth of 40 m in the borehole, where due to technical problems only two shorter monitored series could have been obtained. Both of them confirmed warming rate, namely 0.0168 °C/year (in 1999) and

slightly higher rate of 0.0240 °C/year in 2003. It is obvious that in the case of Kocelovice the warming rate of both series is lower by approximately 0.013 °C/year. This difference is caused by impact of local anthropogenic structures in urban area where the Spořilov hole is located. Quantification of this phenomenon is described in chapter 5.

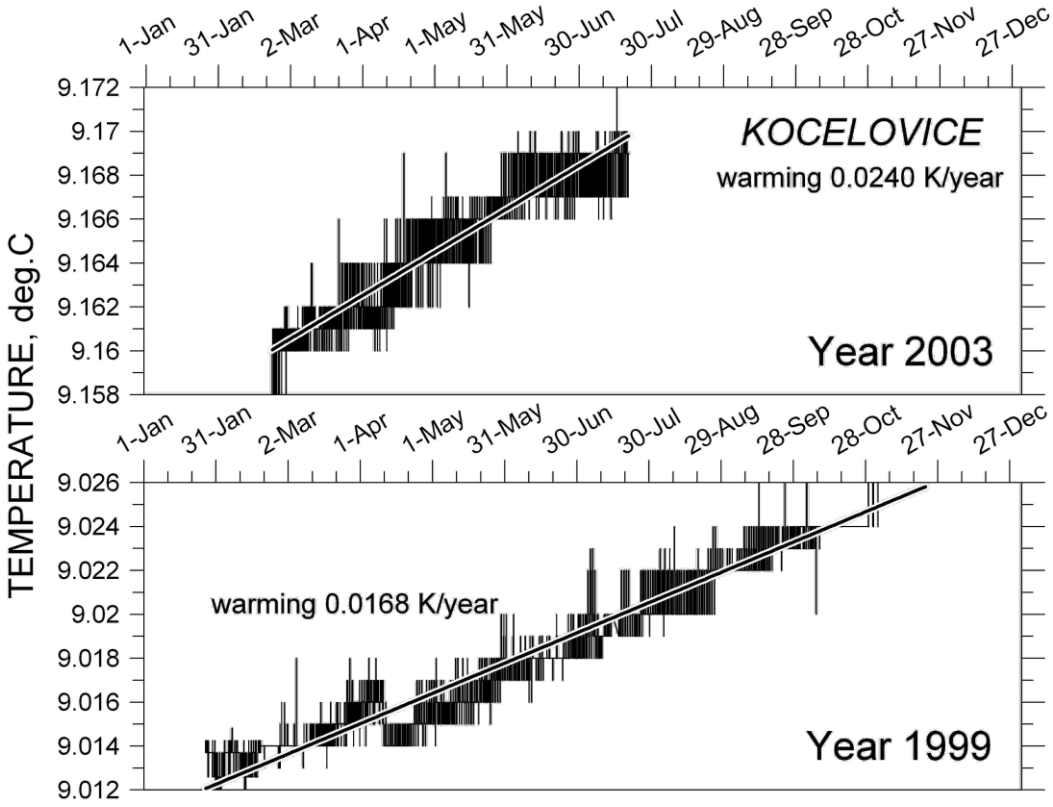

Figure 3. Results of temperature monitoring at depth of 40 m (Kocelovice hole). Two records correspond to 1999 and 2003 monitoring series.

2. Thermal diffusivity from subsurface temperature series

In order to model time changes of subsurface temperature field and to separate the individual transient signals, it is necessary to know the temperature diffusivity (TD) of the environment. The temperature diffusivity depends on the mineral composition of the soil / rock, its porosity and water saturation. In this work, two ways of calculating TD from long-term temperature series are presented. In both cases the influence of convective heat transfer (meteoric water infiltration) on the subsurface temperature field is discussed.

2.1. Estimation based on the error function solution of the heat conduction equation

In a thin layer of soil to the depth of the range of daily temperature variations, this method brings the possibility to observe detailed changes of thermal diffusivity during the year. Method uses solution of heat conduction equation in one dimensional homogenous environment by error function (Carlslaw a Jeager, 1957), which has the form

$$T(z,t) = \Delta T \, erfc \frac{z}{2\sqrt{kt}} \qquad (1)$$

where T is temperature, t time, z depth, and k is thermal diffusivity. For the estimation of the impact of N temperature steps, we can modify equation to the following form

$$T(z,t) = T_0 + \left(T_1 - T_0\right) \operatorname{erfc} \frac{z}{2\sqrt{k\left(t - t_0\right)}} + \left(T_2 - T_1\right) \operatorname{erfc} \frac{z}{2\sqrt{k\left(t - t_1\right)}} + \ldots\ldots\ldots + \left(T_{n+1} - T_n\right) \operatorname{erfc} \frac{z}{2\sqrt{k\left(t - t_n\right)}} \qquad (2)$$

The Matlab code based on this approach enables us to compute downward penetration of temperature changes from the surface, or from a given level in the soil profile, to the depth in given time intervals. The code was written to allow calculations in floating time windows of varying length. Synthetic temperature series for different values of TD

(with step $1x10^{-8}$ $m^2.s^{-1}$) are automatically compared with observed temperature time series in given depth. The TD value minimizing the standard deviation of difference between the measured and computed temperature series is considered the best approximation of reality. The **Figure 4** shows the change of standard deviation for short time intervals in summer and winter in 2008 in Evora (Portugal). The minimum of curves determines the best value of TD.

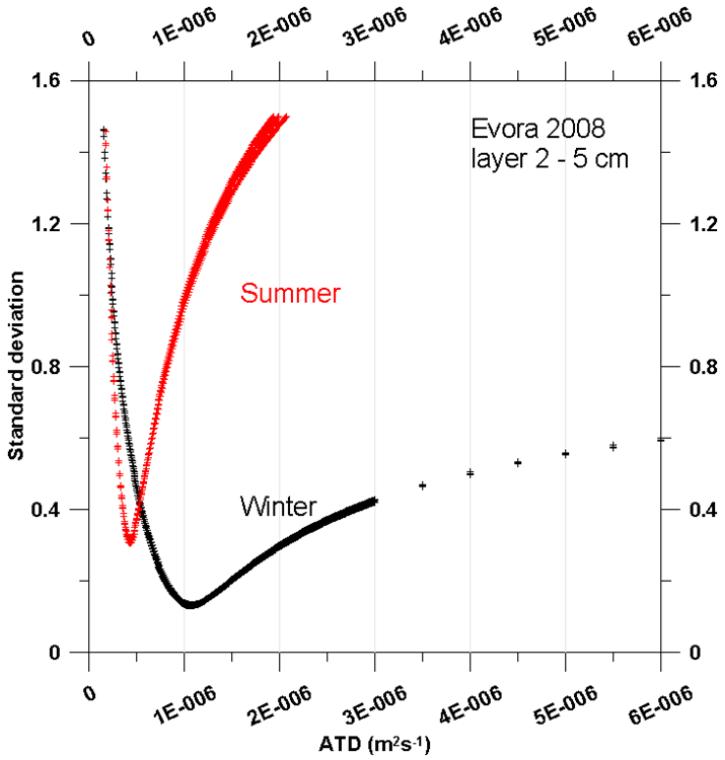

Figure 4. Example of estimation of TD in summer and winter days in Evora.

The climate in southern Portugal is characterized by alternating dry summer and rainy winter periods. **Figure 5** shows the record of air (2 m) and soil (2 cm) temperature measured in 2008. Due to the absence of vegetation cover at the observatory, there is a substantial surface heating and drying of soil during the summer months. **Figure 6** presents the results of TD estimation between the years 2008 and 2013. There are clearly visible seasonal variations in the 2-5 cm layer related to the change of moisture, when the TD increases more than twice during the wet period. However, this dependence decreases significantly at a depth of 5-10 cm. It is also evident in **Figure 7** depicting a dependence of monthly averages of TD on the number of rainy days in individual months.

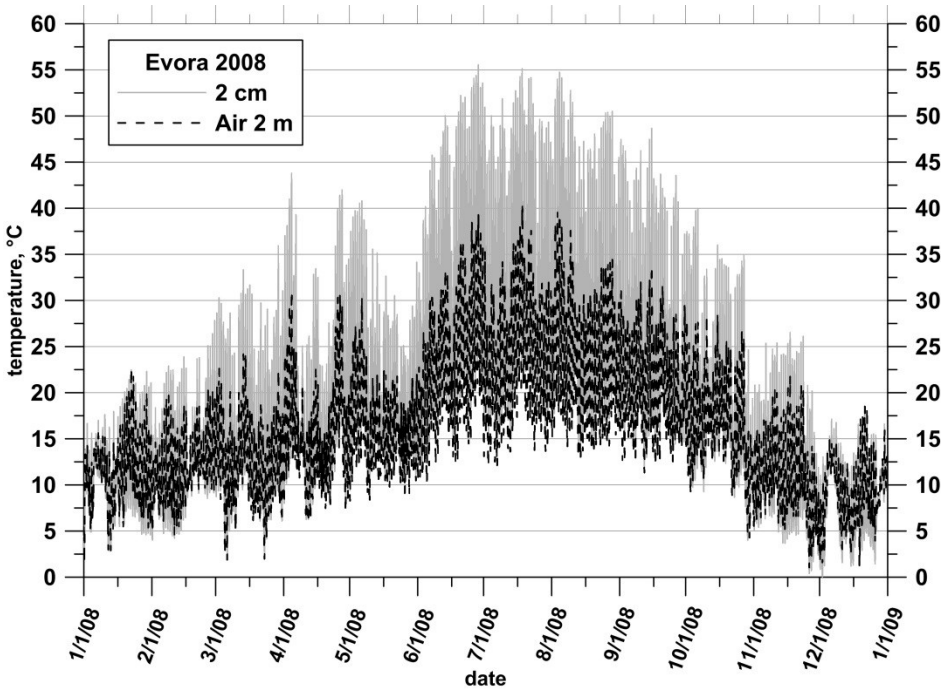

Figure 5. Air and ground temperature fluctuation at Evora observatory during 2008.

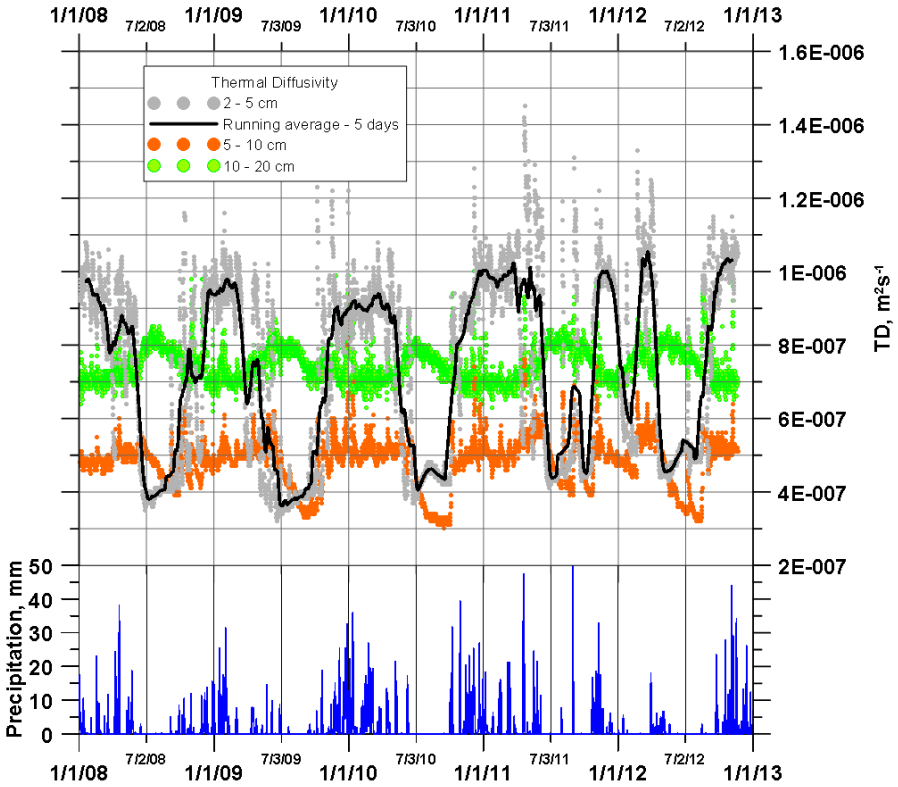

Figure 6. Seasonal changes of thermal diffusivity of soil connected with daily sums of precipitations.

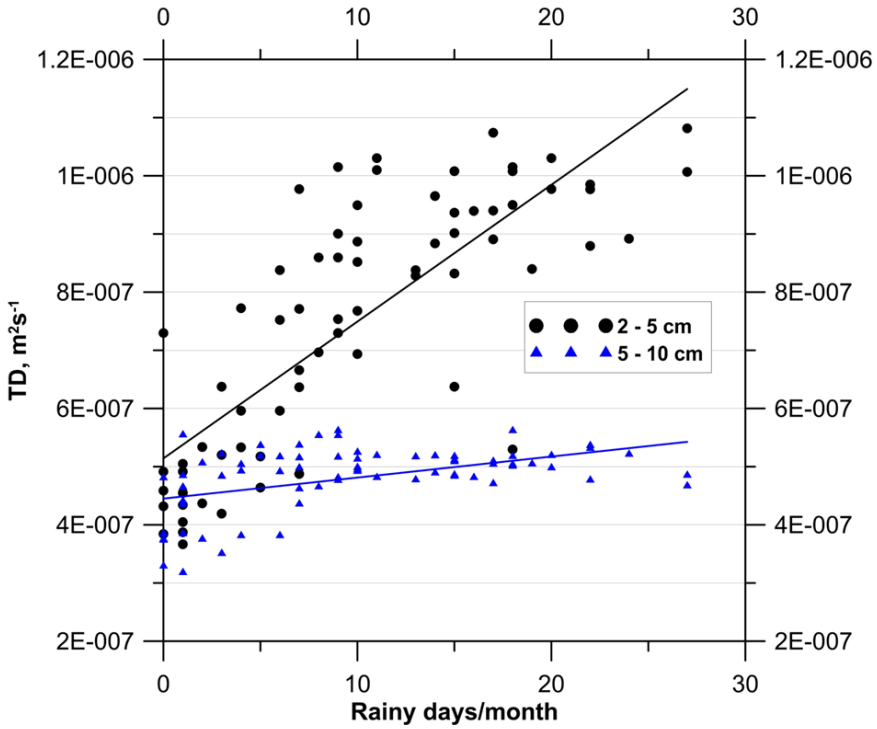

Figure 7. Dependence of the monthly TD averages on the number of rainy days per month in Evora in years 2008 – 2013.

It is evident that the method used above allows a detailed monitoring of changes in TD related to the soil moisture changes during the year. The case of Evora is an extreme one due to the absence of vegetation cover and alternating hot dry and wet periods. Nevertheless, seasonal variations decline rapidly with depth. In case of Malence, where measurement are carried out in a meadow in a clayey soil, the seasonal variations are significantly attenuated below a depth of 5 cm (**Figure 9**).

2.2. Estimation based on periodical boundary condition

Another way of calculating TD is based on solving the heat conduction equation assuming a periodic boundary condition. For that reason it is possible to process the temperature series up to the range of annual variations. **Figure 8** shows the results of temperature monitoring at Malence (MBCO) observatory, where the annual wave is visible to the depth of 10 m. Practical algorithms for the calculation of the thermal diffusivity k from the soil temperature measurements were proposed e.g. by Horton et al. (1983), Lamba and Khambete (1991) or Hurley and Wiltshire (1993). These

algorithms are based on a 1-D solution of the heat conduction equation in a semi-infinite homogeneous medium,

$$\frac{\partial T}{\partial t} = k \frac{\partial^2 T}{\partial z^2} \qquad (3)$$

with a periodic surface boundary condition of period $2\pi/\omega$

$$T(z=0,t) = T_0 + A_0 \sin(\omega t - \varepsilon_0), \quad (4)$$

where t is time, z is depth, T is temperature. T_0, A_0, and ε_0 represent mean surface temperature, amplitude and phase of the surface temperature wave, respectively. The underground temperature at depth z can be calculated

$$T(z,t) = T_0 + z.gradT + A_0 e^{-z/d} \sin(\omega t - z/d - \varepsilon_0), \qquad (5)$$

where $gradT$ is geothermal gradient and $d = \sqrt{2k/\omega}$ is damping depth of the surface temperature wave. In other words, the amplitude of the surface wave decreases exponentially as $A(z)=A_0 \cdot e^{-z/d}$ and its phase increases linearly as $\varepsilon(z)=\varepsilon_0+z/d$ with increasing depth. As seen, the above solution applies to the uniform strata only. To estimate the thermal diffusivity within a given layer we have applied the following two methods. They use the amplitude and/or the phase lag of the temperature wave at depths z_1 and z_2 and the frequency of the investigated surface temperature wave (Horton et al., 1983), namely, the Amplitude algorithm (AA) that calculates k from the equation (5) as

$$k = \frac{\omega(z_1 - z_2)^2}{2\ln(A_1/A_2)^2} \qquad (6)$$

and Phase algorithm (PA) giving

$$k = \frac{\omega(z_1 - z_2)^2}{2(\varepsilon_1 - \varepsilon_2)^2}. \qquad (7)$$

Here A_1, ε_1 and A_2, ε_2 are the amplitudes and phase lags of the temperature waves at depths z_1 and z_2, respectively. The k-value represents the thermal diffusivity within the (z_1, z_2) interval.

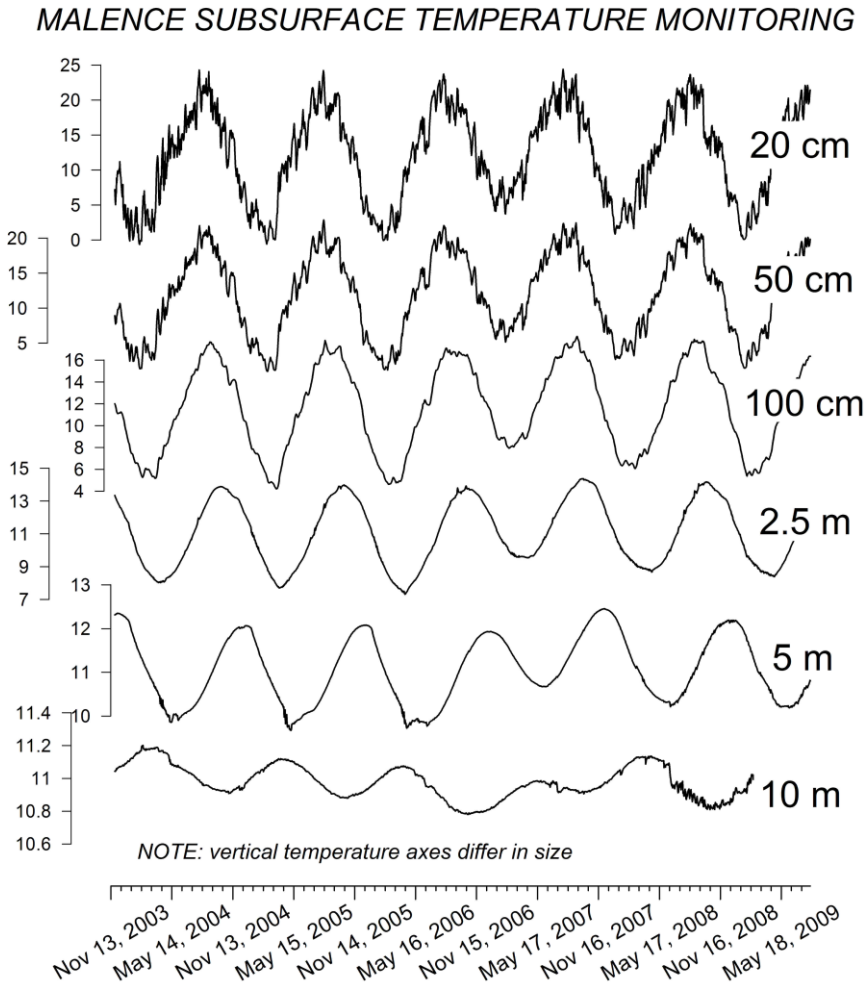

Figure 8. Time series of daily temperature averages at different depths in the borehole Malence.

2.2.1. Conduction-Convection (CCA) algorithm

Both AA and PA provide certain estimates of the thermal diffusivity only for a vertically homogeneous medium without convective heat transport. Subsurface fluid movements represent one of the most common and serious factors disturbing the underground temperature field. Even very small water flows could significantly distort the temperature (see e.g. Bodri and Čermák, 2005, and the references therein) and thus affect the estimated k-value. It is also known, that the thermal diffusivity depends upon soil water content. It increases with an increase of the rock moisture at low water contents (when the effect of increasing thermal conductivity prevails) and then gradually decreases with increasing water contents at high water (e.g. Viswanadham and Rao, 1972; Farouki, 1986). The Conduction-Convection algorithm (CCA) for the subsurface thermal diffusivity determination incorporates the impact of vertical water movement and thus takes into account the possibility of the advective heat transfer. The

detailed examining of this method by field experiments was performed by Gao et al. (2008, 2009).

In a porous medium with undeformable solid matrix and incompressible fluid, the 1-D equations for conservation of mass and energy can be expressed:

$$\frac{\partial v}{\partial z} = 0, \frac{\partial T}{\partial t} + \frac{C_f}{C} v\theta \frac{\partial T}{\partial z} = k \frac{\partial^2 T}{\partial z^2}, \qquad (8)$$

where C and C_f are the volumetric heat capacities of the medium and fluid, respectively, θ is the volumetric water content of the soil and v is the pore (distance) velocity. Product of θ and v is Darcy fluid velocity. Negative velocity corresponds to the fluid flow towards the surface. Further on, values of the parameter

$$W = \partial k / \partial z - \frac{C_f}{C} \theta v, \qquad (9)$$

are considered, the second part of which, $- Cf/C * \theta * v$, defined Gao et al. (2008) as the fluid flux density. Shao et al. (1998) and Gao et al. (2003, 2008) suggested an analytical solution of Eqs. (8) and the following expressions for the calculation of k

$$k = -\frac{(z_1 - z_2)^2 \omega \ln(A_1 / A_2)}{(\varepsilon_1 - \varepsilon_2)[(\varepsilon_1 - \varepsilon_2)^2 + \ln^2(A_1 / A_2)]} \qquad (10)$$

and W

$$W = \frac{\omega(z_1 - z_2)}{(\varepsilon_1 - \varepsilon_2)} \left[\frac{2 \ln^2(A_1 / A_2)}{(\varepsilon_1 - \varepsilon_2)^2 + \ln^2(A_1 / A_2)} - 1 \right]. \qquad (11)$$

This technique is generally known as the Conduction-Convection algorithm (CCA). At W=0 (purely conductive heat transfer in a homogeneous subsurface) one obtains $\varepsilon_1 - \varepsilon_2 = \ln(A_1/A_2)$ and equation (10) reduces to the formulae (6) or (7).

2.2.2. Spectral analysis of data

To obtain the annual temperature wave at a given depth we applied the Fourier analysis on measured data, which is a conventional method for analyzing time series data to determine the amplitude, phase and the power (mean square amplitude) as a function of frequency. Daily mean temperature series were subjected to the windowing Fourier transform method to estimate their heterogeneity spectra. The calculated values of the amplitude and phase (**Table 1**) monotonously decrease with depth in the upper 10 m.

Except of the annual wave, the spectra do not contain any distinct peaks that may indicate the presence of other periodic processes.

Depth (m)	Amplitude (K)	Phase (rad)
0.02	8.28425	-0.46042
0.05	8.10476	-0.48170
0.10	7.89128	-0.50976
0.20	7.55725	-0.55585
0.50	6.59817	-0.69859
1	5.32925	-0.92259
2.5	2.73109	-1.53812
5	0.93930	-2.48123
10	0.09850	-4.74586

Table 1. *Amplitude and phase of the annual wave.*

Interval (m)	k_{AA}[a]	k_{PA}[a]	k_{CCA}[a]	W (m/s)
0.02-0.05	0.187	0.198	0.198	0.81×10^{-8}
0.05-0.10	0.350	0.316	0.316	-1.77×10^{-8}
0.10-0.20	0.533	0.469	0.468	-2.74×10^{-8}
0.20-0.50	0.487	0.440	0.440	-2.11×10^{-8}
0.50-1.00	0.546	0.496	0.496	-2.12×10^{-8}
1.00-2.50	0.502	0.592	0.590	4.00×10^{-8}
2.50-5.00	0.547	0.699	0.694	6.50×10^{-8}
5.00-10.0	0.490	0.485	0.456	-0.19×10^{-8}

Table 2. *TD and parameter W calculated for different depth intervals ([a] k_{AA}, k_{PA} and k_{CCA} were calculated by the AA, PA and CCA methods, respectively, and are given in 10^{-6} m^2/s).*

2.2.3. Calculation of TD and parameter W

The values of the parameters *k* and *W* calculated by the three algorithms mentioned above from amplitudes and phase lags of the annual temperature wave are presented in **Table 2**. As seen, all three algorithms gave reasonable results. The k-values estimated from the amplitude and phase angle by the AA and PA are consistent, their relative differences are below 12%, only in the layers 1 - 2.5 m and 2.5 - 5 m the PA values are larger by 18% and 28%, respectively. Both methods detect obvious vertical heterogeneity of the TD that equals to ~0.2-0.3x10^{-6} m^2/s in the top 5-10 cm of the soil and increases to the values of 0.5-0.7x10^{-6} m^2/s within the 0.1-10 m layer. TD estimated

by error function algorithm in three upper soil layers (**Figure 9**) shows good match in layers without seasonal variations. In the 2-5 cm layer where TD fluctuations occur as the soil dries in the summer months, the value is slightly higher than that given by "periodic" solution.

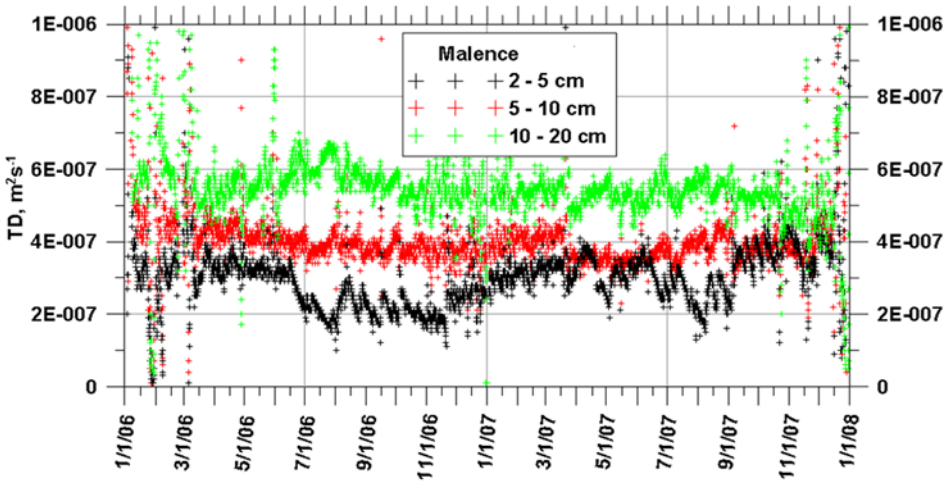

Figure 9. TD estimated by error function algorithm in the upper soil layer at Malence.

As seen, the k-values obtained by the CCA that specifies on a presence of the subsurface fluid flow, revealed a good agreement with the results given by only conduction solution. This is especially true for the PA and CCA results. As follows from formula (5) for the T(z,t), the natural logarithm of amplitude and the phase lag are linear functions of depth in a semi-infinite homogeneous medium.

Figure 10 shows how closely this relationship is obeyed by the amplitudes and phases of the annual waves determined in the individual depths down to 10 m in these particular conditions. The regression lines of the logarithm of amplitude and the phase lag yield a mean thermal diffusivity of 0.51x10-6 m2/s and 0.55x10-6 m2/s, respectively. The zero depth intercepts of the regression lines also yield estimates of the amplitude and phase lag of the annual ground surface temperature signal, 8.29 °C and -0.465 radian, respectively, which are close to the values determined for the depth of 2 cm (Table 1). As mentioned above, for the amplitude and phase lag calculations the solution of conductive heat equation under periodic boundary condition was used. The linear regressions of the logarithm of amplitude and/or the phase lag with depth yield coefficients of determination 0.9999 and 0.9991, respectively. It is evident that heat conduction dominates in the entire domain.

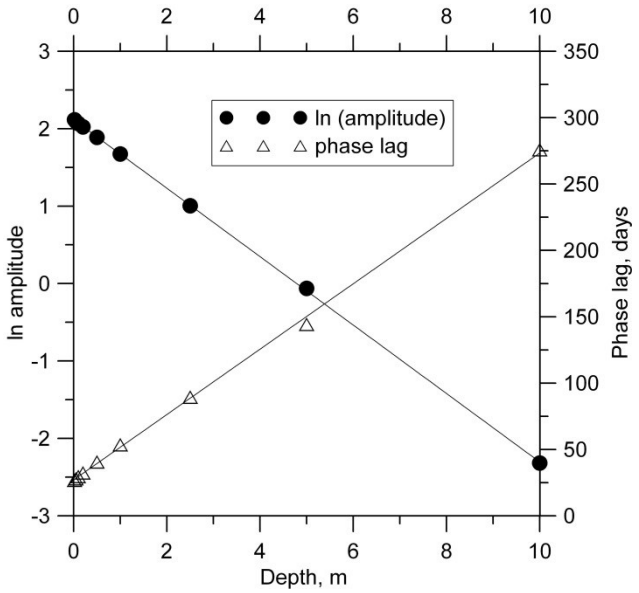

Figure 10. The natural logarithm of amplitude and the phase lag as functions of depth and their linear regressions. The regression lines yield estimates of mean thermal diffusivity between the surface and the depth of 10 m. The zero depth intercepts of the regression lines also provide estimates of the amplitude and phase lag of the annual ground surface temperature signal.

3. Impact of anthropogenic structures on subsurface temperature field

As mentioned in chapter 3 discrepancy between the regional climate change and observed temperature response in subsurface was discovered in urban area at Spořilov, Prague. The second studied locality, where the heat urban island effect appeared, is borehole Še-1 situated in industrial area in Šempeter, Slovenia. The temperature logs of Šempeter borehole display a U-shape with a minimum at the depth of 65 – 70 m migrating downwards at the rate of about 1 m per year, and a gradual warming at the rate of 0.01 – 0.02 K per year.

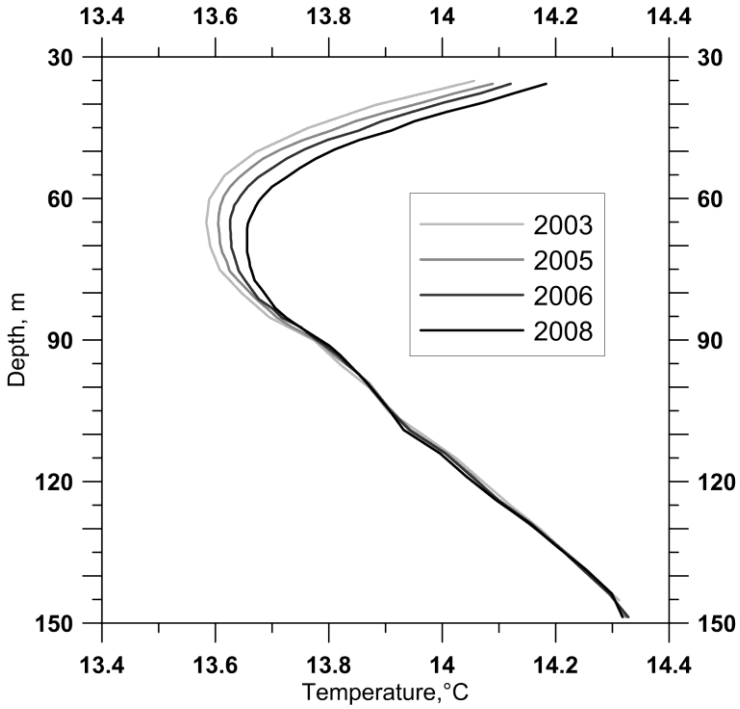

Figure 11. Temperature logs in the borehole Še-1, Slovenia, measured in the years 2003, 2005, 2006 and 2008 (from left to right) at the depth section 40 m – 150 m.

3.2. Numerical modeling

The mathematical modeling of thermal effects of the anthropogenic changes in surroundings of the boreholes and of the regional climatic changes on subsurface temperature field has been done using software packages FRACTURE (Kohl and Hopkirk, 1995) and commercial code COMSOL Multiphysics. Three-dimensional time-variable geothermal models (cube, length of the sides 1000 m) of the boreholes' sites were compiled with the aim to distinguish in the observed transient component of the

temperature logs the part caused by construction of new buildings and other anthropogenic structures in surroundings of the boreholes, and the part generated by the ground surface temperature warming due to the surface air temperature rise. The 3D models of the two studied localities (Spořilov, Prague and Šempeter, Slovenia) were composed taking into account the substantial anisotropy of thermal conductivity of rocks. The role of convective transfer of heat in the flat or subdued topography around the boreholes was assumed to be negligible and was not considered (see chapter 2, Smerdon et al, 2003).

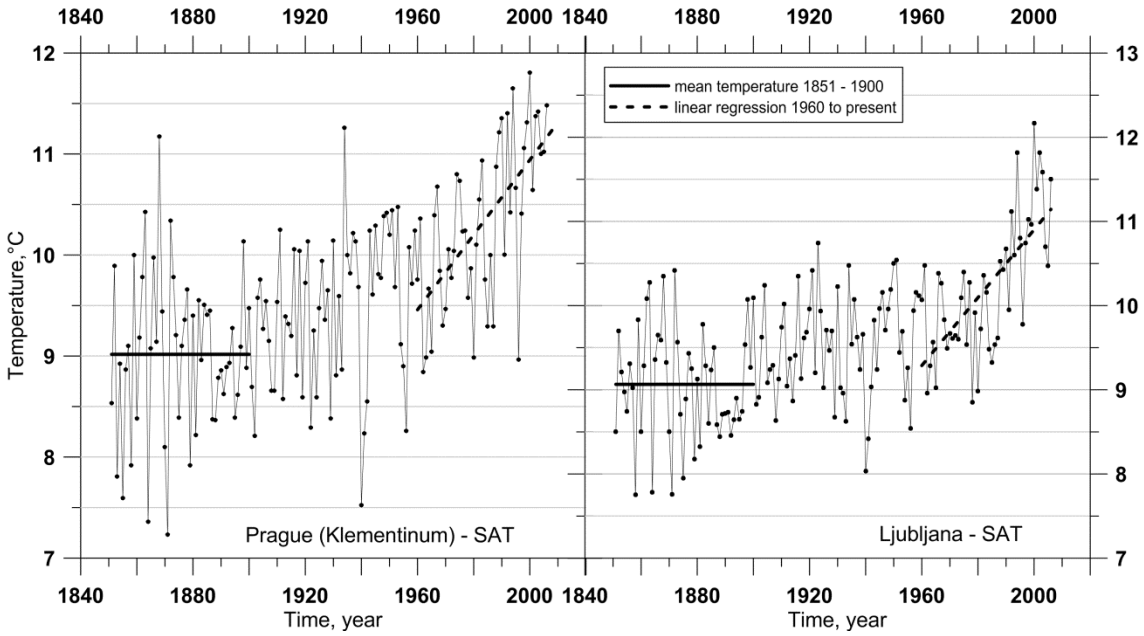

Figure 12. Mean annual surface air temperatures (SAT) recorded at meteorological stations in Prague (Klementinum), Czechia and in Ljubljana, Slovenia.

The zero heat flow was used as the low boundary condition at the depth of 1000 m (Smerdon and Stieglitz, 2006). The boundary condition of the zero heat flow together with zero heat sources within the model imply that all modeled variations of the subsurface temperature are caused by the spatial and temporal changes of the ground surface temperature, which was the upper boundary condition of the models. Because the surroundings of the boreholes can be approximated by a horizontal plain, the spatial variations of the ground surface temperature are given by a pattern of the different types of surface (grass, asphalt, sand, buildings,..). With the exception of buildings, under which a constant temperature was assumed, the ground surface temperature was subjected to the temporal variations consistent with variations of the mean annual air

temperatures observed at the nearby meteorological stations. To estimate mean annual temperatures of the individual surfaces, results of the aforementioned long-term monitoring of the soil temperatures were used. Because at the beginning of the 20th century the boreholes' surroundings were grassy areas without buildings, the average air temperature of the period 1851 – 1900 observed at meteorological stations in Prague and Ljubljana (**Figure 12**) was used as the initial temperature of the corresponding models. The temporal development of the models started therefore in the year 1900. The time series of the mean annual air temperatures recorded at meteorological stations in Prague (Klementinum) and Ljubljana **(Figure 12)** display a similar pattern with significant warming in the last 50 years (the average warming rate of 0.04°C per year in both cases). Mean temperature in the second half of the 19th century was 9.02°C in Prague and 9.07°C in Ljubljana.

3.3. Borehole GFU-2 in Prague

First we tried to model the temperature – time series observed in the borehole GFU-2 in Prague at the depth of 38.3 m in the period 1994 - 2008 as a pure response of the subsurface temperatures to the air temperature warming trend observed at the meteorological station Prague (Klementinum), about 7 km away from the borehole. When we used the air temperature variations as the surface boundary condition in transient solution of the heat conduction equation in the geothermal model of the site, we obtained for the depth 38.3 m and the period 1994 - 2008 the time – temperature series shown in **Figure 13**. The warming pattern can be divided into three time periods. The average increase of temperature was 0.020°C per year in 1994 – 1998, then (especially due to the very cold year 1996) it was 0.010°C per year in 1999 – 2001 and finally again 0.021°C per year in the third period 2002 - 2008. The average warming rate of the whole explored period 1994 – 2008 was 0.017°C. Comparing the calculated warming rate (**Figure 13**) yielded by the SAT variations (**Figure 12**) with the rate of the observed curve (**Figure 14**), we see appreciable quantitative difference. Namely, the mean annual warming rate for the whole period of observation is 0.034 °C per year instead of the calculated rate of 0.017 °C per year. However, it is obvious from **Figure 13** that also the observed temperature increase varies in time and that the curve can be divided into several time intervals with respect to the warming trend. The measured temperature increase amounts to 0.022°C/year in 1994 – 1995, to 0.029°C/year in 1996

– 1999, to 0.024°C/year in 1999 – 2000, to 0.038°C/year in 2001 - 2004 and to 0.036 °C/year after the year 2004.

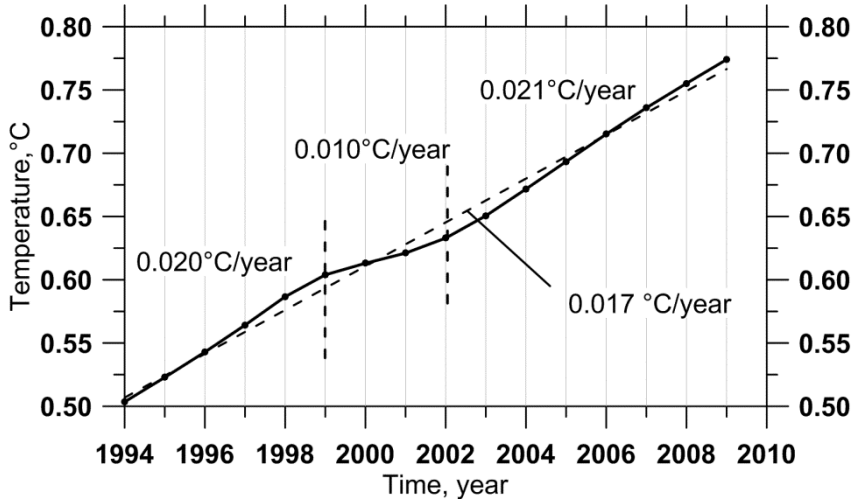

Figure 13. Time – temperature variations at 38.3 m of the GFU-2 borehole calculated as a subsurface temperature response to the surface air temperature variations only.

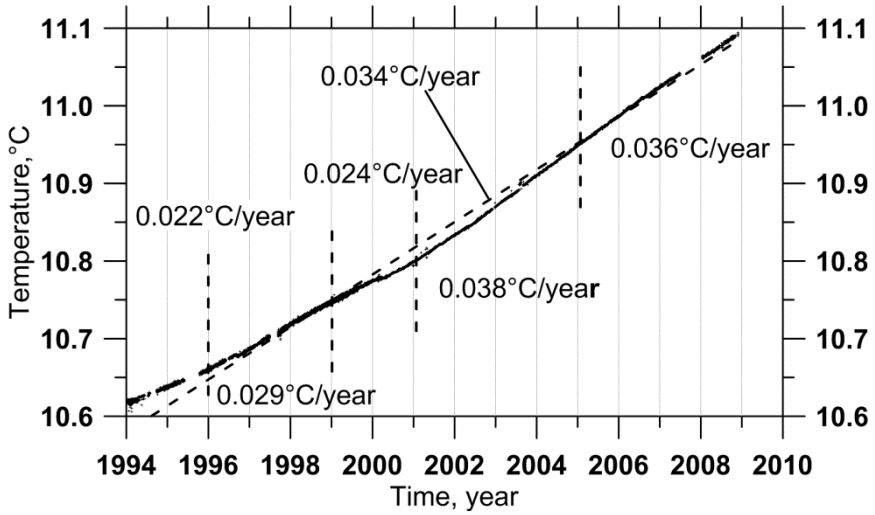

Figure 14. The observed time – temperature series at 38.3 m in the GFU-2 borehole divided into periods of approximately constant warming rate. The warming trend of the whole observational period 1994 – 2008 is 0.034 °C per year.

As stated above, the average rate of warming in the borehole GFU-2 during the entire observational period is two times larger than the calculated warming rate caused by warming trend of the SAT. In searching for sources of this discrepancy we explored the effects of anthropogenic structures in the immediate surroundings of the borehole. **Figure 15** shows configuration of these structures and the boreholes. There are asphalt

surfaces, a house with the ground plan of 20 m x 20 m and a red clay playing field (a tennis court). The rest of the area is covered mostly by grass. The asphalt surfaces and the playing field were built at the turn of the 1950s into the 1960s, the house was constructed in 1992 and has been used since 1993.

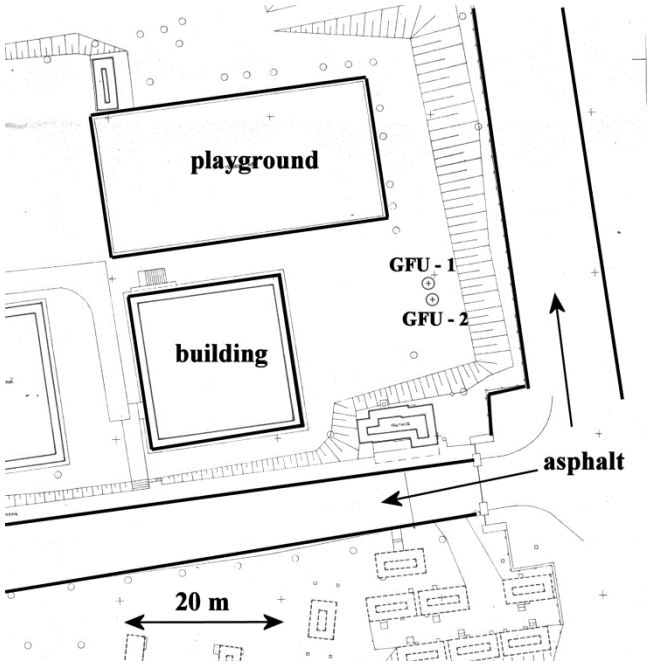

Figure 15. Block plan of the immediate surroundings of borehole GFU-2 in Prague – Spořilov.

The effects of the surface anthropogenic structures on the subsurface temperature field were evaluated by considering different offsets between the mean annual temperature of the ground and the air according to the type of the surface, based on the results of the aforementioned long-term monitoring of the soil temperatures. The offset for the playground was assumed similar to that observed for sand, 1 – 2 °C and the offset for asphalt was taken in accord with observations as 3 – 4 ° C. Zero offset was considered for the prevailing grassy surface (see the text below). First, we evaluated the effect of the structures constructed at the turn of the 1950s into the 1960s, i.e. the playground and the asphalt surfaces and then separately the effect of the house used since 1993. The resulting time-temperature variations, calculated for the point of observation at the depth of 38.3 m in borehole GFU-2, are depicted in **Figure 16a** (the playground and the asphalt surfaces) and **Figure 16b** (the house). They show the pure effect of the

structures' construction, because the ground surface temperatures were kept constant in time. It is obvious that the surface structures have an essential impact, albeit varying in time, on the measured warming in the borehole. It can be seen from **Figure 16a** that dynamics of the subsurface temperature response to the construction of the playground and asphalt areas has diminished appreciably after 1980 – 90, still before the beginning of the monitoring. On the contrary, the temperature signal of the house built 20 m apart from the borehole in 1992 reached the observational point after the year 1996 only and its warming rate culminated in the period 1999 – 2004. It means that the effect of the anthropogenic structures on the observed warming rate in borehole GFU-2 was minimal in the beginning of the observations. It corresponds well with the fact that the observed warming (**Figure 14**) is only by 0.003 °C higher than the modeled effect of the air temperature rise in the first years of the monitoring (**Figure 13**). On the other side, the period of the largest warming caused by the house, 1999 – 2004, overlaps partially with the period of the minimum warming generated by the air temperature rise due to the very cold year 1996. That is why the effect of the house is clearly visible in the observed data after the year 2001 only (**Figure 14**).

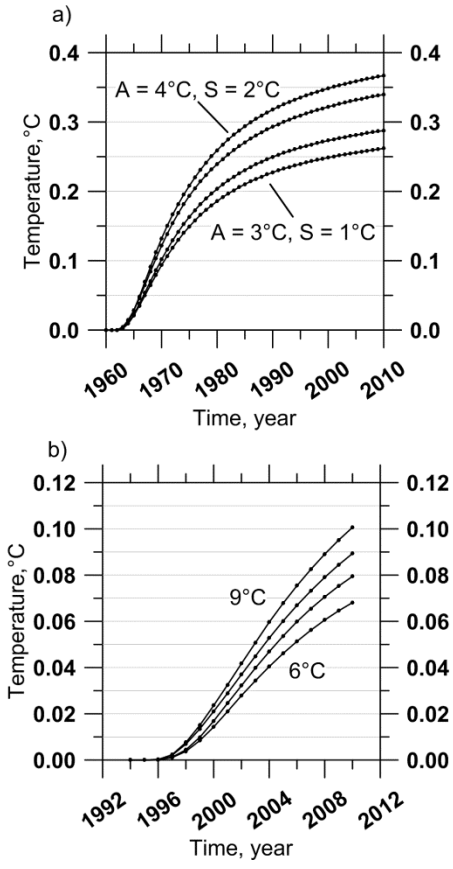

Figure 16. Time – temperature changes in borehole GFU-2 at the depth of 38.3 m calculated as a response of the subsurface temperature to construction of the anthropogenic structures in surroundings of the borehole; a) – effect of asphalt (A) and sandy (S) areas with different combinations of the ground surface temperature offset with respect to the grassy surface. The magnitude of the warming increases with increasing offset from (A = 3 °C, S = 1 °C) via (A = 3 °C, S = 2 °C), (A = 4 °C, S = 1 °C) to (A = 4 °C, S = 2 °C), b) – effect of the warmer ground below the house with respect to the grassy surrounding for offsets 6 °C, 7 °C, 8 °C and 9 °C.

The calculated time-temperature variation due to SAT (**Figure 13**) indicates only moderate warming rate of 0.021 °C per year after 2001, the transient effect of the house construction should diminish gradually and the effect of the hard anthropogenic surfaces (asphalt, playground) should be minimal after 2004 (**Figure 16a,b**). Calculations based on the model taking into account the SAT variations, the temperatures of asphalt and playground higher than grass by 4°C and 1.5°C, respectively, and the constant temperature of 20 °C at the base of the house, yielded warming rate of 0.030 °C per year in the period 2005 – 2008. It is substantially less than the observed warming rate of 0.036 °C per year.

In search for explanation of this disagreement we explored the possibility that the offset between the mean annual ground surface temperature and the mean annual SAT has changed during the monitoring. Usually it is assumed that this ground – air coupling is constant on the time scale of decades and longer, but can vary on the inter-annual scale depending on variations of meteorological factors like thickness and duration of snow cover, precipitation, solar irradiation etc.

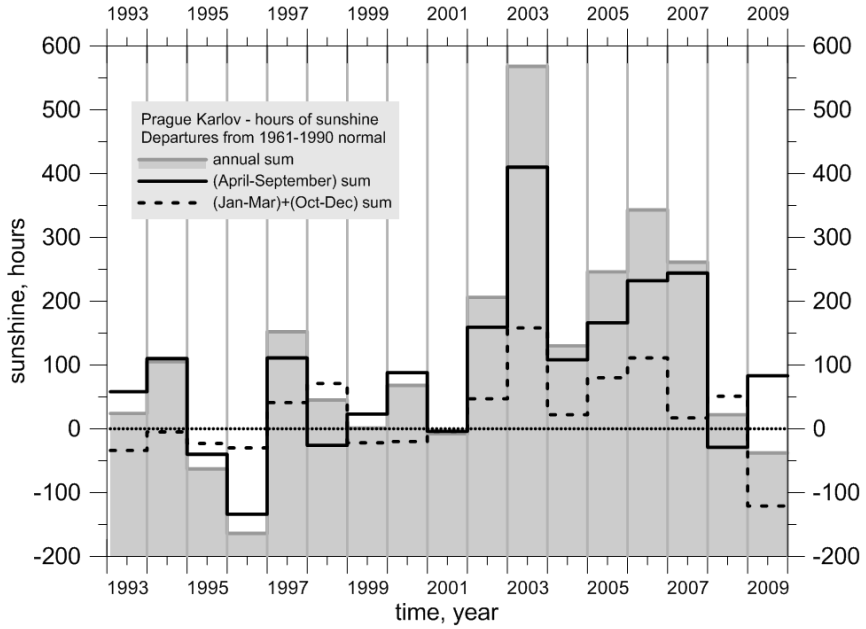

Figure 17. Number of sunny hours measured at the meteorological station Prague – Karlov in the period 1994 – 2008.

An important source of data for the mathematical modeling of thermal effects of the anthropogenic changes in surroundings of the boreholes, namely mean annual ground temperatures under different types of surface, were the records from the observational

polygon located about 150 m from the boreholes in Prague, also on the grounds of the Institute of Geophysics. Here, the continuous monitoring of soil temperatures under various types of surface (grass, sand, bare soil and asphalt) together with air temperature and other meteorological elements has been running since 2003. Temperatures are measured by calibrated platinum sensors Pt-1000 in five-minute intervals at the depths of 2, 5, 10, 20 and 50 cm. The monitoring indicates that, in the period 2003-2008, the difference between the mean annual temperature of the ground at the depth of 2 cm and the air temperature at 5 cm varied in the range 0,2 - 0,8 °C for grass, 1,5 – 2 °C for sand and bare soil and 4 – 5°C for asphalt. Inter-annual variation of the difference for the individual types of surface in the given period of 6 years is affected mostly by the number of sunny hours in summer months and to a certain degree by snow cover in winter.

When we checked records from the nearest meteorological station Prague – Karlov, about 5 km away from the borehole, the only parameter that showed systematic trend since the beginning of 1990s was the annual sum of the sunny hours. As can be seen from **Figure 17**, which shows the annual sum of sunny hours in the period 1993 – 2008 at Prague - Karlov, the sum fluctuated closely around its long-term standard of 1630 hours (1961 – 1990) prior to 2002, but was significantly above the standard in the period 2002 – 2007. As mentioned earlier, the difference between the mean annual temperature of asphalt and air during 6 years of the soil – air temperature monitoring on premises of the Institute of Geophysics in Prague fluctuated between 4 – 5°C. The maximum difference, almost 5°C, was observed in the year 2003, which was also the year of the highest annual sum of the sunny hours. Therefore it seems reasonable to assume that the difference of mean annual ground and air surface temperatures is sensitive, at least for surfaces with a low albedo, on the sum of the sunny hours. This assumption was taken into consideration in the final model, where the difference between asphalt and air was set on 3.5°C prior the year 2002 and to 4.5 °C since 2002. In the case of the playing field it was 1°C, increased by 0.5°C since 2002. The mean annual temperature of grass was equal to that of air. The resulting time-temperature series is shown in **Figure 18**. The resulting curve can be divided into several time periods according to the warming rate again. Now, the warming pattern agrees fairly well with the observed one: 0.023°C/year in 1994 – 1995, 0.029°C/year in 1996 - 1998, 0.024°C/year in 1999 - 2001 and 0.036°C/year after the year 2001. It is remarkable how well the final model reproduces not only the rate of warming, but also the absolute level

of the subsurface temperatures. After adding 0.77 °C to the temperature calculated for the depth of 38.3 m, which corresponds to the undisturbed gradient of 20 °C/ km observed in the lower part of borehole GFU-1, the temperature differs from the observed one by 0.18°C only (10.91 °C instead of 11.09 °C) at the end of 2008. As mentioned above, the difference between the mean annual ground temperature under grass and the mean annual temperature of air was 0.2 – 1.2 °C during the 6-year monitoring period. The resulting difference of 0.18 °C is therefore at the lower margin of this interval. The reason for this may lie in full-grown trees situated in the surroundings of the borehole.

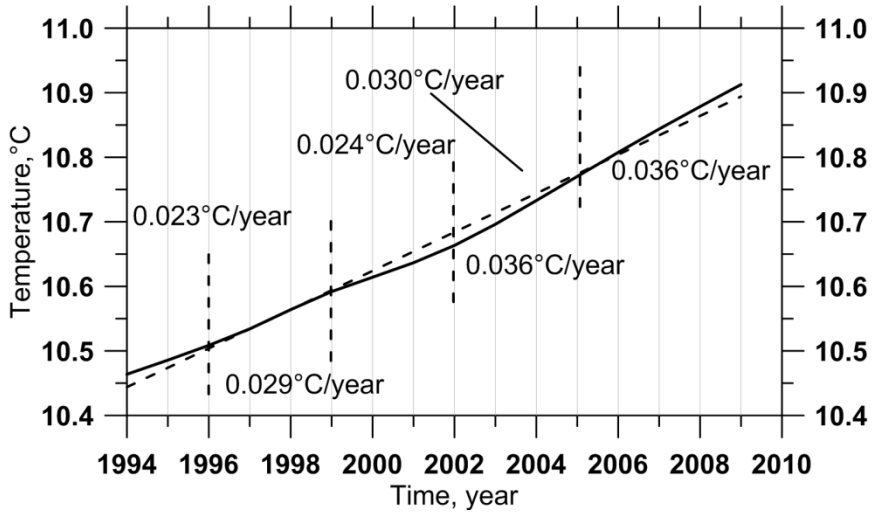

Figure 18. Time – temperature variations at 38.3 m in the GFU-2 borehole calculated by the final model as a subsurface temperature response to the surface air temperature variations together with the effect of the anthropogenic structures.

3.4. Borehole Še-1 in Šempeter

The borehole Še-1 is located in the industrial zone of the town Šempeter. A large sporting hall is situated in the borehole's close vicinity with adjacent asphalt areas, a small playing field and also industrial halls and asphalt roads further away (see **Figure 19**). The whole agglomeration was built during the second half of the 1970s. The site of the borehole is warmer than in Prague, the long-term ground surface temperature extrapolated from the temperature logs is nearly 13 °C compared to 9.5 °C in Prague. The long-term mean of the annual sum of the sunny hours at the near meteorological station Bilje is around 2000 (Mesečni bilten ARSO 2009), which is by 370 hours more

than in Prague. As mentioned above, the upper 90 m of the borehole passes through unconsolidated Quaternary sediments characterized by alternating sandy and clayey layers with different thermal properties. Whereas samples of these Quaternary sediments were not available, we estimated values of thermal conductivity and thermal diffusivity of the individual layers using our laboratory measurements on similar rock types, and published data (Abu-Hamdeh and Reeder, 2000, Shan Xiong Chen, 2008). Effect of this fine layered structure on transient temperature is substantial. When the structure is approximated by a homogeneous model of the same thermal resistance, the resulting transient profile differs appreciably. This is demonstrated in **Figure 19** which shows downward propagation of SAT changes simulated by the transient layered model and the transient homogeneous model. **Figure 19** depicts also the difference of the two profiles. It amounts to several tenths of degree in the upper part of the borehole. The layered, more realistic model was used in simulating the effect of the anthropogenic structures in 3-D models.

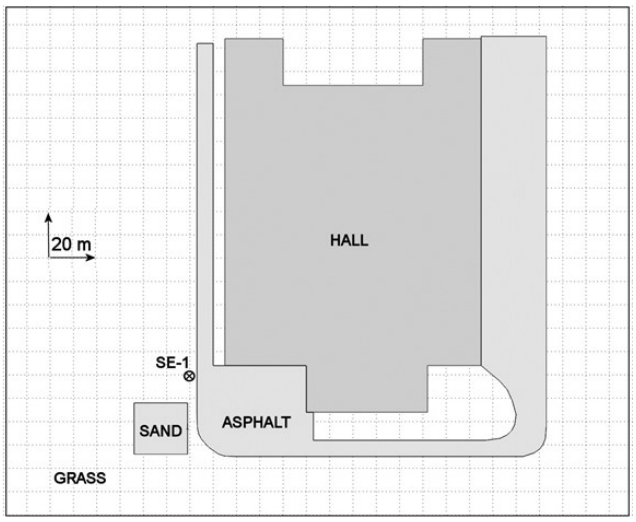

Fig. 19. Block plan of surroundings of the borehole Še-1.

The individual effects of the regional climatic and local anthropogenic forcing together with their composite effect on the subsurface temperature field in the borehole Še-1 are shown in **Figure 20** in a form of transient components of the temperature – depth profiles. They are compared with the observed transient component. All profiles are related to the year 2008. Variations of the mean annual SAT series observed at meteorological station Ljubljana were used as the climatic forcing. The offsets chosen for the ground surface temperatures of the individual types of surface were similar to

that in Prague, 3.5°C for asphalt and 1.5°C for the playground. Temperature below the sporting hall was considered between 15°C through 20°C in the individual versions. The best fit to the observed profile was achieved for 17°C. The transient component of both the observed and the simulated temperature logs was obtained by subtracting from the profile its linear part fitted to the depth section 150 – 400 m, where the transient component is negligible in comparison with the uppermost 100 m of the borehole.

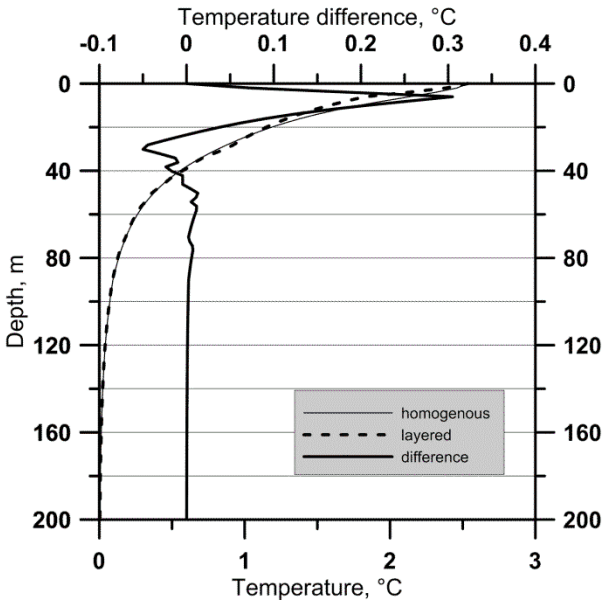

Figure 19. Synthetic transient temperature – depth profiles and their difference in the borehole Še-1 calculated by layered and homogeneous transient geothermal models of the same thermal resistance as a response to climate change.

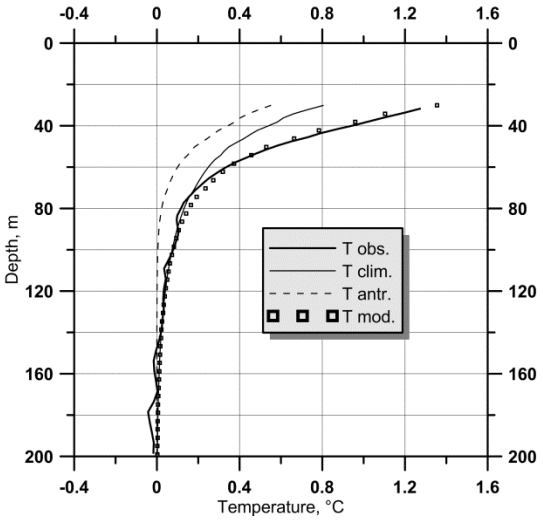

Figure 20. Transient components of the temperature – depth profiles in the borehole Še-1 in 2008 generated (i) by the individual effects of the regional climatic (Tclim) and

local anthropogenic (Tantr) forcings and (ii) by their composite effect (Tmod) compared with the observed transient component (Tobs).

The warming effect of the anthropogenic structures is about 50 % of that caused by the SAT warming at the depth of 50m and becomes negligible below 100 m. The impact of climatic signal attenuates more slowly with depth than the anthropogenic one and becomes smaller than one hundredth of degree below 160 m. The sum of the two signals approximates fairly well the observed transient component of the Še-1 temperature logs.

Conclusions

The thesis has shown that the present subsurface temperature field can be strongly influenced both by the recent regional climatic changes and by thermal effects of local anthropogenic structures. On the other side the influence of water movement on subsurface temperature field caused by a meteoric water infiltration is negligible and heat conduction dominates in vadose zone. Only the thinnest layer of soil to a depth of 5 cm is affected by changes in moisture and the induced seasonal variations of thermal diffusivity can affect heat transfer in the shallow subsurface, especially in places where the significant alternation of hot dry and cooler wet periods occurs.

The results of the study indicate that the factor of “thermal pollution” due to local anthropogenic effects in precise temperature logs must be taken into account seriously both in the terrestrial heat flow studies and in the ground surface temperature history reconstructions. Especially for the climatic studies based on the temperature logs, selection of boreholes or borehole sites should always consider this possible problem.

Acknowledgements

I would like to express my gratitude to my supervisor RNDr. Jan Šafanda, CSc. for his cooperation and many useful advices to find best way in my work. I would also like to thank RNDr. Vladimír Čermák, DrSc.for his encouragement and cooperation on data processing. I thank my wife for patience…

List of papers included in the thesis

P1. **Dědeček P**., Šafanda J., Rajver D.,(2012): Detection and quantification of local anthropogenic and regional climatic transient signals in temperature logs from Czechia and Slovenia*, Climatic Change 113 (3-4), DOI: 10.1007/s10584-011-0373-5*

P2. **Dědeček P**., Rajver D., Čermák V., Šafanda J., Krešl M., (2013): Six years of ground–air temperature tracking at Malence (Slovenia): thermal diffusivity from subsurface temperature data, *J. Geophys. Eng. 10 (2013) 025012 (9pp) doi:10.1088/1742-2132/10/2/025012*

P3. Čermák V., **Dědeček P.,** Šafanda J. and Krešl M. (2010): Climate warming: evidence stored in shallow subsurface. In: *Przybylak, R.; Majorowicz, J.; Brázdil, R.; Kejna, M. (Eds.) The Polish Climate in the European Context: An Historical Overview, DOI 978-90-481-3167-9_11, Springer Science+Business Media B.V. 2010,*

References

Abu-Hamdeh NH, Reeder RC. (2000): Soil thermal conductivity: effects of density, moisture, salt concentration, and organic matter. *Soil Science Society of America Journal 2000;64:1285–1290.*

Beltrami, H. (2002): Climate from borehole data: Energy fluxes and temperatures since 1500. *Geophysical Research Letters 29 (23)*

Beltrami, H., Kellman, L. (2003): An examination of short- and long-term air-ground temperature coupling. *Global and Planetary Change 38 (3-4), 291-303.*

Bense, V., Beltrami, H. (2007): Impact of horizontal groundwater flow and localized deforestation on the development of shallow temperature anomalies. *Journal of Geophysical Research, 112, F04015, doi:10.1029/2006JF000703.*

Bodri L and Čermák V 2005. Borehole temperatures, climate change and the pre-observational surface air temperature mean: Allowance for hydraulic conditions, *Global Planet.Change 45 265-276*

Carslaw HS and Jaeger JC 1957 Conduction of Heat in Solids (2nd edition). *Clarendon Press Oxford 510 pp*

Chen, S.X.(2008): Thermal conductivity of sands. *Heat Mass Transfer 44:1241–1246*

Farouki OT 1986 Thermal Properties of Soils. *Series on rock and soil mechanics Vol. 11. In: Trans Tech.Publ. Clausthal-Zellerfeld Germany 136 pp.*

Gao Z, Fan X and Bian L 2003 An analytical solution to one-dimensional thermal conduction-convection in soil *Soil Sci. 168 99-107*

Gao Z, Lenschow DH, Horton R, Zhou M, Wang L and Wen J 2008 Comparison of two soil temperature algorithms for a bare ground site on the Loess Plateau in China *J.Geophys.Res. 113 D18105 doi:10.1029/2008JD010285*

Gao Z, Wang L and Horton R 2009 Comparison of six algorithms to determine the soil thermal diffusivity at a site in the Loess Plateau of China, *Hydrol.Earth Syst.Sci. Discuss. 6 2247-2274.*

Harris, R.N., Chapman, D.S. (1997): Borehole temperatures and a baseline for 20th-century global warming estimates. *Science 275 (5306).*

Horton R, Wierenga, PJ and Nielsen, DR 1983. Evaluation of methods for determination apparent thermal diffusivity of soil near the surface. *Soil.Sci.Soc.Am.J. 47 23-32*

Hurley S and Wiltshire RJ 1993 Computing thermal diffusivity from soil temperature measurements, *Computers and Geosciences 19 475-477*

IPCC 2001, Houghton JT, Ding Y, Griggs DJ, Noguer M, van der Linden PJ, Dai X, Maskell K, Johnson CA. (eds) (2001) Climate change 2001: the scientific basis. *Cambridge University Press, Cambridge*

Kohl, T., Hopkirk, R. J. (1995): "Fracture" – A simulation code for forced fluid flow and transport in fractured, porous rock. *Geothermics 24 (3), 333 – 343.*

Lamba BS and Khambete NN 1991 Analysis of subsoil temperature at various depths by Fourier technique, *Mausam 42 269-274.*

Lewis, T. J., Wang, K. (1992): Influence of Terrain on Bedrock Temperatures, Paleogr., Paleoclim.,Paleoecol. *Global and Planetary Change 98, 87–100*

Majorowicz, J.A., Skinner,W.R. (1997): Potential causes of differences between ground and surface air temperature warming across different ecozones in Alberta, Canada. *Glob. Plan. Change 15,79–91.*

Majorowicz, J.A., Skinner, W.R. (1997): Anomalous ground surface warming vs. surface air warming in the Canadian Prairie provinces. *Clim. Change 37, 485– 500.*

Majorowicz, J., Safanda, J. (2005): Measured versus simulated transients of temperature logs — a test of borehole climatology. *J. Geophys. Eng. 2 (4), 291–298.*

Mesečni bilten (Monthly Bulletin) Arso environmental agency of the republic of Slovenia (ARSO), *Ministry for Environment and Spatial Planning, 2009, XVI(12), 31–45. Available: http://www.arso.gov.si/ oagenciji/knjižnica/mesečni bilten/*

Nitoiu, D., Beltrami, H. (2005): Subsurface thermal effects of land use changes. *Journal of Geophysical Research – Earth Surface 110 (F1).*

Pollack HN, Chapman DS (1993) Underground records of changing climate. *Sci Am 268(6):44–49*

Rajver D, Šafanda J and Dědeček P 2006 Monitoring of air-ground temperature coupling and examples of shallow subsurface warming in Slovenia *Geologija 49/2 279-293.*

Šafanda J (1994) Effects of topography and climatic changes on temperature in borehole GFU-1, Prague. *Tectonophysics 239:187–197*

Shao, M., Horton, R. and Jaynes, D.B., 1998. Analytical solution for one-dimensional heat conduction-convection equation. *Soil Sci.Soc.Am.J., 62, 123-128.*

Smerdon, J. E., Pollack, H. N., Enz, J. W., Lewis, M. J. (2003): Conduction-dominated heat transport of the annual temperature signal in soil. *Journal of Geophysical Research, 108(B9), 2431.*

Smerdon, J. E., Stieglitz, M. (2006): Simulating heat transport of harmonic temperature signals in the Earth's shallow subsurface: Lower-boundary sensitivities. *Geophysical Research Letters, 13 (4).*

Štulc P (1995) Return to thermal equilibrium of an intermittently drilled hole: theory and experiment. Tectonophysics 241:35–45

Viswanadham Y and Ramanadham R 1969 The thermal diffusivity of red sandy soil at Waltair Pure Appl.Geophys. 74 195-205.

WMO (2019) WMO Statement on the State of the Global Climate in 2018, *ISBN 978-92-63-11233-0*

Woodbury, AD., Bhuiyan AKMH, Hanesiak J, and Akinremi OO (2009): Observations of northern latitude ground-surface and surface-air temperatures, *Geophys. Res. Lett., 36, L07703, doi:10.1029/2009GL037400*

Supplement

Papers included in the thesis

Climatic Change
DOI 10.1007/s10584-011-0373-5

Detection and quantification of local anthropogenic and regional climatic transient signals in temperature logs from Czechia and Slovenia

Petr Dědeček · Jan Šafanda · Dušan Rajver

Received: 3 August 2011 / Accepted: 16 November 2011

Abstract The paper reports on detection and quantification of the impact of local anthropogenic structures and regional climatic changes on subsurface temperature field. The analyzed temperature records were obtained by temperature monitoring in a borehole in Prague-Spořilov (Czechia) and by repeated logging of a borehole in Šempeter (Slovenia). The observed data were compared with temperatures yielded by mathematical 3D time-variable geothermal models of the boreholes' sites with the aim to decompose the observed transient component of the subsurface temperature into the part affected by construction of new buildings and other anthropogenic structures in surroundings of the boreholes and into the part affected by the ground surface temperature warming due to the surface air temperature rise. A direct human impact on the subsurface temperature warming was proved and contributions of individual anthropogenic structures to this change were evaluated. In the case of Spořilov, where the mean annual warming rate reached 0.034°C per year at the depth of 38.3 m during the period 1993–2008, it turned out that about half of the observed warming can be attributed to the air (ground) surface temperature change and half to the human activity on the surface in the immediate vicinity of the borehole. The situation is similar in Šempeter, where the effect of the recently built surface anthropogenic structures is detectable down to the depth of 80 m and the share of the anthropogenic signal on the non-stationary component of the observed subsurface temperature amounts to 30% at the depth of 50 m.

1 Introduction

Geothermal research based primarily on the temperature-depth logs measured in several hundred meters to several kilometers deep boreholes provides information on the energetic balance of the Earth (Pollack et al. 1993). However, the information stored in the transient component of the temperature-depth profiles, which is considered as a noise in the terrestrial heat flow determinations, can be used as a valuable archive of the past climatic changes (Harris

P. Dědeček (✉) · J. Šafanda
Institute of Geophysics, Czech Academy of Science, Boční II/1401, 141 31 Prague, Czech Republic
e-mail: pd@ig.cas.cz

D. Rajver
Geological Survey of Slovenia, Dimičeva 14, Ljubljana, Slovenia

Published online: 07 December 2011

and Chapman 1997; Beltrami 2002; Šafanda et al. 2004). The steady-state part of the subsurface temperature corresponds to the long-term annual mean of the ground surface temperature. The seasonal and inter-annual surface temperature variations propagate downward and disappear at the depth of 15–25 m. In case of a climatic change, however, the long-term annual mean of the surface temperature changes and this transient signal propagates much deeper—to hundreds of meters for the centennial and millennial climatic changes and to first kilometers for the glacial—interglacial cycles. By solving the inverse problem, the history of the ground surface temperature (GST) variations can be reconstructed from this transient component obtained by a precise temperature logging and by removing the steady-state part of the temperature-depth profile. For the climatic interpretation of the reconstructed ground surface temperature history, it is necessary to know how the long-term difference between the mean annual ground and surface air temperatures (SAT) behaves. The extent to which the SAT change will be reflected in the GST change depends especially on the albedo of the ground, intensity of solar radiation and magnitude of the ground isolation that can be formed for instance by a vegetation or snow cover (Lewis and Wang 1992; Majorowicz and Skinner 1997a, b; Smerdon et al. 2003; Majorowicz and Safanda 2005). Transfer of heat from the surface into the ground (soil) and into the bedrock takes place mainly by the heat conduction. In winter, when air temperatures decrease below zero, the latent heat released or consumed during phase changes of water within the active layer can influence appreciably the heat transfer (Beltrami and Kellman 2003; Smerdon et al. 2003; Woodbury et al. 2009) leading to a certain decoupling between SAT and GST. Beside the natural causes, the activities of people have been involving more and more in forming the Earth's surface. Human impact is either passive, when human activity changes the albedo or isolation of the Earth's surface, thereby altering the SAT–GST relation, or active, when heat is supplied into or extracted from the ground with the use of geothermal (ground source) heat pumps, for example. Humans began to radically alter temperature relations on the earth surface with the arrival of agriculture, when they started to deforest landscape and cultivate soil. Extensive deforestation of landscape and/or conversion into the arable land that took place in the past and continue in many regions of the world today, altered completely SAT–GST relations in that areas (Majorowicz and Skinner 1997a, 1997b; Nitoiu and Beltrami 2005; Bense and Beltrami 2007). Another substantial change has been brought by urbanization. Urban agglomerations, apart from extensive paved surfaces with a low albedo (asphalt, concrete) that absorb sunshine, bring also an active energy exchange due to heated or cooled buildings. As a contribution to better understanding of this complex problem we report here on detection and quantification of the simultaneous impact of local anthropogenic structures and regional climatic changes on the subsurface temperature field at two sites in the Central Europe, in Czechia and Slovenia. The similar topics have been recently addressed for instance by Ferguson and Woodbury (2004, 2007), who reported on temperatures measured in shallow boreholes inside the city of Winnipeg, which were several degrees higher than temperatures measured at the same time in agricultural areas in the immediate vicinity of the city or by Taniguchi et al. (2005, 2007) and Huang et al. (2009), who described the impact of urbanization on subsurface temperature field inside and around several big Asian cities.

2 Data set

The first studied locality is situated on the premises of the Institute of Geophysics in Prague (50°02.5′N, 14°28.7′E, 275 m a.s.l.) with a subdued topography. Two boreholes were drilled here to the depths of 150 m and 40 m in 1992, which passed through a 4 m thick

layer of embankment underlain by weathered and gradually compact shale of Ordovician age. The bedding of the shale is inclined from horizontal direction towards north under the average angle of 60°. Thermal conductivity measured in a great detail along the entire length of the deeper borehole (GFÚ-1) displays strong anisotropy with mean value of 3.2 W/mK along the bedding and 2.2 W/mK perpendicular to it (Šafanda 1994). The shallower borehole (GFU-2) was fitted with a chain of thermistors placed in a narrow plastic tube plugged at the bottom and filled with oil. The space between the tube and the borehole's wall was "gritted". Continuous measurements of subsurface temperatures have been taking place here since 1994, together with surface air temperature monitoring in the height of 0.05 m and 2 m above the surface. Thermistors are fitted in pairs, so that an error in the case of a drift of some of the sensors is minimized. Two sixteen year long time—temperature series registered by this monitoring system at the depths of 20 m and 38.3 m (the deepest point of the thermistor chain) are depicted in Fig. 1. They document subsurface warming, the rate of which decreases with depth. The series measured at 20 m is still modulated by the annual waves of the ground surface temperature. The deeper borehole GFU-1, 15 cm in diameter, has been logged repeatedly within inserted plastic tube of 5 cm diameter. The groundwater level varying around the depth of 7 m is the same within and outside the tube. The temperature logging is done usually once a year by calibrated probes in a step-by-step regime with a depth increment between 2 m and 5 m. The logging tools had a resolution of 1–3 mK and an absolute accuracy of several hundredths °C (Wilhelm et al. 2004). The repeated logs in the borehole GFÚ-1 (Fig. 2) clearly indicate a downward propagating warming, the rate of which agrees with values observed at the corresponding depths by the continuous monitoring in the shallower borehole GFU-2.

The second studied locality is the borehole Še-1 in Šempeter (45°55.28′N, 13°37.95′E, 68 m a.s.l) located in the southwestern part of Slovenia in a flat terrain of an industrial zone. The borehole is 1,541 m deep, was drilled in 1994 and encountered in the upper 90 m Quaternary sediments (alternation of sandy and clayey layers) which are followed by fine grained sedimentary rocks (marly shales, silty marls, siltstones, sandstones) of mostly Middle Eocene age with approximately horizontal position of bedding along its entire length. The thermal conductivity was measured only in lower part of the borehole and the mean value from several samples in section 500–1,000 m was 2.4 W/mK along the bedding and 1.9 W/mK perpendicular to it. The borehole was logged in 2003 and then repeatedly in

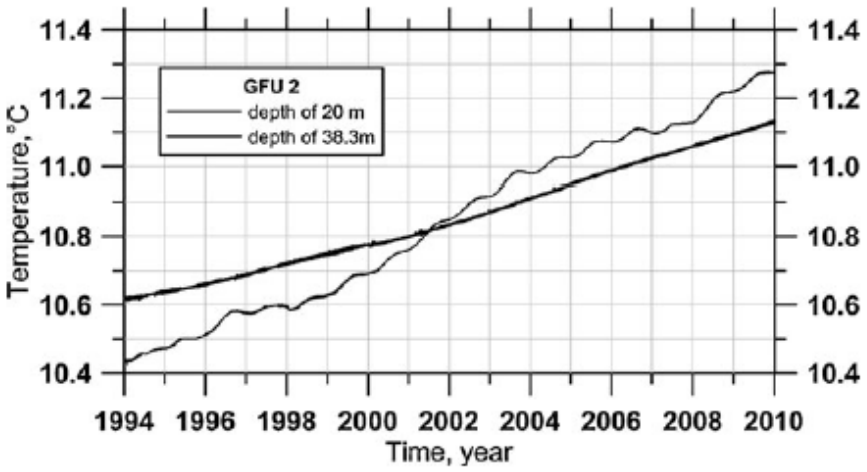

Fig. 1 Sixteen years' time series of continuous temperature monitoring at two different depths of the borehole GFU-2 in Prague, Czechia

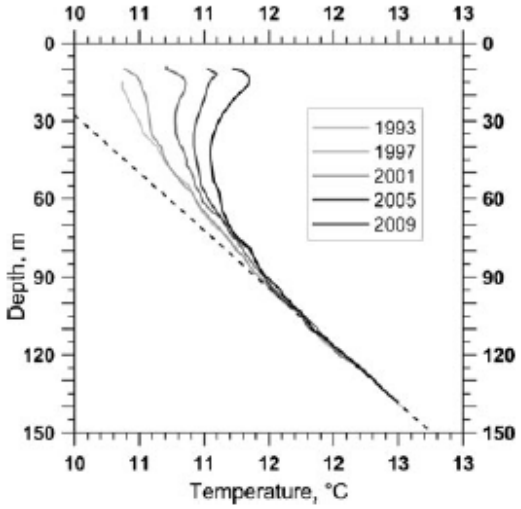

Fig. 2 Temperature logs in the borehole GFU-1,Prague, measured between the years 1993 and 2009

2005, 2006 and 2008 by the same logging tool and technique as in the case of the borehole GFU-1 mentioned above. The temperature—depth profiles observed at the depth section 35–150 m, well below the depth of penetration of the ground temperature annual wave, are shown in Fig. 3. The borehole is cased and filled by groundwater, the level of which varies in the depth interval 13–16 m. The temperature logs display a U-shape with a minimum at the depth of 65–70 m migrating downwards at the rate of about 1 m per year, and a gradual warming at the rate of 0.01–0.02 K per year.

An important source of data for the mathematical modeling of thermal effects of the anthropogenic changes, were the mean annual ground temperatures under different types of surface. They were measured at the observational polygon located about 150 m from the boreholes in Prague, also on the grounds of the Institute of Geophysics. Here, the continuous monitoring of soil temperatures under various types of surface (grass, sand, bare soil and asphalt)

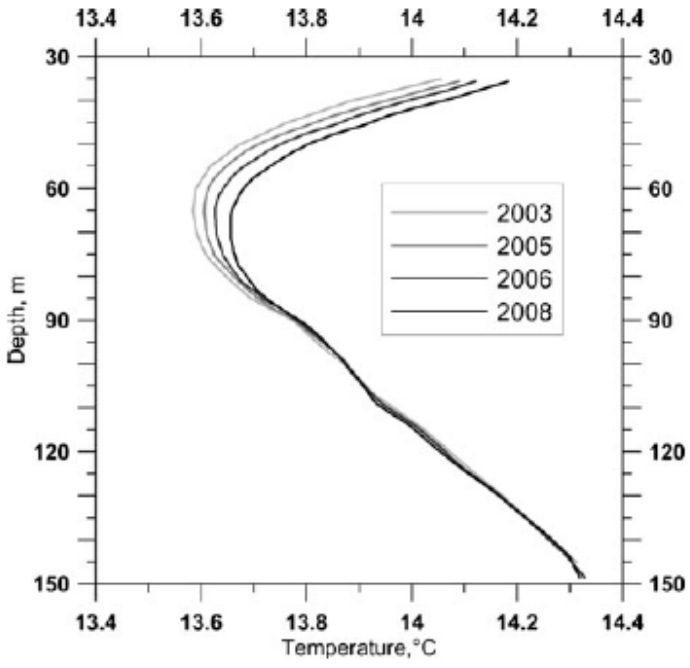

Fig. 3 Temperature logs in the borehole Še-1, Slovenia, measured in the years 2003, 2005, 2006 and 2008 (*from left to right*) at the depth section 40 m–150 m

together with air temperature and other meteorological elements has been running since 2003. Temperatures are measured by calibrated platinum sensors Pt-1000 in five-minute intervals at the depths of 2, 5, 10, 20 and 50 cm. The monitoring indicates that, in the period 2003–2008, the difference between the mean annual temperature of the ground at the depth of 2 cm and the air temperature at 5 cm varied in the range 0.2–0.8°C for grass, 1.5–2°C for sand and bare soil and 4–5°C for asphalt (Dědeček et al. 2010). Inter-annual variation of the difference for the individual types of surface in the given period of 6 years is affected mostly by the number of sunny hours in summer months and to a certain degree by snow cover in winter.

3 Results of modeling

The mathematical modeling of thermal effects of the anthropogenic changes in surroundings of the boreholes and of the regional climatic changes on subsurface temperature field has been done using software packages FRACTURE (Kohl and Hopkirk 1995) and commercial code COMSOL Multiphysics. Three-dimensional time-variable geothermal models (cube, length of the sides 1,000 m) of the boreholes' sites were compiled with the aim to distinguish in the observed transient component of the temperature logs the part caused by construction of new buildings and other anthropogenic structures in surroundings of the boreholes, and the part generated by the ground surface temperature warming due to the surface air temperature rise. The 3D models of the two studied localities were composed taking into account the substantial anisotropy of thermal conductivity of rocks. The role of convective transfer of heat in the flat or subdued topography around the boreholes was assumed to be negligible and was not considered (Smerdon et al. 2003).

The zero heat flow was used as the low boundary condition at the depth of 1,000 m (Smerdon and Stieglitz 2006). The boundary condition of the zero heat flow together with zero heat sources within the model imply that all modeled variations of the subsurface temperature are caused by the spatial and temporal changes of the ground surface temperature, which was the upper boundary condition of the models. Because the surroundings of the boreholes can be approximated by a horizontal plain, the spatial variations of the ground surface temperature are given by a pattern of the different types of surface (grass, asphalt, sand, buildings,..). With the exception of buildings, under which a constant temperature was assumed, the ground surface temperature was subjected to the temporal variations consistent with variations of the mean annual air temperatures observed at the nearby meteorological stations. To estimate mean annual temperatures of the individual surfaces, results of the aforementioned long-term monitoring of the soil temperatures were used. Because at the beginning of the 20th century the boreholes' surroundings were grassy areas without buildings, the average air temperature of the period 1851–1900 observed at meteorological stations in Prague and Ljubljana (Fig. 4) was used as the initial temperature of the model. The temporal development of the model started therefore in the year 1900. The time series of the mean annual air temperatures recorded at meteorological stations in Prague (Klementinum) and Ljubljana (Fig. 4) display a similar pattern with significant warming in the last 50 years (the average warming rate of 0.04°C per year in both of cases). Mean temperature in the second half of the 19th century was 9.02°C in Prague and 9.07°C in Ljubljana.

3.1 Borehole GFU-2 in Prague

First we tried to model the temperature—time series observed in the borehole GFU-2 in Prague at the depth of 38.3 m in the period 1994–2008 (Fig. 1) as a pure response of the

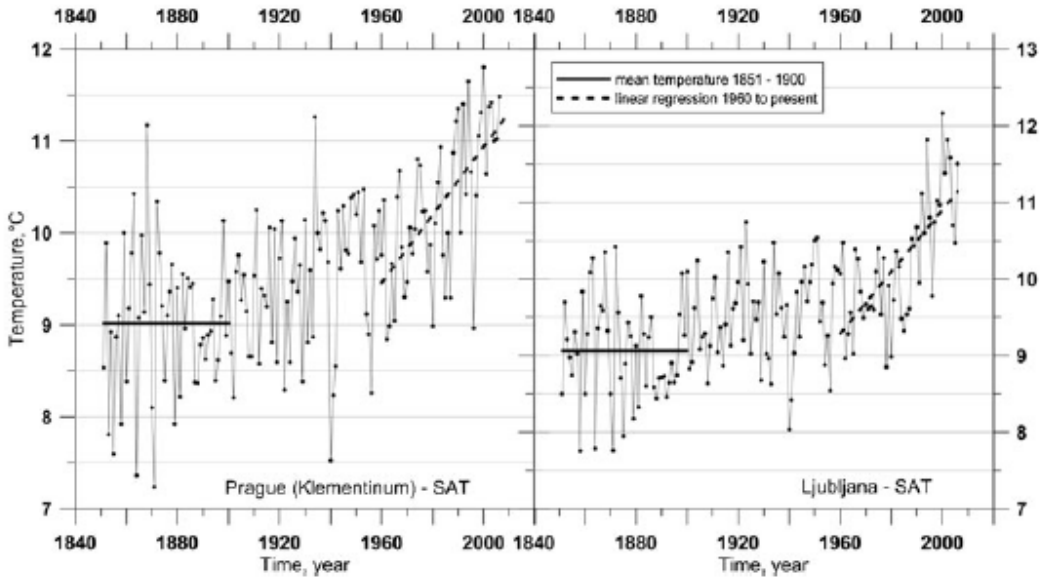

Fig. 4 Mean annual surface air temperatures (SAT) recorded at meteorological stations in Prague (Klementinum), Czechia and in Ljubljana, Slovenia

subsurface temperatures to the air temperature warming trend observed at the meteorological station Prague (Klementinum), about 7 km away from the borehole. When we used the air temperature variations as the surface boundary condition in transient solution of the heat conduction equation in the geothermal model of the site, we obtained for the depth 38.3 m and the period 1994–2008 the time—temperature series shown in Fig. 5. The warming pattern depicted in Fig. 5 can be divided into three time periods. The average increase of temperature was 0.020°C per year in 1994–1998, then (especially due to the very cold year 1996) it was 0.010°C per year in 1999–2001 and finally again 0.021°C per year in the third period 2002–2008. The average warming rate of the whole explored period 1994–2008 was 0.017°C.

Comparing the calculated warming rate (Fig. 5) yielded by the SAT variations (Fig. 4) with the rate of the observed curve (Fig. 6), we see appreciable differences.

Namely, the mean annual warming rate for the whole period of observation is 0.034°C per year instead of the calculated rate of 0.017°C per year. However, it is obvious from Fig. 6 that also the observed temperature increase varies in time and that the curve can be

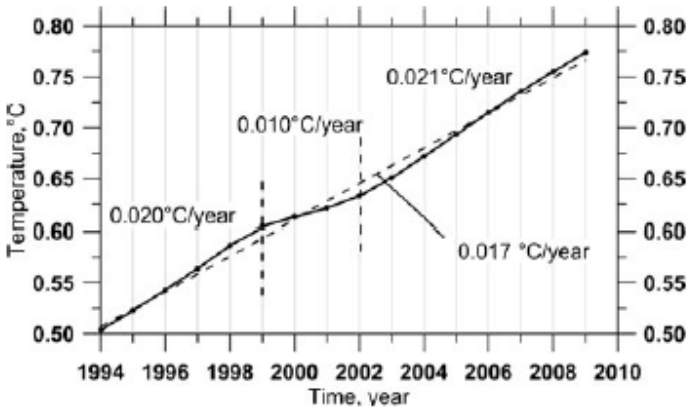

Fig. 5 Time—temperature variations at 38.3 m of the GFU-2 borehole calculated as a subsurface temperature response to the surface air temperature variations only. The warming trend of the whole period 1994–2008 is 0.017°C per year

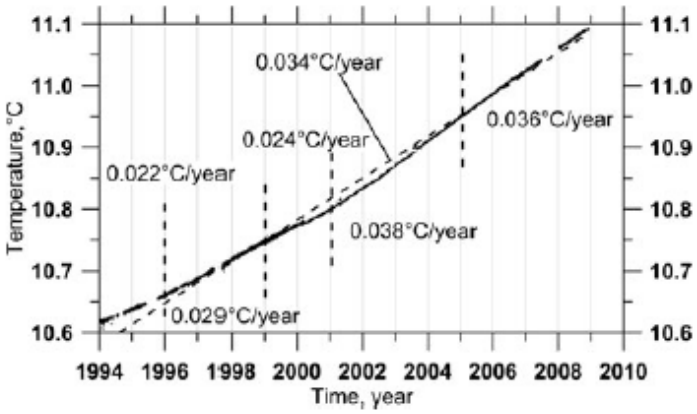

Fig. 6 The observed time—temperature series at 38.3 m in the GFU-2 borehole divided into periods of approximately constant warming rate. The warming trend of the whole observational period 1994–2008 is 0.034°C per year

divided into several time intervals with respect to the warming trend. The measured temperature increase amounts to 0.022°C/year in 1994–1995, to 0.029°C/year in 1996–1999, to 0.024°C/year in 1999–2000, to 0.038°C/year in 2001–2004 and to 0.036°C/year after the year 2004.

As stated above, the average rate of warming in the borehole GFU-2 during the entire observational period is two times larger than the calculated warming rate caused by warming trend of the SAT. In searching for sources of this discrepancy we explored the effects of anthropogenic structures in the immediate surroundings of the borehole. Figure 7 shows configuration of these structures and the boreholes. There are asphalt surfaces, a house with the ground plan of 20 m×20 m and a red clay playing field (a tennis court). The rest of the area is covered mostly by grass. The asphalt surfaces and the playing field were built at the turn of 1950s into 1960s, the house was constructed in and has been used since 1993.

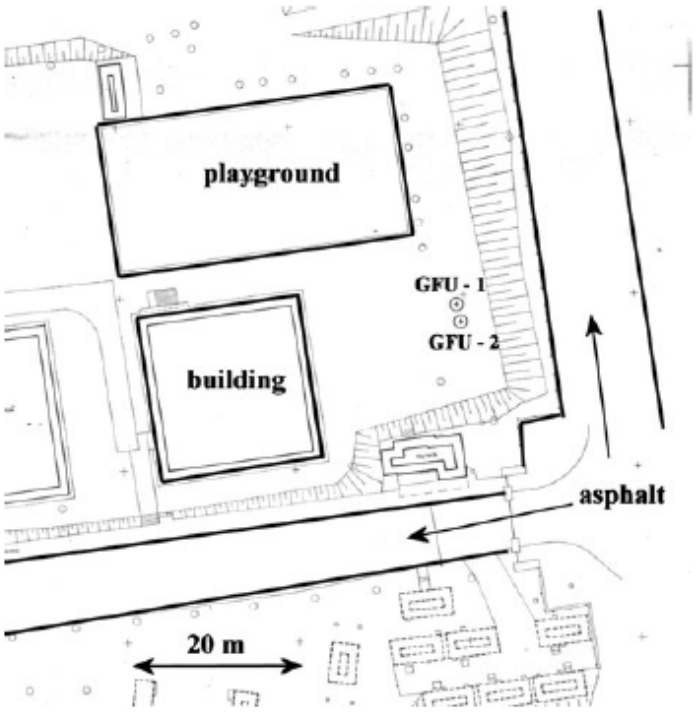

Fig. 7 Block plan of the immediate surroundings of borehole GFU-2 in Prague—Spořilov

The effects of the surface anthropogenic structures on the subsurface temperature field were evaluated by considering different offsets between the mean annual temperature of the ground and the air according to the type of the surface, based on the results of the aforementioned long-term monitoring of the soil temperatures. The offset for the playground was assumed similar to that observed for sand, 1–2°C and the offset for asphalt was taken in accord with observations as 3–4°C. Zero offset was considered for the prevailing grassy surface (see the text below). First, we evaluated the effect of the structures constructed at the turn of 1950s into 1960s, i.e. the playground and the asphalt surfaces and then separately the effect of the house built in 1993. The resulting time-temperature variations, calculated for the point of observation at the depth of 38.3 m in borehole GFU-2, are depicted in Fig. 8a (the playground and the asphalt surfaces) and Fig. 8b (the house). They show the pure effect of the structures' construction, because the ground surface temperatures were kept constant in time. It is obvious that the surface structures have an essential impact, albeit varying in time, on the measured warming in the borehole. It can be seen from Fig. 8a that dynamics of the subsurface temperature response to the construction of the playground and asphalt areas has diminished appreciably after 1980–90, still before the beginning of the monitoring. On the contrary, the temperature signal of the house built

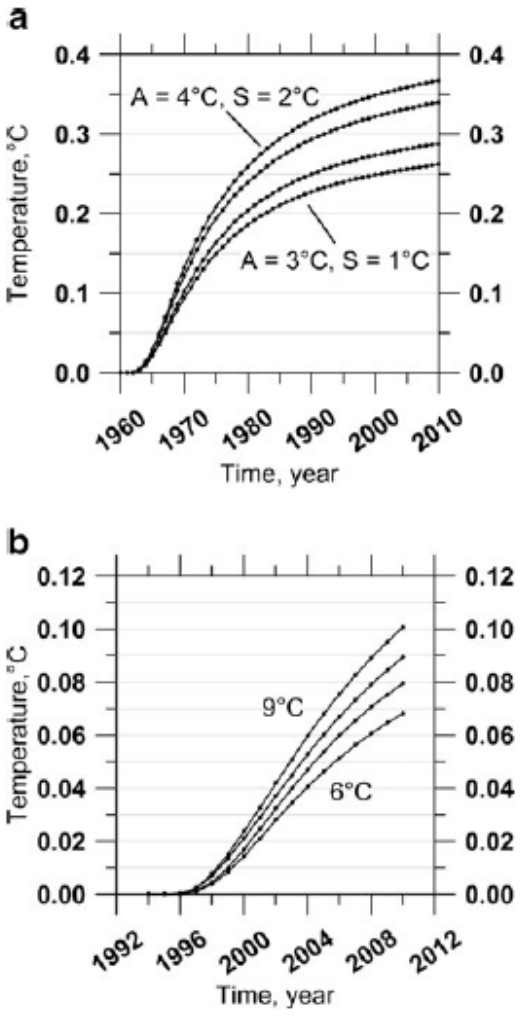

Fig. 8 Time—temperature changes in borehole GFU-2 at the depth of 38.3 m calculated as a response of the subsurface temperature to construction of the anthropogenic structures in surroundings of the borehole; **a** effect of asphalt (A) and sandy (S) areas with different combinations of the ground surface temperature offset with respect to the grassy surface. The magnitude of the warming increases with increasing offset from (A=3°C, S=1°C) via (A=3°C, S=2°C), (A=4°C, S=1°C) to (A=4°C, S=2°C), **b** effect of the warmer ground below the house with respect to the grassy surrounding for offsets 6°C, 7°C, 8°C and 9°C

20 m apart from the borehole in 1993 reached the observational point after the year 1996 only and its warming rate culminated in the period 1999–2004. It means that the effect of the anthropogenic structures on the observed warming rate in borehole GFU-2 was minimal in the beginning of the observations. It corresponds well with the fact that the observed warming (Fig. 6) is only by 0.003°C higher than the modeled effect of the air temperature rise in the first years of the monitoring (Fig. 5). On the other side, the period of the largest warming caused by the house, 1999–2004, overlaps partially with the period of the minimum warming generated by the air temperature rise due to the very cold year 1996. That is why the effect of the house is clearly visible in the observed data after the year 2001 only (Fig. 6).

The calculated time-temperature variation due to SAT (Fig. 5) indicates only moderate warming rate of 0.021°C per year after 2001, the transient effect of the house construction should diminish gradually and the effect of the hard anthropogenic surfaces (asphalt, playground) should be minimal after 2004 (Fig. 8a,b). Calculations based on the model taking into account the SAT variations, the temperatures of asphalt and playground higher than grass by 4°C and 1.5°C, respectively, and the constant temperature of 20°C at the base of the house, yielded warming rate of 0.030°C per year in the period 2005–2008. It is substantially less than the observed warming rate of 0.036°C per year (Fig. 6).

In search for explanation of this disagreement we explored the possibility that the offset between the mean annual GST and the mean annual SAT has changed during the monitoring. Usually it is assumed that this ground—air coupling is constant on the time scale of decades and longer, but can vary on the inter-annual scale depending on variations of meteorological factors like thickness and duration of snow cover, precipitation, solar irradiation etc. From all the parameters recorded on the nearest meteorological station Prague—Karlov, about 5 km away from the borehole, only the annual sum of the sunny hours revealed a systematic trend since the beginning of 1990s. This can be seen from Fig. 9, which shows departures of annual, "summer" (Apr—Sep) and "winter" (Jan-Mar plus Oct-Dec) sums of sunny hours from their 1961—1990 averages observed on this station. A closer look at this trend shows that the higher annual sums observed in the period 2002—2007 have a source mostly in higher number of sunny hours in the warmer or "summer" half of the year, which is decisive for a magnitude of the solar irradiance effect on the SAT—GST difference. As a matter of fact, the short day and the low position of the sun above the horizon together with the large cloudiness make the effect of winter solar irradiance on the SAT—GST difference practically negligible in comparison with the situation in summer in the Central Europe (50 °N). As mentioned earlier, the difference between the mean annual temperature of asphalt and air during 6 years of the soil—air temperature monitoring on premises of the Institute of Geophysics in Prague fluctuated between 4 and 5°C. The maximum difference, almost 5°C, was observed in the year 2003, which was also the year of the highest "summer" sum of the sunny hours. Therefore it seems reasonable to assume that the difference of mean annual ground and air surface temperatures is sensitive, at least for surfaces with a low albedo, on the sum of the "summer" sunny hours. This assumption was taken into consideration in the final model, where the difference between asphalt and air was set on 3.5°C prior the year 2002 and to 4.5°C since 2002. In the case of the playing field it was 1°C, increased by 0.5°C since 2002. The mean annual temperature of grass was equal to that of air. The resulting time-temperature series is shown in Fig. 10. The resulting curve can be divided into several time periods according to the warming rate again. Now, the warming pattern agrees fairly well with the observed one: 0.023°C/year in 1994–1995, 0.029°C/year in 1996–1998, 0.024°C/year in 1999–2001 and 0.036°C/year after the year 2001. It is remarkable how well the final model

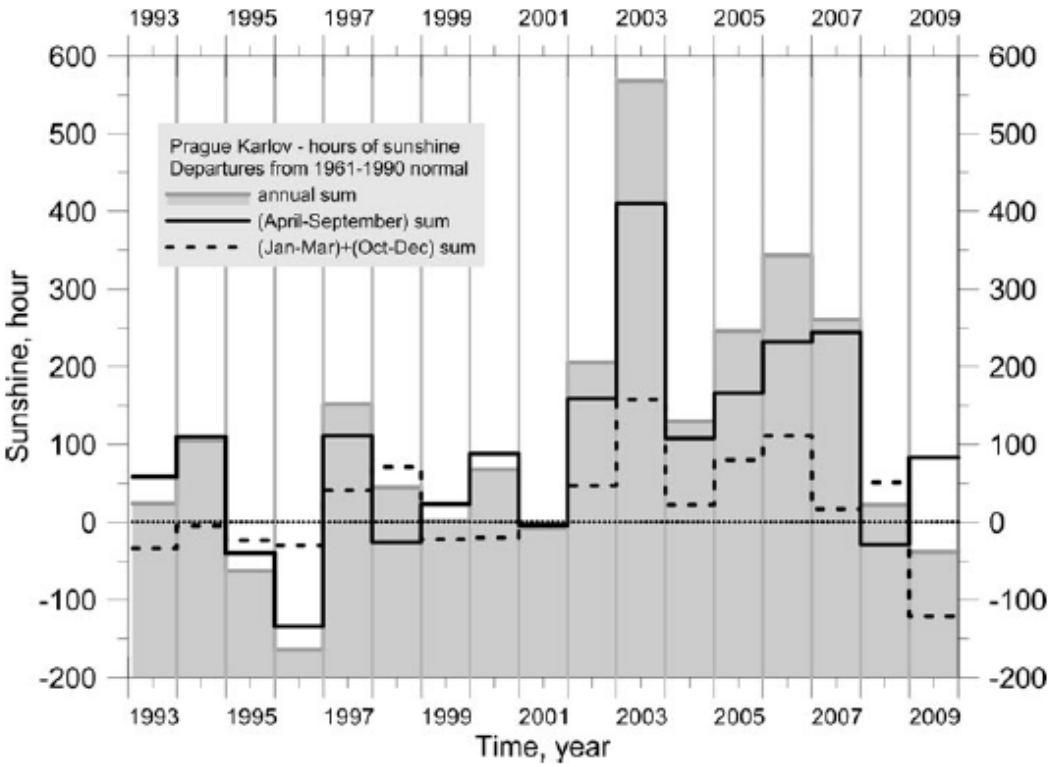

Fig. 9 Departures of annual, "summer" (Apr–Sep) and "winter" (Jan-Mar and Oct-Dec) sums of sunny hours from their 1961–1990 averages (amounting to 1631, 1187 and 444 h, respectively) observed on meteorological station Prague-Karlov in the period 1993–2009

reproduces not only the rate of warming, but also the absolute level of the subsurface temperatures. After adding 0.77°C to the temperature calculated for the depth of 38.3 m, which corresponds to the undisturbed gradient of 20°C/km observed in the lower part of borehole GFU-1, the temperature differs from the observed one by 0.18°C only (10.91°C instead of

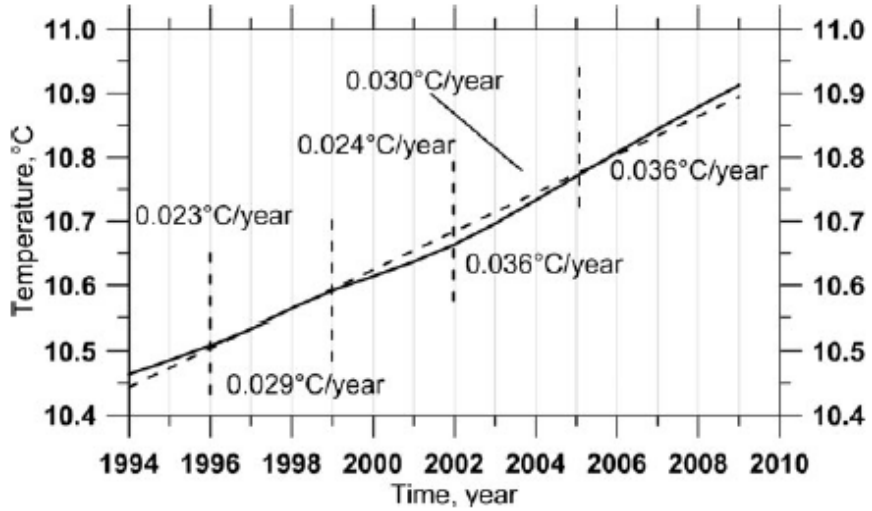

Fig. 10 Time—temperature variations at 38.3 m in the GFU-2 borehole calculated by the final model as a subsurface temperature response to the surface air temperature variations together with the effect of the anthropogenic structures

11.09°C) at the end of 2008. As mentioned above, the difference between the mean annual ground temperature under grass and the mean annual temperature of air was 0.2–1.2°C during the 6-year monitoring period. The resulting difference of 0.18°C is therefore at the lower margin of this interval. The reason for this may lie in full-grown trees situated in the surroundings of the borehole.

3.2 Borehole Še-1 in Šempeter

The aim of the mathematical modeling in Šempeter was to fit the transient component of the repeated temperature logs of the borehole Še-1 (Fig. 3). The borehole Še-1 is located in the industrial zone of the town Šempeter. A large sporting hall is situated in the borehole's close vicinity with adjacent asphalt areas, a small playing field and also industrial halls and asphalt roads further away (see Fig. 11). The whole agglomeration was built during the second half of 1970s. The site of the borehole is warmer than in Prague, the long-term ground surface temperature extrapolated from the temperature logs is nearly 13°C compared to 9.5°C in Prague. The long-term mean of the annual sum of the sunny hours at the near meteorological station Bilje is around 2000 (Mesečni bilten ARSO 2009), which is by 370 h more than in Prague. As mentioned above, the upper 90 m of the borehole passes through unconsolidated Quaternary sediments characterized by alternating sandy and clayey layers with different thermal properties. Whereas samples of these Quaternary sediments were not available, we estimated (see Table 1) values of thermal conductivity and thermal diffusivity of the individual layers using our laboratory measurements on similar rock types, and published data (Abu-Hamdeh and Reeder 2000; Chen 2008). Effect of this fine layered structure on transient temperature is substantial. When the structure is approximated by a homogeneous model of the same thermal resistance, the resulting transient profile differs slightly. This is demonstrated in Fig. 12 which shows downward

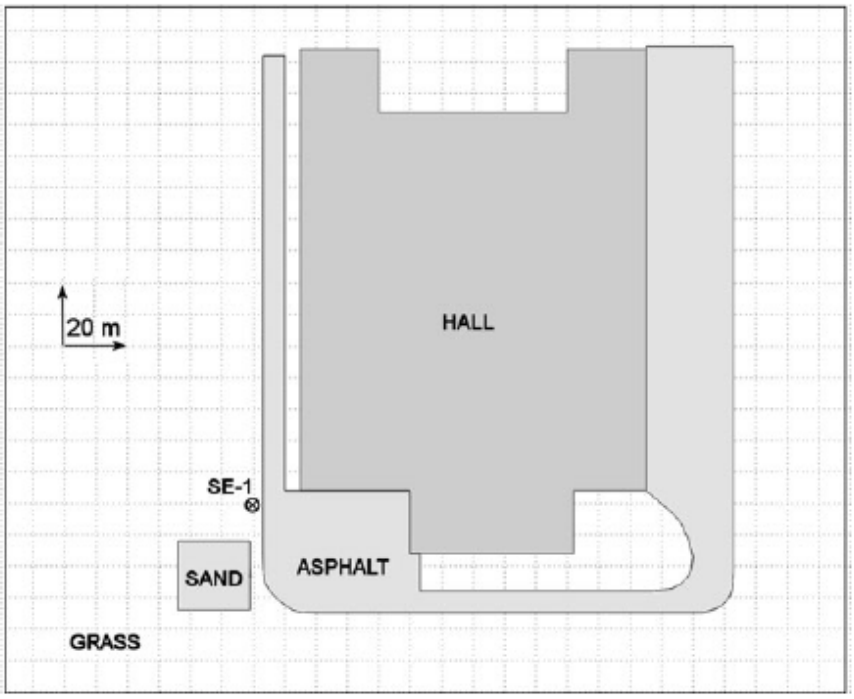

Fig. 11 Block plan of surroundings of the borehole Še-1

Table 1 Estimated values of thermal properties (*TC* thermal conductivity, *TD* thermal diffusivity) in the upper part of the borehole Še-1

Depth (m)	Type of sediment	TC (W/mK)	TD (m^2s^{-1})
0–6	dry clayey sand	1	4.6E-07
6–29.5	gravel with sand	2.2	1.0E-06
29.5–35.3	clay	1.2	5.6E-07
35.3–38.7	gravel with sand	2.2	1.0E-06
38.7–43.2	clay	1.2	5.6E-07
43.2–45.2	sand	2.2	1.0E-06
45.2–51	clay	1.2	5.6E-07
51–54	gravel with sand	2.2	1.0E-06
54–56.7	clay	1.2	5.6E-07
56.7–71.3	clayey sand	1.7	7.9E-07
71.3–75.2	clay	1.2	5.6E-07
75.2–90	clayey gravel	1.7	7.9E-07
90+	Eocene layers	2.2	1.0E-06

propagation of SAT changes simulated by the transient layered model and the transient homogeneous model. Figure 12 depicts also the difference of the two profiles. It amounts to several tenths of degree in the uppermost 20 m of the borehole, but stays within 0.05°C below this depth. Because it is difficult to discriminate which of the two models fits better the observed data—in the upper 20 m the temperature is strongly influenced by seasonal variations not considered in the simulations, and below 20 m the differences are rapidly diminishing with depth to the noise level—the layered, more realistic model was used in simulating the effect of the anthropogenic structures in 3-D models.

The individual effects of the regional climatic and local anthropogenic forcing together with their composite effect on the subsurface temperature field in the borehole Še-1 are

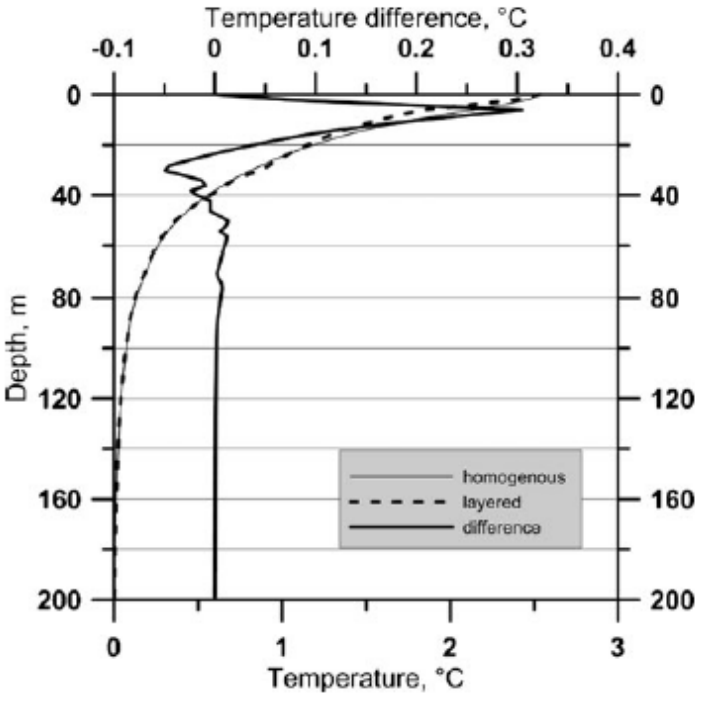

Fig. 12 Synthetic transient temperature—depth profiles in the borehole Še-1 calculated as a response to climate change by layered and homogeneous transient geothermal models of the same thermal resistance. Also shown is the difference of the profiles (upper abscissa)

shown in Fig. 13 in a form of transient components of the temperature—depth profiles. They are compared with the observed transient component. All profiles are related to the year 2008. Variations of the mean annual SAT series observed at meteorological station Ljubljana were used as the climatic forcing. The offsets chosen for the ground surface temperatures of the individual types of surface were similar to that in Prague, 3.5°C for asphalt and 1.5°C for the playground. Temperature below the sporting hall was considered between 15°C through 20°C in the individual versions. The best fit to the observed profile was achieved for 17°C. The lower temperature of 17°C accords with a character of the building there, which is a sports hall heated usually to a lower temperature than an office building like that in Prague.

The transient component of both the observed and the simulated temperature logs was obtained by subtracting from the profile its linear part fitted to the depth section 150–400 m, where the transient component is negligible in comparison with the uppermost 100 m of the borehole.

The warming effect of the anthropogenic structures is about 30% of the total warming at the depth of 50 m and becomes negligible below 100 m. The impact of climatic signal attenuates slower with depth than the anthropogenic one and becomes smaller than one hundredth of degree below 160 m. The sum of the two signals approximates fairly well the observed transient component of the Še-1 temperature logs.

4 Conclusions

The study has shown that the present subsurface temperature field observed and monitored at two localities in the Central Europe is strongly influenced both by the recent regional climatic changes and by thermal effects of local anthropogenic structures. It was possible, by means of the 3D mathematical simulations in transient geothermal models, to separate the transient signals of the two sources and to show that they are of a similar magnitude at the studied sites.

A precise quantitative evaluation of contributions of individual anthropogenic structures is definitely a complex problem. Nevertheless, due to the availability of the data obtained by 6 year monitoring of the ground-air temperature coupling for different types of surface,

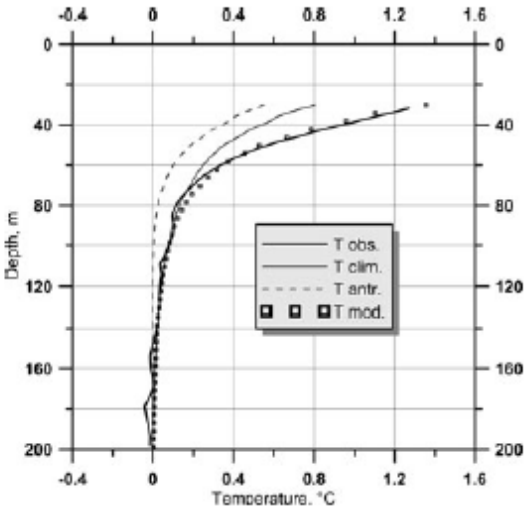

Fig. 13 Transient components of the temperature—depth profiles in the borehole Še-1 in 2008 generated (i) by the individual effects of the regional climatic (T_{clim}) and local anthropogenic (T_{antr}) forcings and (ii) by their composite effect (T_{mod}) compared with the observed transient component (T_{obs})

we were able to estimate the magnitude of the mean annual ground-air differences in surroundings of the boreholes and to use them in the simulations. The situation is complicated by the inter-annual variations of these differences, which depend on varying intensity of solar irradiance, height and duration of snow cover and other meteorological factors. This introduces another source of uncertainty into the simulations. Considering the temperature effects of the long-term trend in the solar irradiance turned out to be important in reproducing the observed temperature-time series in Prague.

The results of the study indicate that the factor of "thermal pollution" due to local anthropogenic effects in precise temperature logs must be taken into account seriously both in the terrestrial heat flow studies and in the ground surface temperature history reconstructions. Especially for the climatic studies based on the temperature logs, selection of boreholes or borehole sites should always consider this possible problem.

Acknowledgements This study was supported by the Czech Science Foundation (projects TOP/08/E014 and P210/11/0183) and also by institutional research programs Z3012916 and K3046108.

References

Abu-Hamdeh NH, Reeder RC (2000) Soil thermal conductivity: effects of density, moisture, salt concentration, and organic matter. Soil Sci Soc Am J 64:1285–1290

Beltrami H (2002) Climate from borehole data: energy fluxes and temperatures since 1500. Geophys Res Lett 29(23)

Beltrami H, Kellman L (2003) An examination of short- and long-term air-ground temperature coupling. Global Planet Change 38(3–4):291–303

Bense V, Beltrami H (2007) Impact of horizontal groundwater flow and localized deforestation on the development of shallow temperature anomalies. J Geophys Res 112:F04015. doi:10.1029/2006JF000703

Chen SX (2008) Thermal conductivity of sands. Heat Mass Tran 44:1241–1246

Dědeček P, Šafanda J, Čermák V, Krešl M (2010) Air—ground temperature coupling—results of the seven year temperature monitoring under different types of surface. Geophys Res Abstracts Vol. 12, EGU2010-11852, 2010 EGU General Assembly

Ferguson G, Woodbury A (2004) Subsurface heat flow in an urban environment. J Geophys Res—Solid Earth 109(B2)

Ferguson G, Woodbury A (2007) Urban heat islands in the subsurface. Geophys Res Lett 34(23)

Harris RN, Chapman DS (1997) Borehole temperatures and a baseline for 20th-century global warming estimates. Science 275(5306)

Huang S, Taniguchi M, Yamano M, Wang C (2009) Detecting urbanization effects on surface and subsurface thermal environment—a case study of Osaka. Sci Total Environ 407:3142–3152

Kohl T, Hopkirk RJ (1995) "Fracture"—a simulation code for forced fluid flow and transport in fractured, porous rock. Geothermics 24(3):333–343

Lewis TJ, Wang K (1992) Influence of terrain on bedrock temperatures, Paleogr., Paleoclim.,Paleoecol. (Global and Planetary Change) 98:87–100

Majorowicz JA, Skinner WR (1997a) Potential causes of differences between ground and surface air temperature warming across different ecozones in Alberta. Canada Glob Plan Change 15:79–91

Majorowicz JA, Skinner WR (1997b) Anomalous ground surface warming vs. surface air warming in the Canadian Prairie provinces. Clim Change 37:485–500

Majorowicz J, Safanda J (2005) Measured versus simulated transients of temperature logs—a test of borehole climatology. J Geophys Eng 2(4):291–298

Mesečni bilten (Monthly Bulletin) Arso environmental agency of the republic of Slovenia (ARSO), Ministry for Environment and Spatial Planning, 2009, XVI(12), 31–45. Available: http://www.arso.gov.si/oagenciji/knjižnica/mesečni bilten/

Nitoiu D, Beltrami H (2005) Subsurface thermal effects of land use changes. J Geophys Res—Earth Surface 110(F1)

Pollack H, Hurter S, Johnson J (1993) Heat-flow from the earth's interior—analysis of the global data set. Rev Geophys 31(3):267–280

Smerdon JE, Pollack HN, Enz JW, Lewis MJ (2003) Conduction-dominated heat transport of the annual temperature signal in soil. J Geophys Res 108(B9):2431

Smerdon JE, Stieglitz M (2006) Simulating heat transport of harmonic temperature signals in the earth's shallow subsurface: lower-boundary sensitivities. Geophys Res Lett 13(4)

Šafanda J (1994) Effects of topography and climatic changes on the temperature in borehole GFU-1, Prague. Tectonophysics 239:187–197

Šafanda J, Szewczyk J, Majorowicz J (2004) Geothermal evidence of very low glacial temperatures on a rim of the Fennoscandian ice sheet. Geophys Res Lett 31(7)

Taniguchi M, Uemura T, Sakura Y (2005) Effects of urbanization and groundwater flow on subsurface temperature in three megacities in Japan. J Geophys Eng 2:320–325

Taniguchi M, Uemura T, Jago-on K (2007) Combined effects of urbanization and global warming on subsurface temperature in four Asian cities. Vadose Zone J 6(3):591–596. doi:10.2136/vzj2006.0094

Wilhelm H, Heidinger P, Šafanda J, Čermák V, Burkhard H, Popov Yu (2004) High resolution temperature measurements in the borehole Yaxcopoil-1, Mexico. Meteoritics Planet Sci 39:813–819

Woodbury AD, Bhuiyan AKMH, Hanesiak J, Akinremi OO (2009) Observations of northern latitude ground–surface and surface–air temperatures. Geophys Res Lett 36:L07703. doi:10.1029/2009GL037400

IOP Publishing Journal of Geophysics and Engineering
J. Geophys. Eng. **10** (2013) 025012 (9pp) doi:10.1088/1742-2132/10/2/025012

Six years of ground–air temperature tracking at Malence (Slovenia): thermal diffusivity from subsurface temperature data

Petr Dědeček[1,3], Dušan Rajver[2], Vladimír Čermák[1], Jan Šafanda[1] and Milan Krešl[1]

[1] Institute of Geophysics, Academy of Sciences of the Czech Republic, Praha, Czech Republic
[2] Geological Survey of Slovenia, Ljubljana, Slovenia

E-mail: pd@ig.cas.cz

Received 5 April 2012
Accepted for publication 10 December 2012
Published 22 March 2013
Online at stacks.iop.org/JGE/10/025012

Abstract
To understand the processes which govern the downward propagation of the surface temperature signal and to quantify the relationship between ground and air temperatures, a borehole climate observatory was established at Malence (Slovenia). A substantial (climate?) warming has been observed; surface air temperature from 2003 to 2009 has been increasing by a rate of more than 0.5 K/year. Temperature difference between ground and air temperatures revealed a typical annual course; during the winter months the ground is warmer than the air, in the summer the ground gets slightly colder, the mean yearly offset value amounting to 1.6 K. Here we report on the thermal diffusivity distribution which was determined for a near-surface 10 m deep section using a number of six-year-long temperature–time data series. The series of daily averaged temperatures were processed by spectral analysis. Thermal diffusivity was calculated from the amplitude and phase angle of annual waves corresponding to different subsurface layers using conduction theory as well as the conduction–convection approach. Both methods lead to the generally similar results and revealed a definite heterogeneity of the subsurface medium. The results proved that the annual scale convective heat transfer did not contribute significantly to the temperature–time variations monitored in the uppermost 10 m depth interval.

Keywords: ground–air temperature coupling, thermal diffusivity, conductive–convective heat transfer

(Some figures may appear in colour only in the online journal)

1. Introduction

The thermal diffusivity of rock is an important parameter that affects transient heat transfer within the Earth. Its knowledge is important for any time-dependent calculations of subsurface temperature changes in response to the ground surface temperature variations regardless of solving a direct problem (Sun and Zhang 2004, Dědeček *et al* 2012), or an inverse problem, notably in paleoclimatic studies (Lewis, 1992, Čermák *et al* 2010). Diffusivity can be assessed from laboratory measurements on collected rock samples by devices of various complexities using e.g. a popular flash method or varied techniques including the steps of periodically heating rock samples with a heat source modulated at an operating frequency. The main shortcomings of all laboratory techniques are (i) problems with the sample preparation, and (ii) the

[3] Author to whom any correspondence should be addressed.

need for expensive equipment requiring heat pulse generation, optical detection and high speed data acquisition, etc (Gróf 2002, and the references therein).

An alternative way to assess the thermal diffusivity of rocks is its determination from measured subsurface (soil) temperatures. Such measurements represent a common geothermal experiment which could provide a wide database for thermal diffusivity determinations in various geological environments. Thermal diffusivity of the subsurface layers depends on their composition and texture (e.g. porosity) as well as on the moisture content. The latter technique provides genuine *in-situ* diffusivity values against laboratory data corresponding to the pre-prepared (often machined) rock samples. Thermal diffusivity values obtained this way can be also directly used for geophysical modelling in various field case studies.

Malence Borehole Climate Observatory (MBCO) in Slovenia was built in 2003 to track the penetration of the surface air temperature (SAT) signal to the shallow subsurface by monitoring soil temperatures at several depth levels down to 10 m. During six years (2003–2009) of permanent activity, unique observational materials have accumulated which have provided a suitable database for such alternative thermal diffusivity assessment. The objective of this paper is to present the subsurface thermal diffusivity for different depth intervals by applying the conduction–convection approach as well as conduction theory alone, and to compare the obtained results. In contrast to similar reported studies done in this respect, usually based on considerably shorter data series (day-to-month length) and on a range of only 10 to 100 cm depth below the surface (Chacko and Renuka 2002, Demetrescu *et al* 2007, Gao *et al* 2009), we report results based of an approximately six-year-long data series covering a full 10 m depth section.

2. Data

In order to study the coupling between the air, soil and bedrock temperatures, the MBCO observatory was established at the borehole V-8/86 at Malence, SE Slovenia (45°52.1′N, 15°24.5′E, 152 m a.s.l.) in November 2003. The borehole is located on the alluvial plain of the Krka river on a rim of a meadow in the rural area of the Krško basin. The basin is filled with tertiary and quaternary sediments and belongs to the large Pannonian basin. The hole was drilled in October 1986 with a diameter of 90–120 mm through 16 m of quaternary clay, sand and gravel, down to the bottom at 100 m through Miocene marl strata, sandier in its upper part and more clayey in its deeper part. The groundwater level in the borehole was 2.5 m below the surface in 1987 and rose to approx. 1.5 m after 2003. During a nine-month period of continuous monitoring in 2006/2007, the groundwater level slightly varied between 1.5 and 1.6 m. It is possible that during high stands of the Krka river, the groundwater can be even closer to the surface. Actually, the site was flooded for several days in 2010. The borehole was cased with a zinc-coated steel tube 1.6 in of inner diameter. Thermal conductivity was measured on the only two available rock samples collected from two different depth sections, 1.7 $Wm^{-1} K^{-1}$ in 0.7 m depth and 1.45 $Wm^{-1} K^{-1}$ in

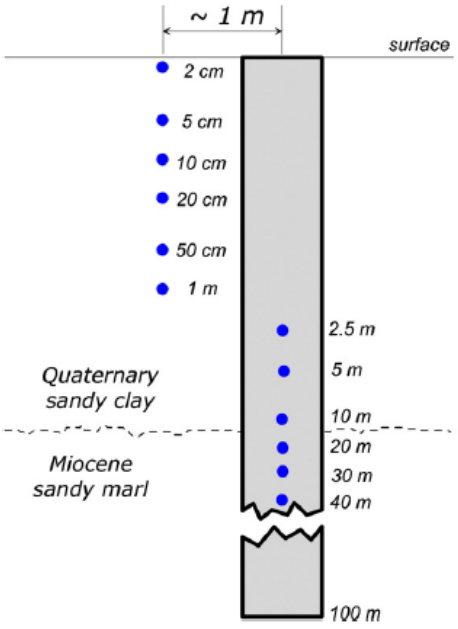

Figure 1. The arrangement of the monitoring experiment (not to scale).

99 m depth. Thermal diffusivity was estimated using typical density and specific heat values and fits into a typical range of 0.6–0.8 $\times$ 10^{-6} $m^2 s^{-1}$. The diffusivity can be even lower due to a high specific heat of the pore water; e.g. for 30% porosity the diffusivity could be as low as 0.4 $\times$ 10^{-6} $m^2 s^{-1}$ (Šafanda *et al* 2007).

As a part of the MBCO instrumentation a chain of platinum sensors (Pt1000, class A, sensitivity of first milliKelvins) for temperature monitoring was installed in 2003 and kept in the hole in the depth interval of 1 to 40 m for a permanent recording experiment (Rajver *et al* 2006). The data logger system (16 channels, 24 bits A/D converter, 16 bits resolution) records air temperatures at 2 m and 0.05 m above the ground level, soil temperatures at 0.02, 0.05, 0.1, 0.2, 0.5 and 1 m below the surface and bedrock temperatures in the borehole at the depths of 2.5, 5, 10, 20, 30 and 40 m. The soil temperature sensors were buried about 1 m beside the borehole (figure 1). All information was collected in preselected 30 min time intervals and for further interpretation the observed temperature data were averaged to furnish series of daily means. The experiment started on 13 November 2003, and is still running; data used in this report cover the period 13 November 2003–1 August 2009.

3. Monitoring results

On long time scales, the land–atmosphere interface is in energy equilibrium, and temperatures measured in each medium reflect this energy balance. The monitoring results of the ground–air temperature coupling may thus provide an important piece of knowledge to understand the complicated energy exchange mechanisms on this interface. Surface and

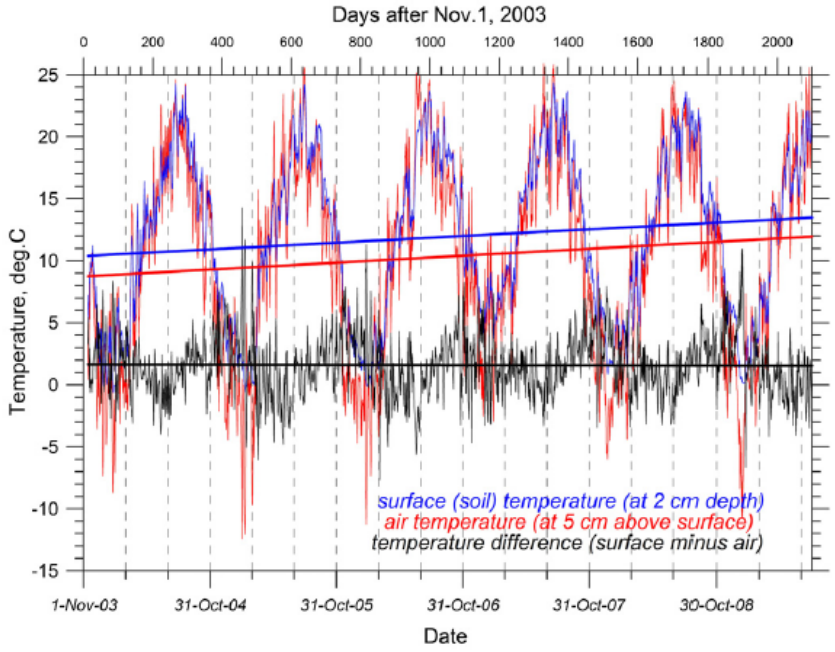

Figure 2. Monitoring records of air temperature at 5 cm height and soil temperature at 2 cm depth together with their difference demonstrating the surface temperature offset.

near-surface ground temperatures in part smooth down the air temperature extremes. The ground surface quality and properties (e.g. absorption, reflectance, colour, humidity) and primarily the existing microvegetation cover play the governing role in the heat transfer across this boundary. The time-varying thermal properties of the surface rocks or seasonal vegetation changes surely do not make the solution of the problem easier. The problem was studied in detail by e.g. Bartlett *et al* (2006), who referred to a number of other authors who investigated the heat transfer mechanisms at the land–atmosphere boundary layer, either using computer models simulating the physics at the interface or those that benefited from the practical observational studies in various land areas (see the many references in Bartlett *et al* 2006). The authors presented their own results from the geothermal observatory at Emigrant Pass (Utah) based on the decade-long monitoring series of the difference of surface ground and air temperatures at 2 m height and reported a persistent 2.47 K offset as ground warming resulting from the incident solar radiation. The offset is largest in the summer (up to 5 K) and falls to nearly 0 K in the winter, the filtered data indicating the inter-annual variability of about 1 K.

Monitoring data from another geothermal observatory at Caravelinha (Portugal), built to a very similar design as the MBCO, validated that soil is substantially warmer than air for most days of the year (by up to 11 K) and slightly colder (by up to 3 K) in short periods during the winter, the four-year mean (2007–2010) amounting to 2.36 K (Šafanda *et al* 2007). The 18-year-long monitoring series obtained from the Sporilov observatory (Czech Republic) provided a small mean ground–air temperature offset of only 0.27 K with no clear annual course and the offset value changing irregularly even on a day and night scale (paper in preparation).

Temperature conditions existing on the ground surface of the MBCO observatory are shown in figure 2, presented as the difference between the soil temperature at 2 cm depth minus the air temperature at 5 cm above the surface. Both records, confirming a substantial warming rate of more than 0.5 K/year during the observational six-year period, nicely track each other with a practically constant difference of ∼1.6 K. Regardless of this constancy, the difference reveals a typical annual course. The ground was generally warmer by up to 5–7 K during the winter months (DJF), but starting in March the difference gradually decreased, changed the sign and during the summer reached its minimum of −4–5 K. The June/July period is thus characterized by colder ground and warmer air. A certain temperature contrast existed even between air temperature at 2 m height and near-surface temperature at the 5 cm height, the former being generally slightly warmer by about 0.4 K and following a similar scenario of the annual cycle. The temperature at 2 m height dominated for most of the year, especially in the winter, but in the summer (JJA) the near-surface temperature took over.

Van Wanbeke (1987) compiled an extensive volume of information based on agriculture data summarizing the effect of the microvegetation cover on the surface ground temperature and reported that the surface was generally warmer than the air. The observed range of temperature offsets amounted from 0 up to 5 K and even more reflecting the sequence 'dense forest–shrub–grass field–sparse vegetation–

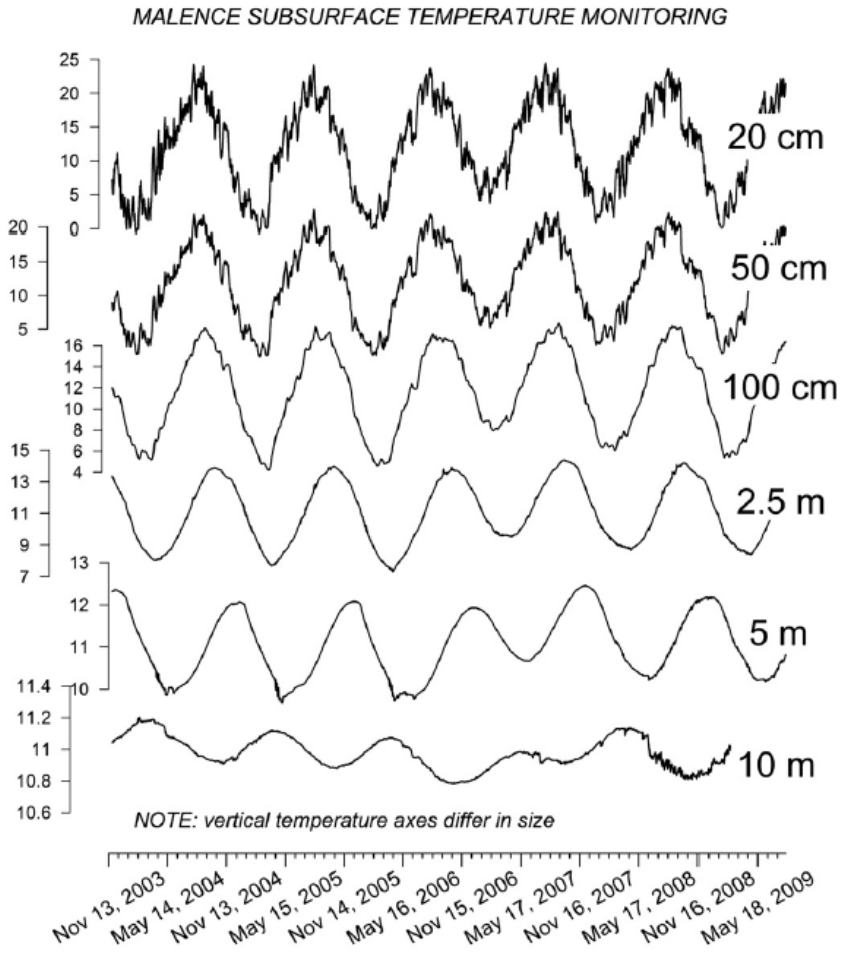

Figure 3. Time series of daily temperature averages at different depths in the borehole Malence.

bare land'. Judging the ground–air temperature offset observed in the MBCO in respect to the analogous values found elsewhere, this tendency was clearly confirmed: Emigrant Pass 2.47 K (exposed granite pluton) (Bartlett *et al* 2006); Caravelinha 2.36 K (gravel) (Šafanda *et al* 2007); MBCO 1.6 K (open meadow); Sporilov 0.27 K (shaded grassland).

The amplitude of diurnal variations rapidly decreases with depth and practically vanishes at ∼50 cm depth. Figure 3 presents the comparison of the daily average temperatures at different depths. As seen, their appearance is very similar within the uppermost 10 m depth interval and illustrates distinct annual variations with progressively damping amplitude. The noise level similarly decreases. While the annual wave appears as the saw-like curve in the series measured just below the surface, it becomes smooth below 1 m depth. Noticeable annual temperature variations then gradually disappear in deeper series, the sign of periodicity vanishes and the time series appear as more or less random temperature fluctuations.

In the upper part (0 to 5 m depth) of the investigated depth interval the annual temperature wave is superposed on a positive linear trend (warming) that operates during the whole observational period. The warming rate achieves 0.4 K/year at 2 cm and progressively decreases to only 0.08 K/year at 5 m depths (table 1).

Table 1. Rate of the linear trend in the daily average temperature–time series, its standard deviation and relative error (=s.d. × 100/slope).

Depth (m)	Slope (10^{-3} K/day)	s.d. (10^{-3} K/day)	Relative error (%)
0.02	1.142 42	0.248 18	21.7
0.05	1.096 95	0.241 41	22.0
0.1	0.998 42	0.233 75	23.4
0.2	0.952 36	0.222 14	23.3
0.5	0.815 33	0.190 58	23.4
1	0.682 81	0.151 21	22.2
2.5	0.348 78	0.075 23	21.6
5	0.210 06	0.027 92	13.3
10	(−0.053 88)	0.003 46	6.4

4. Calculation of the thermal diffusivity

4.1. Conduction theory

A general solution of the conduction of heat in solids and its various applications can be found in Carslaw and Jaeger (1959). Practical algorithms for the calculation of the thermal diffusivity k from the soil temperature measurements were proposed e.g. by Horton *et al* (1983), Lamba and Khambete (1991) or Hurley and Wiltshire (1993). These algorithms are based on a 1D solution of the conductive heat equation in a semi-infinite homogeneous medium,

$$\frac{\partial T}{\partial t} = k\frac{\partial^2 T}{\partial z^2} \tag{1}$$

with a periodic surface boundary condition of period $2\pi/\omega$:

$$T(z=0,t) = T_0 + A_0 \sin(\omega t - \varepsilon_0), \tag{2}$$

where t is the time, z the depth and T the temperature. T_0, A_0 and ε_0 represent mean surface temperature, amplitude and phase of the surface temperature wave, respectively. The underground temperature at depth z can be calculated as

$$T(z,t) = T_0 + z \cdot \text{grad}\, T + A_0\, \mathrm{e}^{-z/d} \sin(\omega t - z/d - \varepsilon_0), \tag{3}$$

where grad$T$ is the geothermal gradient and $d = \sqrt{2k/\omega}$ is the damping depth of the surface temperature wave. In other words, the amplitude of the surface wave decreases exponentially as $A(z) = A_0 \cdot \mathrm{e}^{-z/d}$ and its phase increases linearly as $\varepsilon(z) = \varepsilon_0 + z/d$ with increasing depth. As seen, the above solution applies to the uniform strata only.

Different methods of the thermal diffusivity calculation employ various sets of parameters and/or forcing frequencies and generally provide far not analogous results. To estimate the thermal diffusivity within a given layer we have applied the following two methods. Both of them use the amplitude and phase lag of the temperature wave at depths z_1 and z_2 and the frequency of the investigated surface temperature wave (Horton *et al* 1983), namely, the amplitude algorithm (AA) that calculates k from equation (3) as

$$k = \frac{\omega(z_1 - z_2)^2}{2\ln(A_1/A_2)^2} \tag{4}$$

and phase algorithm (PA) giving

$$k = \frac{\omega(z_1 - z_2)^2}{2(\varepsilon_1 - \varepsilon_2)^2}. \tag{5}$$

Here A_1, ε_1 and A_2, ε_2 are the amplitudes and phase lags of the temperature waves at depths z_1 and z_2, respectively. The k-value represents the thermal diffusivity within the (z_1, z_2) interval.

4.2. Conduction–convection algorithm

Both AA and PA provide certain estimates of the thermal diffusivity only for a vertically homogeneous medium without convective heat transport. Subsurface fluid movements represent one of the most common and serious factors disturbing the underground temperature field. Even very small water flows could significantly distort the temperature (see e.g. Bodri and Čermák (2005), and the references therein) and thus affect the estimated k-value. It is also known, that the thermal diffusivity depends upon soil water content. It increases with an increase of the rock moisture at low water contents and then gradually decreases with increasing water contents at high water contents (e.g. Viswanadham and Jagan Mohana Rao (1972), Farouki (1986)). The conduction–convection algorithm (CCA) for the subsurface thermal diffusivity determination incorporates the impact of vertical water movement and thus takes into account the possibility of the advective heat transfer. A detailed examination of this method by field experiments was performed by Gao *et al* (2008, 2009).

In a porous medium with an undeformable solid matrix and incompressible fluid, the 1D equations for conservation of mass and energy can be expressed:

$$\frac{\partial v}{\partial z} = 0, \qquad \frac{\partial T}{\partial t} + \frac{C_f}{C} v\theta \frac{\partial T}{\partial z} = k\frac{\partial^2 T}{\partial z^2}, \tag{6}$$

where C and C_f are the volumetric heat capacities of the medium and fluid, respectively, θ is the volumetric water content of the soil and v is the pore (distance) velocity. The product of θ and v is Darcy fluid velocity. Negative velocity corresponds to the fluid flow towards the surface. Further on, we will consider values of the parameter $W = \partial k/\partial z - \frac{C_f}{C}\theta v$, the second part of which, $-C_f/C * \theta * v$, was defined by Gao *et al* (2008) as the fluid flux density.

Shao *et al* (1998) and Gao *et al* (2003, 2008) suggested an analytical solution of equations (6) and the following expressions for the calculation of k:

$$k = -\frac{(z_1 - z_2)^2 \omega \ln(A_1/A_2)}{(\varepsilon_1 - \varepsilon_2)[(\varepsilon_1 - \varepsilon_2)^2 + \ln^2(A_1/A_2)]} \tag{7}$$

and W

$$W = \frac{\omega(z_1 - z_2)}{(\varepsilon_1 - \varepsilon_2)}\left[\frac{2\ln^2(A_1/A_2)}{(\varepsilon_1 - \varepsilon_2)^2 + \ln^2(A_1/A_2)} - 1\right]. \tag{8}$$

This technique is generally known as the conduction–convection algorithm (CCA). At $W = 0$ (purely conductive heat transfer in a homogeneous subsurface) one obtains $\varepsilon_1 - \varepsilon_2 = \ln(A_1/A_2)$ and equation (7) reduces to (4) or (5).

5. Heterogeneity spectra

To obtain the annual temperature wave at a given depth we applied the Fourier analysis on measured data, which is a conventional method for analyzing time series data to determine the amplitude, phase and power (mean square amplitude) as a function of frequency. Daily mean temperature series were subjected to the windowing Fourier transform method to estimate their heterogeneity spectra. The pre-processing included linear de-trending of the signals and the 'tapering' with a 10% Hanning window applied on both sides of the records before Fourier transformation. The resulting spectra are shown in figure 4.

In accordance with a tentative 'by-eye' inspection of temperature series, Fourier transform plots exhibit a clear peak corresponding to the annual wave for all series up to 10 m depth. The calculated values of the amplitude and phase (table 2) monotonously decrease with depth in the upper 10 m. Except for the annual wave, the spectra do not contain any

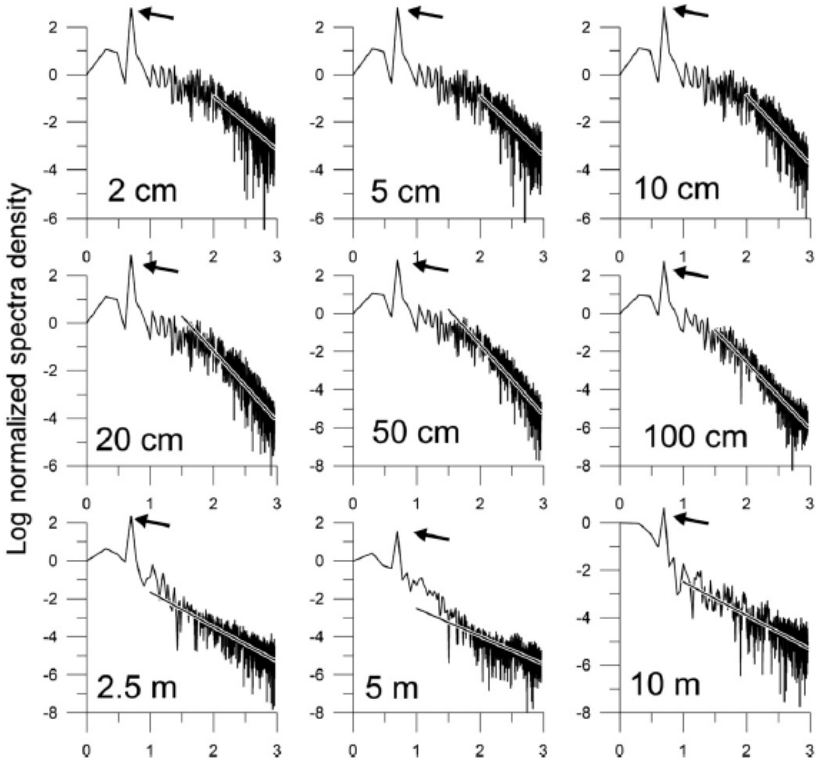

Figure 4. Power spectra of daily temperature averages at borehole Malence. The frequencies are normalized to the lowest frequency in the spectrum and the power spectral density to that at the lowest frequency. Note: the arrows mark the annual wave.

Table 2. Amplitude and phase of the annual wave.

Depth (m)	Amplitude (K)	Phase (rad)	Interval[a]	Slope (*b*-value)
0.02	8.284 25	−0.460 42	2.0–3.0	−2.26
0.05	8.104 76	−0.481 70	2.0–3.0	−2.53
0.10	7.891 28	−0.509 76	2.0–3.0	−2.93
0.20	7.557 25	−0.555 85	1.5–3.0	−2.93
0.50	6.598 17	−0.698 59	1.5–3.0	−3.70
1	5.329 25	−0.922 59	1.5–3.0	−3.47
2.5	2.731 09	−1.538 12	1.0–3.0	−1.82
5	0.939 30	−2.481 23	1.0–3.0	−1.47
10	0.098 50	−4.745 86	1.0–3.0	−1.42

[a] interval of the logarithm of the normalized frequency for which slope was calculated.

distinct peaks that may indicate the presence of other periodic processes.

On the other hand, all spectra exhibit broadband random fluctuations, corresponding to the power law trend $E(\omega) \sim \omega^{-b}$ (scaling behaviour). Here ω is the frequency ($\omega = 2\pi/\tau$, τ is period) and E is the power spectral density. Different values of b represent the cases of the 'coloured noise' (Ladoy *et al* 1991). The b-parameter is thus an important quantity as it foreshadows the nature of the temperature forming processes. The white noise (random fluctuations) spectral exponent amounts to 0 (flat section of the spectrum). As seen in figure 4, the length of the flat sections in the calculated spectra progressively decreases with depth, and disappears below 2.5 m depth. The b-values calculated for the descending parts of the spectra range between 1 and 3 (table 2). The spectral exponents (b-values) for the uppermost series vary between 2 and 3, which indicate that the temperature variations are a product of a long memory (persistent) process with positive correlation of the successive increments. In the case of $b = 3$ (10 and 20 cm depth), the correlation coefficient between two successive increments is 1, which indicates the operation of the close-to-deterministic process that can be modelled by conventional differential equations (like e.g. pure conduction).

The situation changes at 2.5 m depth, where b abruptly decreases to 2. This spectral exponent characterizes an ordinary Brownian noise with random (non-correlated) successive increments. An explanation for the abrupt change of b might be the fact that temperatures at 1 m and above are measured in the soil, whereas temperatures at 2.5 m and below are measured in the water filled borehole. The spectral exponent decreases for the deeper temperature series ($1 < b < 2$), that is characteristic for the anti-persistent process (when inversely correlated fluctuations dominate). Such complexity reflects the number of processes contributing to heat transfer in a compositionally and structurally heterogeneous subsurface.

Table 3. Thermal diffusivity and parameter W calculated for different depth intervals.

Interval (m)	k_{AA}[a]	k_{PA}[a]	k_{CCA}[a]	W (m/s)
0.02–0.05	0.187	0.198	0.198	0.81×10^{-8}
0.05–0.10	0.350	0.316	0.316	-1.77×10^{-8}
0.10–0.20	0.533	0.469	0.468	-2.74×10^{-8}
0.20–0.50	0.487	0.440	0.440	-2.11×10^{-8}
0.50–1.00	0.546	0.496	0.496	-2.12×10^{-8}
1.00–2.50	0.502	0.592	0.590	4.00×10^{-8}
2.50–5.00	0.547	0.699	0.694	6.50×10^{-8}
5.00–10.0	0.490	0.485	0.456	-0.19×10^{-8}

[a] k_{AA}, k_{PA} and k_{CCA} were calculated by the AA, PA and CCA methods, respectively, and are given in 10^{-6} m^2 s^{-1}.

6. Results

The subsurface temperature distribution depends on a variety of external factors, such as e.g. absorbed radiation energy, cloud cover, precipitation, as well as internal factors, such as rock composition, conductivity, porosity and mineralogy. Numerous authors have detected significant seasonal variations of the thermal diffusivity calculated from *in-situ* temperature measurements (Viswanadham and Ramanadham, 1969, Gao *et al* 2009). We have used the parameters of the annual periodic wave to exclude seasonal variations of the estimated thermal diffusivity. The amplitude and phase angle values calculated by the harmonic analysis (section 4) at different depths are summarized in table 2.

The amplitudes of the annual temperature variations show a downward exponential decrease that is clearly detectable up to 10 m depth. The damping depth of the annual temperature wave equals to 2.24 m for the thermal diffusivity $k = 0.5 \times 10^{-6}$ m^2 s^{-1}. One can estimate that at the investigated site the amplitude of the surface annual wave should fall to ~0.001 K at 20 m.

The values of the parameters k and W calculated by the three algorithms mentioned above from amplitudes and phase lags of the annual temperature wave are presented in table 3. As seen, all three algorithms gave reasonable results. The k-values estimated from the amplitude and phase angle by the AA and PA are consistent, their relative differences are below 12%, only in the layers 1–2.5 m and 2.5–5 m are the PA values larger by 18% and 28%, respectively. Both methods detect obvious vertical heterogeneity of the thermal diffusivity that equals to ~0.2–0.3 $\times$ 10^{-6} m^2 s^{-1} in the top 5–10 cm of the soil and increases to the values of 0.5–0.7 $\times$ 10^{-6} m^2 s^{-1} within the 0.1–10 m layer. According to Farouki (1986) the value of 0.5×10^{-6} m^2 s^{-1} is characteristic for the soils with bulk density of 1200–1500 kg m^{-3} with clay content between 0% and 60% and volumetric water content of less than 0.1 m^3 m^{-3}. Garratt (1992) gave the value of ~0.5×10^{-6} m^2 s^{-1} for clay soil with the volumetric water content of 0.2 m^3 m^{-3}.

As seen, the k-values obtained by the CCA that specifies on a presence of the subsurface fluid flow, revealed good agreement with the above results. This is especially true for the PA and CCA results. One of the restrictions of the CCA is that that formulae (7) and (8) for k and W, respectively, are correct only for cases when k does not vary with depth (Gao *et al* 2008). The parameter W is a sum of the vertical gradient of diffusivity, $\partial k/\partial z$, and the water flux density, $-C_f/C * \theta * v$ (see Gao *et al* (2008), equation 3). It means that interpretation of W in terms of the vertical groundwater flow is only approximate and assumes implicitly that the vertical gradient of diffusivity is appreciably smaller than the water flux density. In such a case, W is proportional to Darcy velocity with a proportionality factor $-C_f/C$. In the study of Gao *et al* (2008) dealing with simulations of the diurnal soil temperature variations in the layer 0.05–0.4 m below the surface, Darcy velocity was expected to point upwards and to attain a few millimetres per day (~-10^{-8} m s^{-1}) during days without precipitation. This upward flow is caused by surface evaporation and its role in the diurnal soil heat flux is quite important. In the case of the annual variations treated in this study, the downward flow of infiltrated water through the vadose zone is assumed to be the main factor determining the convective heat flux and therefore influencing the shape of the annual temperature wave in the individual depths. Mean annual Darcy velocity through the vadose zone can be estimated as a share of the annual amount of precipitation at the Malence study site, about 1140 mm (the 1961–1990 mean) (Mesečni bilten ARSO, see http://www.arso.gov.si/oagenciji/knjižnica/mesečnibilten/bilten2011.htm) that infiltrates to the groundwater level. The magnitude of this share, about 500 mm, was estimated from the formula of Turc (1954) for an annual amount of evapotranspiration and from the water budget equation (Krüger *et al* 2001). The Turc's formula requires, besides precipitation, knowledge of the mean annual air temperature. The six-year average (2003–2009) of this quantity attained 11.0 °C in Malence. It implies Darcy velocity of 500 mm/year or $1.6 * 10^{-8}$ m s^{-1} through the vadose zone.

The heat capacity of water C_f equals 4.187 MJ (m^3 · K)$^{-1}$. The heat capacity of soil depends on its type, is affected by the water content and varies in a wide range. For instance, the measurements by Abu-Hamdeh (2003) disclosed that the volumetric heat capacity ranged from 1.5 to 3.5 MJ (m^3 K)$^{-1}$ for clay and from 1.1 to 3.0 MJ (m^3 K)$^{-1}$ for sand at moisture contents from 0 to 0.25 kg kg^{-1} within a density range of 1200–1400 kg m^{-3}. Thus, the expected range of $C_f/C * \theta * v$ would be (1.2–3.8) $*1.6 *10^{-8}$ m s^{-1} = (1.9–6.0) $*10^{-8}$ m s^{-1}. As can be seen from table 3, the estimated values of thermal diffusivity are quite stable in the depth range of 0.05–1 m. It means that the vertical gradient of diffusivity is very small and the water flux density should be close to the W-parameter within this zone. As mentioned above, the vadose zone was about 1.5 m thick during most of the temperature observation period. Therefore, the value of W should correspond to the above estimate (1.9–6.0) $*10^{-8}$ m s^{-1} within the depth range of 0.05–1.5 m. As seen in table 3, it is really the case. The absolute values of W range between (1.8–2.7) $*10^{-8}$ m s^{-1}, i.e. in a lower part of the interval corresponding to the rate of the annual infiltration and typical values of the volumetric heat capacity. The sign of W is negative, because water migrates downwards. In comparison, absolute values of the water flux density in the uppermost 0.4 m revealed by Gao *et al* (2008), $W \sim 10^{-6}$ m s^{-1}, are by two orders of magnitude higher. It is

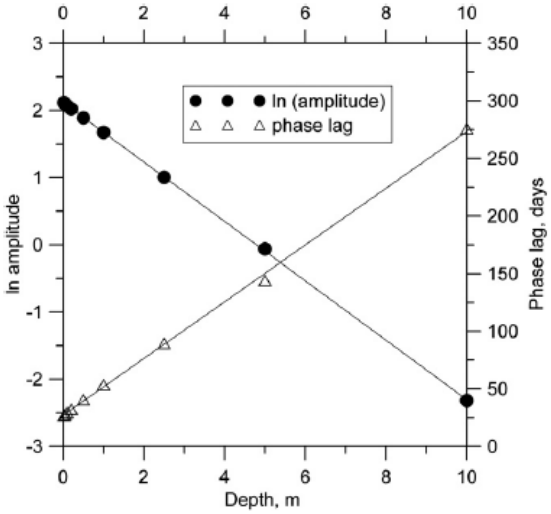

Figure 5. The natural logarithm of amplitude and the phase lag as functions of depth and their linear regressions. The regression lines yield estimates of mean thermal diffusivity between the surface and the depth of 10 m. The zero depth intercepts of the regression lines also provide estimates of the amplitude and phase lag of the annual ground surface temperature signal.

evident that, contrary to our case, they are not proportional to the assumed Darcy velocity of several millimetres per day, i.e. to some $5*10^{-8}$ m s^{-1}, generated by surface evapotranspiration, but most probably they are determined by much higher values of the vertical gradient of diffusivity. The same might apply to the W-values obtained in Malence for the layers 1–2.5 m and 2.5–5 m, which are larger by two and three times, respectively, and have the opposite sign than those within the vadose zone, and also for W in the lowermost layer 5–10 m, which changes the sign again, but its value is by one order of magnitude smaller than the values within the vadose zone. The vertical gradient of diffusivity between the centres of the four lowermost layers calculated from their k_{CCA} values (table 3) amounts to $+9*10^{-8}$, $+5*10^{-8}$ and $-6*10-8$ m s^{-1}, respectively. These values are of the same order of magnitude (in the layers 1–2.5 m and 2.5–5 m) as, or higher (in the layer 5–10 m) than the W-values calculated for the three lowermost layers. It means that these W-values are very, probably strongly, influenced by the diffusivity gradient and cannot be used for a reliable characterization of the water flow below the vadose zone. High vertical gradient of diffusivity can be expected in the uppermost layer 0.02–0.05 m, where the 'water-flux' interpretation of W indicates an upward flow. It is therefore difficult to judge, whether the W-value reflects here the effect of the evapotranspiration near the surface or is a result of a 'random' interference of the two terms contributing to W.

As follows from formula (3) for the $T(z, t)$, the natural logarithm of amplitude and the phase lag are linear functions of depth in a semi-infinite homogeneous medium. Figure 5 shows how closely this relationship is obeyed by the amplitudes and phases of the annual waves determined in the individual depths down to 10 m in these particular conditions. The regression lines of the logarithm of amplitude and the phase lag yield a mean thermal diffusivity of 0.51×10^{-6} and 0.55×10^{-6} m^2 s^{-1}, respectively. The zero depth intercepts of the regression lines also yield estimates of the amplitude and phase lag of the annual ground surface temperature signal, 8.29 °C and −0.465 radian, respectively, which are close to the values determined for the depth of 2 cm (table 2). As mentioned above, for the amplitude and phase lag calculations the solution of the conductive heat equation under the periodic boundary condition was used. The linear regressions of the logarithm of amplitude and/or the phase lag with depth yield coefficients of determination 0.9999 and 0.9991, respectively. It is evident that heat conduction dominates in the entire domain.

7. Concluding remarks

The thermal diffusivity of the subsurface soil layer was estimated from the amplitude and phase angles of the annual temperature wave which were obtained by the harmonic analysis of daily mean temperature variations at nine different depths within a 10 m subsurface depth interval. Two algorithms based on the pure conductive heat transfer approach at the homogeneous medium provided highly consistent results that are in good agreement with each other. The values are also in reasonable agreement with the previous estimates based on the thermal conductivity measurements and estimates of porosity, density and specific heat.

Coupled conduction–convection heat transfer occurs in the subsurface when a significant amount of water percolates vertically. To examine the possibility of the subsurface fluid movement and its influence on the calculated k-values we have applied the CCA based on the analytical solution of the heat transfer equation including an advective term. Low values of parameter W found at all depth levels showed that on the annual scale the convective heat transfer did not contribute significantly to the temperature changes monitored in the uppermost 10 m depth interval. This is confirmed by high level correlation between the logarithm of amplitude and depth as well as between the phase lag of damped annual temperature waves and depth (see the text above and figure 5). Therefore, in this particular case, the assumption used in the reconstruction of the ground surface temperature history from the current deep temperature–depth profiles, namely that the low-frequency changes of the surface temperature like the annual wave and multi-year and secular variations propagate downwards mainly by the heat conduction, is true.

Acknowledgments

Most of the reported studies were done under the cooperation program between the Academy of Sciences of the Czech Republic and the Geological Survey of Slovenia. The support was provided by the Grant Agency of the Czech Republic (project GACR P210/11/0183) and by the project of large research infrastructure CzechGeo, grant no. LM2010008. The manuscript was read by two anonymous reviewers, both of whom proposed a number of constructive comments which were thankfully accepted.

References

Abu-Hamdeh N H 2003 Thermal properties of soils as affected by density and water content *Biosyst. Eng.* **86** 97–102

Bartlett M G, Chapman D S and Harris R N 2006 A decade of ground air temperature tracking at Emigrant Pass Observatory, Utah *J. Clim.* **19** 3722–31

Bodri L and Čermák V 2005 Borehole temperatures, climate change and the pre-observational surface air temperature mean: allowance for hydraulic conditions *Glob. Planet. Change* **45** 265–76

Carslaw H S and Jaeger J C 1959 *Conduction of Heat in Solids* 2nd edn (Oxford: Clarendon) 510 pp

Čermák V, Dědeček P, Šafanda J and Krešl M 2010 Climate warming: evidence stored in shallow subsurface *The Polish Climate in the European Context: An Historical Overview* ed R Przybylak, J Majorowicz, R Brázdil and M Kejna (Berlin: Springer)

Chacko P T and Renuca G 2002 Temperature mapping, thermal diffusivity and subsoil heat flux at Kariavattom of Kerala *Proc. Indian Acad. Sci. (Earth Planet. Sci.)* **111** 79–85

Dědeček P, Šafanda J and Rajver D 2012 Detection and quantification of local anthropogenic and regional climatic transient signals in temperature logs from Czechia and Slovenia *Clim. Change* **113** 787–801

Demetrescu C, Nitoiu D, Boroneant C, Marica A and Lucaschi B 2007 Thermal signal propagation in soils in Romania: conductive and non-conductive processes *Clim. Past Discuss.* **3** 469–500

Farouki O T 1986 *Thermal Properties of Soils. Series on Rock and Soil Mechanics* vol 11 (Germany: Trans Tech) 136 pp

Gao Z, Fan X and Bian L 2003 An analytical solution to one-dimensional thermal conduction-convection in soil *Soil Sci.* **168** 99–107

Gao Z, Lenschow D H, Horton R, Zhou M, Wang L and Wen J 2008 Comparison of two soil temperature algorithms for a bare ground site on the Loess Plateau in China *J. Geophys. Res.* **113** D18105

Gao Z, Wang L and Horton R 2009 Comparison of six algorithms to determine the soil thermal diffusivity at a site in the Loess Plateau of China *Hydrol. Earth Syst. Sci. Discuss.* **6** 2247–74

Garratt J R 1992 *The Atmospheric Boundary Layer* (Cambridge: Cambridge University Press) 335 pp

Gróf G 2002 The thermal diffusivity measurement of anthracite by the flash method in the green and calcite state *Period. Polytech. Ser. Mech. Eng.* **46** 159–75

Horton R, Wierenga P J and Nielsen D R 1983 Evaluation of methods for determination apparent thermal diffusivity of soil near the surface *Soil. Sci. Soc. Am. J.* **47** 25–32

Hurley S and Wiltshire R J 1993 Computing thermal diffusivity from soil temperature measurements *Comput. Geosci.* **19** 475–7

Krüger A, Ulbrich U and Speth P 2001 Groundwater recharge in Northrhine-Westfalia predicted by a statistical model for greenhouse gas scenarios *Phys. Chem. Earth Part* B **26** 853–61

Ladoy P, Lovejoy S and Schertzer D 1991 Extreme variability of climatological data: scaling and intermittency *Non-Linear Variability in Geophysics* ed D Schertzer and S Lovejoy (The Netherlands: Kluwer) pp 241–50

Lamba B S and Khambete N N 1991 Analysis of subsoil temperature at various depths by Fourier technique *Mausam* **42** 269–74

Lewis T (ed) 1992 Climatic change inferred from underground temperatures *Glob. Planet. Change* **6** 71–281 (special issue)

Rajver D, Šafanda J and Dědeček P 2006 Monitoring of air-ground temperature coupling and examples of shallow subsurface warming in Slovenia *Geologija* **49/2** 279–93

Šafanda J, Rajver D, Correia A and Dědeček P 2007 Repeated temperature logs from Czech, Slovenian and Portuguese borehole climate observatories *Climat. Past* **3** 453–62

Shao M, Horton R and Jaynes D B 1998 Analytical solution for one-dimensional heat conduction-convection equation *Soil Sci. Soc. Am. J.* **62** 123–8

Sun S and Zhang X 2004 Effect of the lower boundary position of the Fourier equation on the soil energy balance *Adv. Atmos. Sci.* **21** 868–78

Turc L 1954 Colcul du bilan de l'eau evaluation en function des precipitations et des temperatures Publication No. 37 des I/Association International d'Hydrology, Assemblée Génrale de Rome, Tome III 188–202

Van Wanbeke A 1987 Soil moisture and temperature regimes of Central America, Caribbean and Mexico *SMSS Tech. Monogr.* **16** 33 pp

Viswanadham Y and Jagan Mohana Rao N 1972 The thermal diffusivity of soil at tropical stations in southern hemisphere *Pure Appl. Geophys.* **101** 247–66

Viswanadham Y and Ramanadham R 1969 The thermal diffusivity of red sandy soil at Waltair *Pure Appl. Geophys.* **74** 195–205

Chapter 11
Climate Warming in the Czech Republic: Evidence Stored in Shallow Subsurface

Vladimir Čermák, Petr Dědeček, Jan Šafanda, and Milan Krešl

11.1 Introduction

There is clear evidence that the world climate has been undergoing a general warming. This warming was typical for the most of the last century, following the previous relatively colder nineteenth century. An important question to answer is whether this warming is just a manifestation of natural climate variability and a certain "return" to previous conditions or an indication of a new (and permanent) trend. What is alarming, is the matter of fact, that the warming rate has been accelerating in the last 3 or 4 decades. The 1990s was the warmest decade of the last century (IPCC 2001) and global mean surface temperature deviations (related to the 1961–1990 average) were in 1998 and in 2002–2007 the absolutely warmest since the world data have been collected in 1861 (NASA 2008, WMO 2005). Also the Czech meteorological records confirmed the growth of the mean annual air temperatures (Kalvová 2001, see also http://www.chmi.cz). The increase of the global mean temperature is accompanied by changes of many climatic and environmental variables (Hansen and Lebedeff 1987; Jones et al. 1999). The observed climate change does not only mean a change of average values, but may present additional changes in climate variability leading to the increasing occurrences of extreme phenomena such as floods or droughts. If the warming is to continue in the future, serious environmental changes present a risk for the population of many countries, see plentiful recent reports presented during the Paris (February 2007) and Brussels (April 2007) IPCC assemblies. The Czech Hydrometeorological Institute published Climate Atlas of Czechia with a detailed description of climate evolution in the Czech Republic for 1961–2000 (Tolasz et al. 2007).

The nonlinear climate system is under effects of many forcing agents – natural (solar and volcanic activity, natural aerosols) as well as anthropogenic (massive deforestation, industrial pollution and emissions of greenhouse gases, land-use).

V. Čermák (✉), P. Dědeček, J. Šafanda and M. Krešl
Geophysical Institute, Czech Academy of Sciences, Praha, Czech Republic
e-mail: cermak@ig.cas.cz

R. Przybylak et al. (eds.), *The Polish Climate in the European Context: An Historical Overview*, DOI 10.1007/978-90-481-3167-9_11,

In order to describe the climate evolution and to attribute it to the individual forcing factors, a robust record of the past climatic changes is required. Equally important is to improve the knowledge of the spatial distribution of the present-day warming rate and its environmental confidence. Direct evidence of climate change and its variability based on instrumental measurements covers only a relatively short period. The longest European temperature records started at the beginning of the eighteenth century (Camuffo and Jones 2002). The Czech longest continuous temperature series covers more than two centuries (Prague-Klementinum), see e.g. Hlaváč (1937) or Brázdil and Budíková (1999). More detailed database of measurements based on a dense station network is available for the last 4 or 5 decades. From all these records, it is possible to detect a significant evidence of gradually changing conditions.

There is an alternative, relatively new, but powerful method (so called borehole climatology), which relies on the inversion of the present-day subsurface temperature-depth profiles into the ground surface temperature history (GSTH) (Čermák, 1971; Lachenbruch and Mareschall, 1986; Pollack and Chapman 1993). For a comprehensive summary of this method see e.g. Pollack and Huang (2000), Majorowicz et al. (2004) or Bodri and Čermak (2007). Inverting almost one hundred borehole temperature logs from the Czech territory into the GST-history revealed a past climate scenario of the last millennium (Bodri and Čermak, 1995, 1997, 1999). Numerous shorter meteorological surface air temperature (SAT) series completed by shallow subsurface temperature monitoring offered a quantitative estimate of the present day warming rate of 0.02–0.04 K/year (Čermak et al. 2000). There is no doubt that combining several approaches, namely the instrumental and proxy data analysis, can enable better understanding of the Earth's climate history and that the knowledge of the past will facilitate a more reliable assessment of the future of the climate system (Harris and Chapman 1998; Huang et al. 2000).

11.2 Rationale

The observed increase of air temperature is linked to the increase of the surface (soil) temperature. The response to changes in the surface conditions slowly penetrates downwards into the shallow subsurface (Fig. 11.1). Subsurface temperature field at depth of several tens to several hundreds of meters contains a record of what has happened on the surface in the past, i.e. the long-term ground surface (soil) temperature history (GSTH). This information can be recovered from present-day borehole temperature-depth profiles and used to reconstruct the GSTH of several past centuries (see e.g. Lewis 1992). Amplitude of the surface temperature changes is attenuated and time delay increases with depth (Čermak et al. 1993). The high-frequency component of the transient temperature signal from the surface is progressively filtered out as it propagates to depth (Pollack and Chapman 1993). Seasonal temperature variations, in dependence on the thermal conductivity and diffusivity of the near surface rock, practically fade out below the depth of 20–30 m. As the (meteorological) air temperature series exhibit certain variability and the relatively

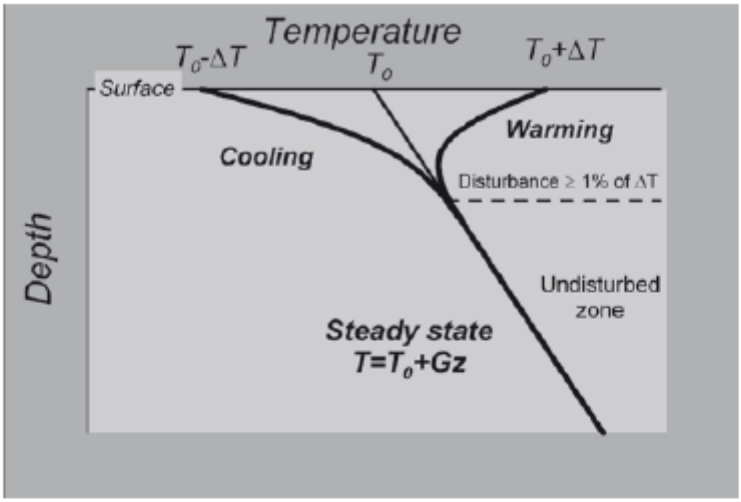

Fig. 11.1 Response of the subsurface temperature field to the change on the surface. Temperature-depth profile measured in a borehole indicates the surface warming/cooling signal as a departure from the (undisturbed) steady-state geotherm

"warmer" and "colder" years may occur irregularly, a relatively long time span is generally needed to provide reliable statistical results. Since the ground smoothes the temperature extremes, the magnitude of the present day climate warming, as the reflection of the long-term climate evolution, can be more easily obtained by the temperature monitoring at shallow depths just below the penetration reach of the seasonal temperature variations and in a considerably shorter time interval.

The geothermal method to reconstruct past climate history addresses the analysis of the downward diffusion of variation of the subsurface temperature field with time. While this method has a low time resolution (being diffusion controlled), it is directly related to the past temperature on the surface (unlike all other proxies). It is an advantage that the time span of most GST-histories extracted from borehole data exceeds that of meteorological SAT data, so they can be used to "extend" the SAT time series back into the pre-instrumental period. This can be done only in case that ground and air temperatures track each other on a long-term scale. Although there are papers suggesting that the climatic temperature record in the Earth is compatible with measured SAT series (e.g. Harris and Chapman 1995), the air and ground temperature coupling is governed by the energy and mass fluxes at the Earth's surface which represent a complex system of competing physical and biological processes (Beltrami and Mareschal 1995). Therefore the effect of other climate variables, such as precipitation and evaporation, transpiration, moisture, soil freezing, snow and vegetation cover changes need to be taken into account (Harris and Chapman 1995; Možný and Kott, 2003). While this fact somehow limits the practical use of the routine inversion procedure, at the same time it offers interesting applications such as detecting long-term changes in the vegetation cover (Čermak and Bodri 2001) and also the possibility to distinguish between the natural and potential anthropogenic components of the present-day warming (Čermak et al. 2000).

11.3 Subsurface Temperature Monitoring

As a part of the "Borehole and Climate" program of the International Geological Correlation Program (IGCP 428), two experimental shallow holes were drilled in two different environments to monitor the depth response to the downwards penetrating signal of the changing surface temperatures. The first 40 m deep hole was drilled in October 1992 on the campus of the Geophysical Institute in Praha Sporilov (50º02'27" N, 14º28'39" E, 275 m a.s.l.). The hole is located on a low E-W trending ridge. The upper four meters of the lithological column represent soil and a man-made loose material backfill of low conductivity (1.7–2.0 W/mK), underlain by silt to clayey shale of gradually increasing conductivity, below 10 m the conductivity is practically constant (3.2 ± 0.2 W/mK) (Šafanda 1994; Štulc, 1995). The corresponding diffusivity of the upper strata is only 0.4×10^{-6} m^2s^{-1}, lower strata is characterized by values of $0.73–0.9 \times 10^{-6}$ m^2s^{-1}.

While the Sporilov hole is located on the rim of a large urban area, the site for the second hole was selected at Kocelovice in south-central Bohemia at a distance of about 70 km SSW of Praha in a typical farming area . The 40 m deep Kocelovice hole (49º28'02.2" N, 13º50'18.7" E, 519 m a.s.l.) was drilled in 1997. The borehole site is near one of the main Czech meteorological stations on a gently grassy slope in slightly undulating terrain. The hole penetrates a compact granite body with a mean conductivity of 3.1 ± 0.1 W/mK, covered by about 1–2 m thick soil layer. The diffusivity was not measured, but can be estimated as $1.2–1.3 \times 10^{-6}$ m^2s^{-1}.

Both holes were equipped with a measuring chain of temperature sensors (thermistors) spaced at selected depth levels covering the whole 0–40 m depth section. Both holes are filled with water, the depth of which slightly varies between 4 and 5 m in Kocelovice hole and is stable at 9 m depth in the Sporilov hole. In addition to the subsurface temperatures, air (SAT) temperatures are monitored at 0.05 m, 1 and 2 m above surface. At Sporilov also precipitation is recorded and at the Kocelovice meteorological station a complete set of various information is completed (wind speed and direction, direct and reflected solar radiation, snow layer thickness, air humidity, soil moisture and vapor tension).

11.4 Monitoring Temperatures

Regular temperature variations at the surface occur at temporal scales, such as diurnal or seasonal/annual. The typical magnitude of the daily variations amounts 10–15ºC, the amplitude of the seasonal variations may amount to 20–30ºC and more. Inter-annual and long-term temperature change patterns are irregular. As the surface, temperature signal propagates downward, its amplitude decreases exponentially with depth due to the diffusive process of heat conduction, each variation vanishes over a vertical distance related to the period of change and to the thermal diffusivity of the ground. The shorter period fluctuations attenuate more rapidly.

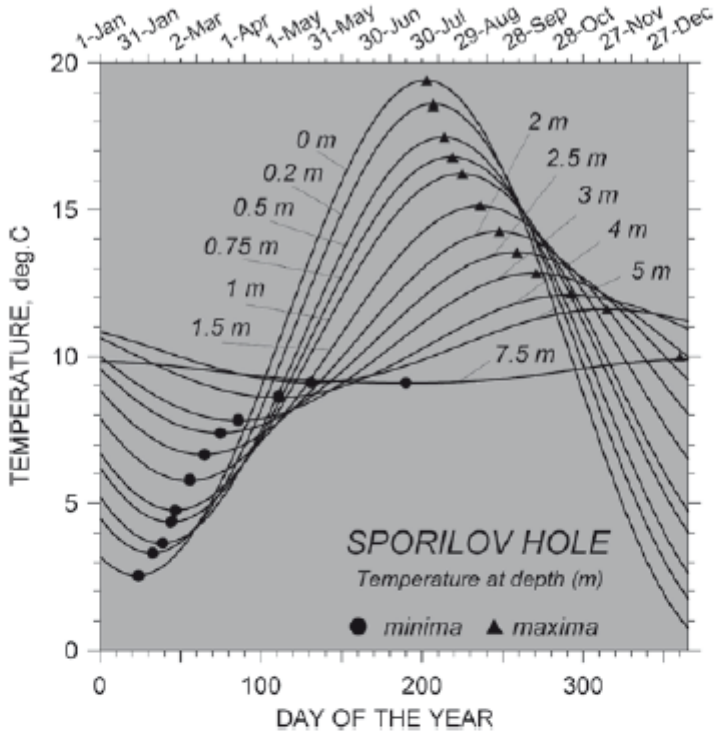

Fig. 11.2 Characteristic temperature distribution in shallow subsurface corresponding to the annual temperature variations on the surface (daily variations ignored). The individual curves illustrate the amplitude decrement and phase delay of the temperature response penetrating downwards. Based on 6-year-long temperature monitoring in the Sporilov hole

Figure 11.2 demonstrates the amplitude attenuation of the temperature signal when propagating downwards and the delay of its phase by presenting the results of the 12-year temperature monitoring in the Sporilov hole. The daily temperature wave is practically not observable below 1 m depth. On the other hand, the temperature at 1 m depth represents integrated average of the daily signal of the previous day(s). Similarly, annual GST oscillations practically vanish at about 15–20 m depth, the temperature field below 20–30 m depth is free of any response to the annual or shorter temperature variations and contains exclusively the fingerprints of longer scale evens with characteristic time of several last years.

The 12-year (1994–2005) record of temperature recorded at 38.3 m depth in the Sporilov hole (Fig. 11.3) clearly demonstrates the yearly increases of temperature (records 2000–2005). Bottom panel summarizes the general temperature increase from 10.63ºC in 1994 to 10.99ºC in 2005 together with early warming rates ranging from 0.02 K/year in 1994 to 0.04 K/year in 2006 (with the mean of 0.0296 K/year). Even when the observed warming rate at depth is not identical with the SAT warming, it can well serve as a certain measure to describe the recent climate evolution.

Figure 11.4 presents monitoring series of temperature at 40 m depth in borehole Kocelovice, where due to technical problems only two shorter monitoring series

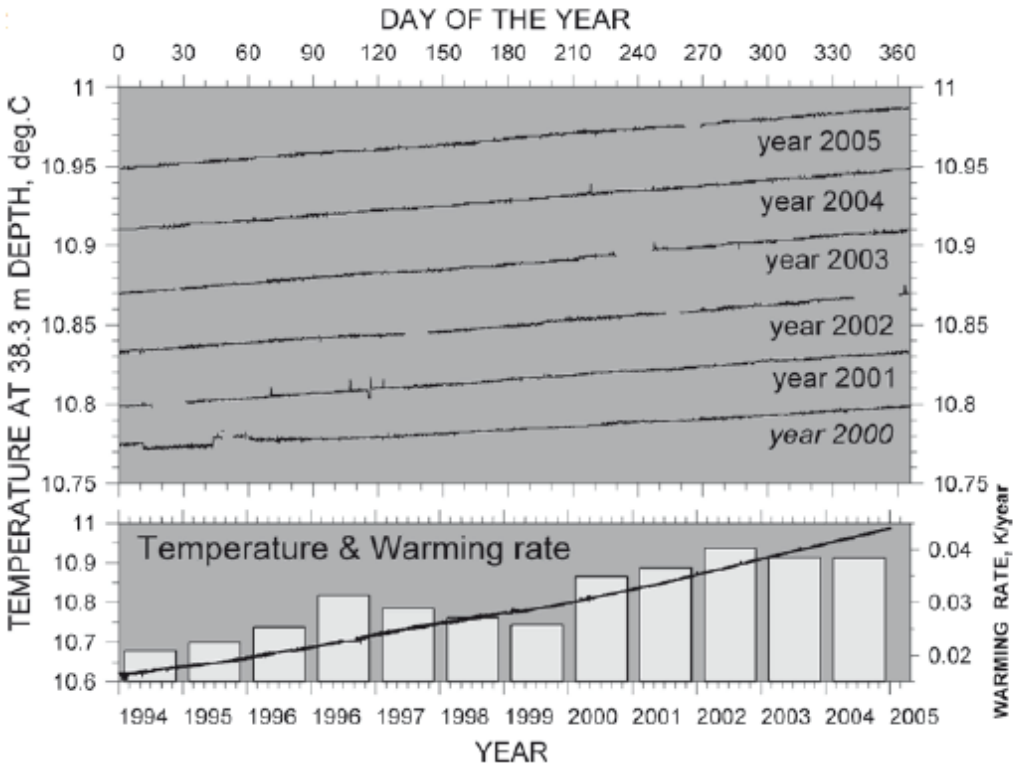

Fig. 11.3 Results of temperature monitoring at 38.3 m depth (Sporilov hole), years 2000–2005. Bottom: the 12-year record together with the warming rates calculated for the individual years

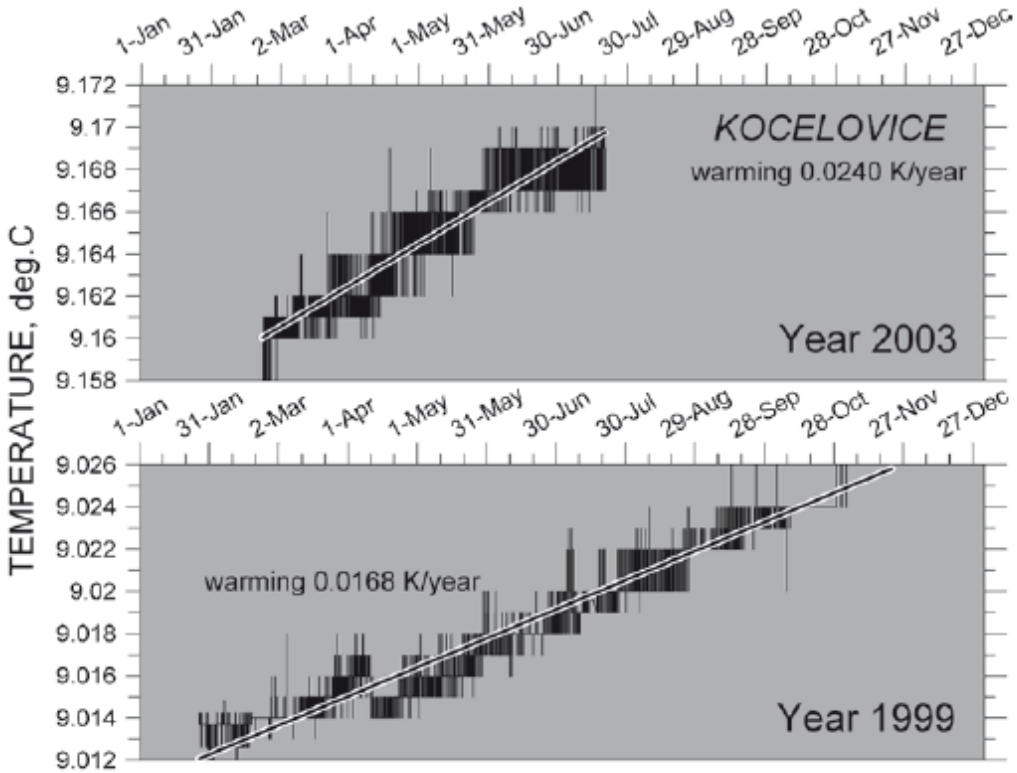

Fig. 11.4 Results of temperature monitoring at 40 m depth (Kocelovice hole). Two records correspond to 1999 and 2003 monitoring series

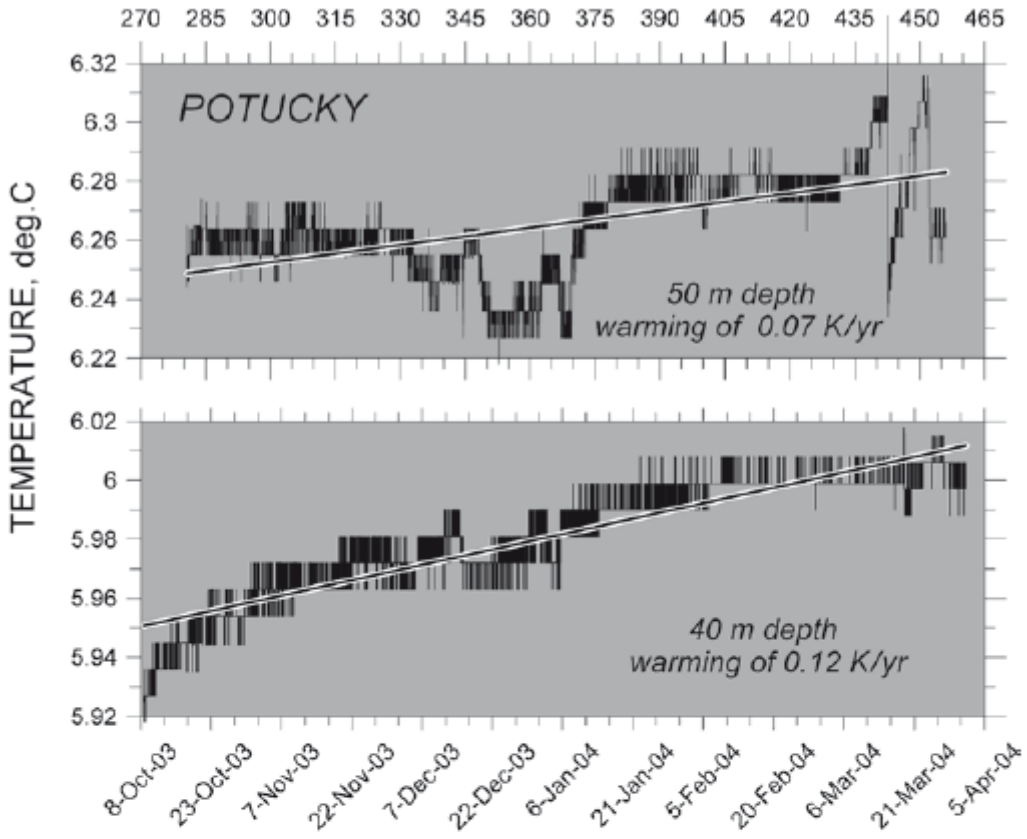

Fig. 11.5 Results of temperature monitoring at 40 and 50 m depths (Potucky hole). Contrary to Sporilov and Kocelovice data, temperature field at Potucky is less stable and obviously disturbed by local hydrogeology

could be obtained, both confirmed warming rate, namely 0.0168 K/year (in 1999) and slightly higher rate of 0.0240 K/year in 2003. In years 2003–2004 a similar experiment was performed in an abandoned hole at Potucky site located in the Ore (Krušné Hory) Mountains, north-western Bohemia (50.43ºN, 12.78ºE, 864 m a.s.l.). The site is in close vicinity of a forested area of coniferous woods (mostly Norwegian spruce, *Picea abies*), and served for several experiments (see further). The temperature data in this hole, however, may be disturbed by complex hydrological conditions in the subsurface and are thus less reliable. The monitoring confirmed surprisingly high warming rates (Fig. 11.5), namely 0.12 K/year at 40 m depth and 0.07 K/year at 50 m depth, which so far are difficult to interpret. It is, however, interesting to mention, that the north-western part of the country belongs to the areas most industrially polluted and that the meteorological SAT record from the near-by station Fichtelberg also revealed a steep increase of air temperature in the last 25 years of 0.0537 K/year (Fig. 11.6).

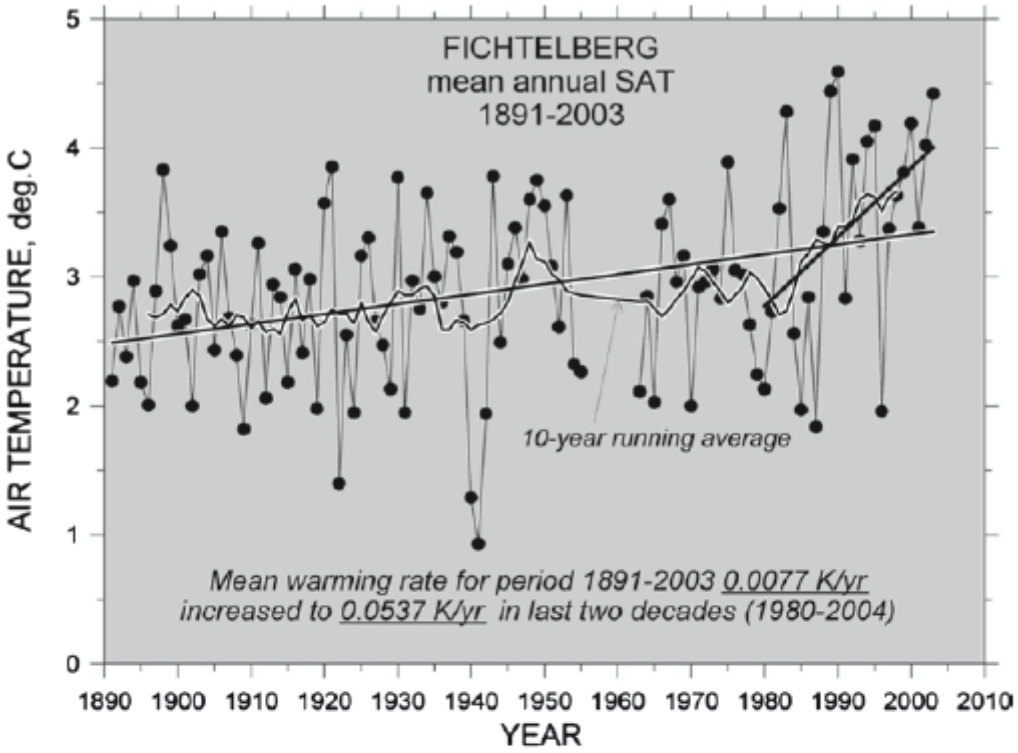

Fig. 11.6 Surface air temperature measured at Fichtelberg meteorological station (1891–2003)

11.5 Surface and Near Surface Effects

11.5.1 Snow Cover and Ground Freezing

Modeling the GST-SAT coupling have confirmed that on longer timescales the GST represents a good SAT indicator and their variations repeat each other (see e.g. González-Rouco et al. 2003, 2006). The problem can be, to what extend the observed GST variations can track SAT changes on a shorter timescale, such as the monthly or yearly series. No doubt, that large spatial-scale GST differences are determined by ground heating by incoming solar radiation, its transformation, distribution and the amount of heat penetrating into the subsurface. Thermal balance on the ground surface is thus determined not only by the actual air temperature, but also by the surface absorption and reflection. Of special concern is the GST-SAT coupling in locations, where e.g. the ground loses a substantial part of information about air cooling in winter because snow insulates the ground and reflects the incoming solar radiations. Even when snow is sporadic, the complicated latent heat effects and winter freezing/thawing processes can complicate the heat transfer. Of similar importance can be the GST-SAT coupling due to rain precipitation producing changes in moisture content, infiltration, evaporation and runoff, as well as the seasonal (micro)vegetation changes and chemical weathering.

To understand the GST-SAT coupling, the experimental site (microclimate station) was built on the campus of the Geophysical Institute in 2002 to monitor the shallow subsurface temperature field below several characteristic surfaces, namely bare soil, sand, grass and asphalt. Air temperatures at 5 and 200 cm above surface as well as soil temperatures at depth levels of 2, 5, 10, 20 and 50 cm are recorded at 5 min interval. All yearly (2003–2005) air temperature averages at 5 cm above the ground are surface dependent, but appeared lower than the soil averages for all types of surface. The differences between air temperature at 5 cm above the ground and the soil temperature at 2 cm depth amounted to 1.4–1.6 K, 1.8–2.0 K, 0.2 -0.4 K, and 4.1–4.8 K for bare soil, sand, grass and asphalt, respectively. These results hint that on the annual scale the soil is warmer than the air and corroborates the similar observations reported by e.g. Backer and Ruschy (1993)) and Putnam and Chapman (1996). The interannual variability is also surface type dependent and ranges within the first tenths of degree Kelvin.

In general, the magnitude of the GST-SAT difference may exhibit significant variations. Subsurface heat conduction as well as the factors related to the movements and/or diffusion of air and/or moisture masses (wind, evaporation/transpiration, vertical soaking of soil moisture and precipitation) tends to equalize air and soil temperatures. Soil temperature generally follows the air temperature course when average SAT is above 0°C, but the GST-SAT coupling is violated at the presence of snow in winter when the air temperature drops below zero. Snow insulates the ground surface and reduces heat loss. As an example Figure 11.7 shows the temperature variations of the air (SAT) temperature together with the 2 cm depth soil data under different surfaces and illustrates the effect of the snow cover on the GST-SAT coupling. During the week February 20–27 the SAT-GST data decoupled, then the coupling started to restore after snow cover thawed away (on January 28) and continued till February 8 when new snow appeared again. For the most of February till the early March the GST-SAT data decoupled again. Similar results were obtained at Potucky (Fig. 11.8), where temperature was recorded at 2 cm depth and 5 cm height above ground. The coupling of the temperatures is almost perfect in fall and spring and breaks down during most of the winter.

Smerdon et al. (2004, 2006) have generalized the results of the above experiments in the relation to several temperature time series measured at other localities, namely at Fargo (North Dakota), Cape Henlopen State Park (Delaware) and Cape Hatteras (North Carolina). These sites represent different kinds of subsurface strata and/or climatic settings located within the mid-latitude zone, and can be used for the spatial consideration. On the annual scale the GST signal (even attenuated and phase shifted) generally follows the SAT variations. The slight differences between annual GST and SAT signals may occur in both winter and summer seasons. The GST-SAT difference depends on the site location and its climate and terrain characteristics. The GST-SAT decoupling at Fargo occurs mainly during the winter, whereas at Capes Henlopen and Hatteras the observed attenuation of the GST signal has taken place during the summer season. The seasonal partitioning of the GST-SAT decoupling is caused mainly by the corresponding partition of the summer precipitation and snow. While the Fargo location is characterised by the modest

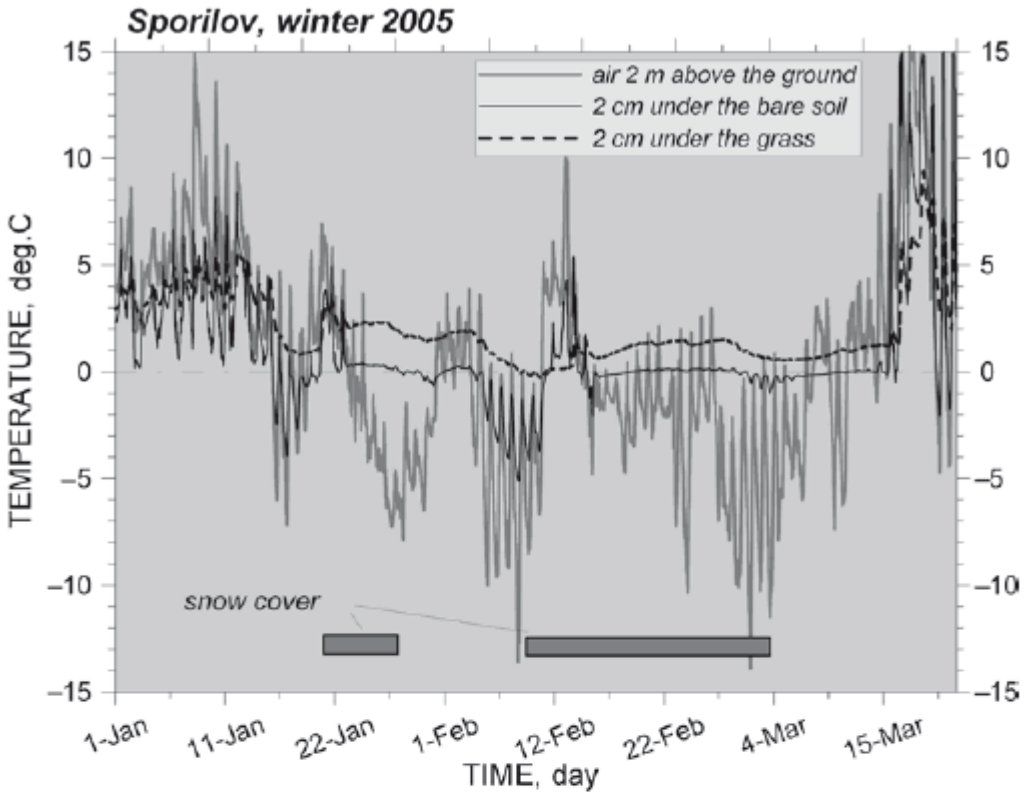

Fig. 11.7 Time series of air (at the height 2 m) and soil temperatures (at 2 cm depth) recorded under different surface at Prague-Sporilov. Soil temperatures follow SAT at temperatures above 0ºC, but are decoupled when the surface is covered by snow

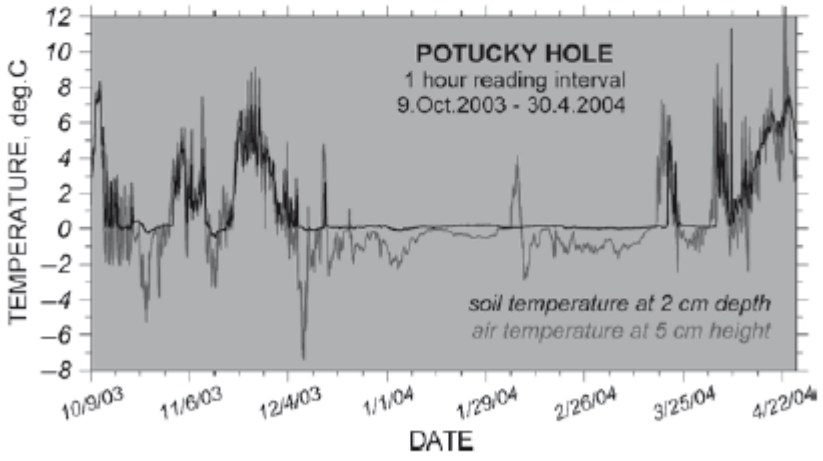

Fig. 11.8 Time series of air (at 5 cm above surface) and soil (at 2 cm depth) temperatures recorded at Potucky hole in 2003–2004 winter. Between mid December 2003 and March 20, 2004, when the ground was covered by snow, soil temperature was practically constant and showed practically no response to the SAT variations

rainfall and significant amount of snow, the Cape Henlopen and Hatteras stations have negligible or no snowfall. Similarly to the Czech monitoring results, the North American stations confirmed influence of the snow cover on the GST-SAT coupling. In all investigated locations snow cover has affected heat transfer in the surface in such a manner that mean daily soil temperature under snow cover was warmer relative to the SAT.

The above experiments have detected also finer features of the GST-SAT decoupling during cold season, such as the dependence of the soil temperature on the thickness of snow layer and snow quality, the date when the first snowfall started, and the effect of the vegetation cover. Numerical modeling by Gosnold et al. (1997) of the GST-SAT tracking in the presence of the snow cover have detected that the winter soil temperatures are more sensitive to the presence or absence of snow rather than to variations in its thickness. Thus, the exact amount of the winter snowfall is unlikely a decisive factor of the GST-SAT coupling in winter. Our monitoring experiments have also revealed certain effect of the surface type on the ground-air temperature tracking. The grassland preserves the snow cover longer than the bare surface, where snow is not isolated from the ground. Combination of snow and grass provides better insulation and the temperature under such surface remains above zero, the rate of snow melting is thus surface dependent. The thicker snow cover is characteristic for the grass. Similar studies were also done by the research group of the Utah University, see for more discussion in Bartlett et al. (2004, 2005, 2006)

It is to be stressed that our results are representative of the typically mid-latitude seasonal GST-SAT relationships, i.e. for mild winters, with relatively less snow and generally late snowfall. Winter temperatures are rarely cold enough to cause a massive soil freezing. At high-latitude regions where SAT temperature remains below 0°C for a considerably longer time, the effect of freezing may even surpass the influence of the snow cover, depending on the date what comes first, snow or frost. Here we can only partly contribute by demonstrating the effect of the soil freeze/thaw events on the GST as reflected by the relatively rare situation on the time series at Potucky site (Fig. 11.9). The period October–December 2003 was characterized by the absence of snow and by two episodes of the sharp air temperature fall below 0°C. The ground temperature at shallow depths of 2 and 10 cm remained almost constant, close to 0°C and to 1–1.5°C, respectively, demonstrating a so-called "zero-curtain effect" that occurs due to latent heat released from the freezing of soil. Recorded temperatures indicated that the soil freezing at Potucky station during this period did not penetrated deeper than 10 cm. The uppermost "active" layer experienced a complex combination of heat transfer from the frozen upper and undisturbed lower layer as well as the heat release from the advancing freezing front, the corresponding temperature-time series reflected pure influence of the freeze/thaw processes on the GST. The anomalous SAT variations were significantly attenuated at the depth of 50 cm with a time delay of days. Temperatures at that depth are lower than the highest positive air temperatures by approx. 3–4 K and may be higher than the lowest negative air temperatures by 8–10 K.

Figure 11.10 shows the ground temperatures under sand and grass surfaces during February 2006 at the Prague-Sporilov station. Due to several frosty days and

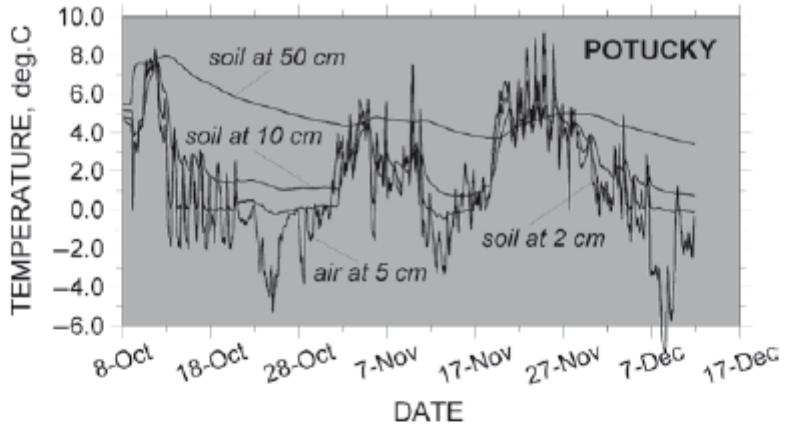

Fig. 11.9 Time series of air (at 5 cm height) and soil temperatures at 2, 10 and 50 cm depth at Potucky hole (October–December 2003)

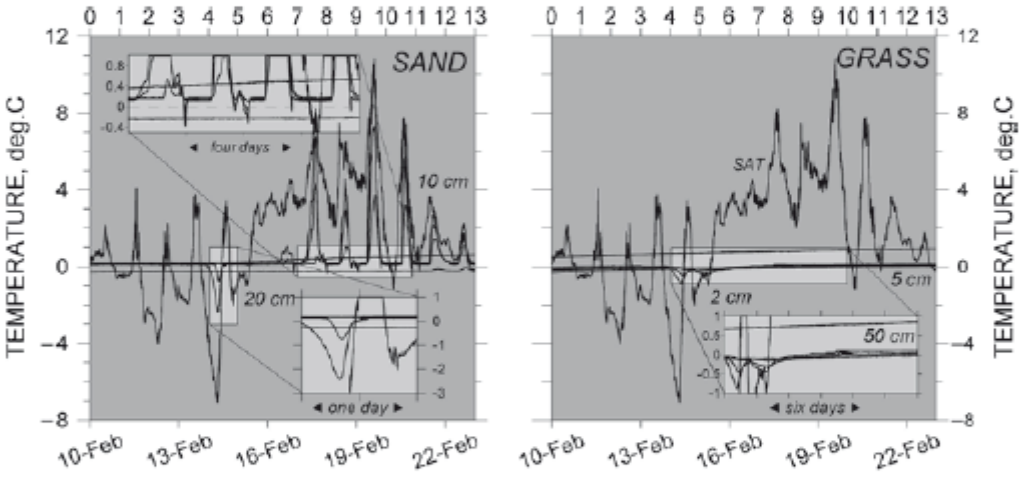

Fig. 11.10 Shallow soil temperatures at different depths below sand and grass surface during short freezing cycles in February 2006. Data from Sporilov hole

absence of snow in January, the subsurface temperature below both surfaces dropped below the freezing point. Temperature at 20 cm depth was stable at approx. 0°C and/or –0.3°C under the grass and the sand, respectively. The higher temperature under the grass occurred due to insulation effect of the vegetation cover. In the first half of February, when SAT was oscillating around zero, the GST under both surfaces remained practically constant. Its sharp decrease between 2 and 5 cm depths was observed only on February 14–15 and was the result of a similar SAT drop. During the second half of February, when the air temperature increased above zero, the subsurface temperature under the sand surface followed the SAT course. However, the phase changes of soil moisture substantially reduced the GST variations. The surface temperature variations vanished at the interface of the frozen and thawed soil layers and remained at zero temperature. Temperature at 20 cm depth

was practically constant, that hints that all heat coming from the surface was spent to melt the soil moisture (Fig. 11.10, left). Under the grass, where insulation of the surface and low thermal diffusivity of the soil slowed down the penetration of the surface warming, at all measured depth soil temperature remained close to 0°C (Fig. 11.10, right).

11.5.2 Rain Precipitation

Summer soil temperature is controlled by combined effect of air temperature variations and soil moisture content. An increase in rainfall during summer season can increase both surface wetness and soil moisture. This requires more energy consumption for evaporation and produces cooling of the ground surface (Yasunari et al. 1991; Matsuyama and Masuda 1998). In principle, such soil moisture feedback mechanism may explain soil cooling during summer, when air temperatures increase. Rain precipitation is thus another factor determining the subsurface thermal regime because it affects the amount of soil moisture and therefore the amount of energy removed from soil by latent heat flux. Because the thermophysical properties of the subsurface rock, like thermal conductivity and heat capacity, depend on the water content, the rainfall can influence not only energy balance of the ground surface-air system, but also thermophysical and/or hydrological characteristics of the ground. Regions with low porosity and permeability will likely be less affected, while less consolidated medium will experience more pronounced changes.

Primarily influence of the precipitation on the GST-SAT coupling occurs on the very short time scales (during and just after rain events) through advective transport of heat by falling water that may significantly contribute to the development of shallow subsurface temperatures. Figure 11.11 displays temperature difference between the ground surface ($T_{z=0}$) and temperature at 2 cm depth measured in a dry and in a rainy period at Prague-Sporilov. During a 10-day interval with no rain the differences have shown quasi-periodic oscillations with maximum positive values in the daytime and negative values at night. The range of variations achieved ~9 K. The temperature differences were negative after rain events over both day and night (air temperature at wet surface is lower than at 2 cm depth, like e.g., June 30-July 2 and/or July 5–6 intervals). Its variations were significantly reduced and ranged within only ~3–4 K. On the other hand, evaporation goes relatively quickly, thus, depending on the rain strength the "dry" regime was restored after 1–2 days after rainfall.

The role of rain precipitation appears to be far more important on seasonal and/or annual scales because of its possible seasonal persistence. In the mid-latitudes snowfall and soil freezing represent generally sporadic events and their effect on the GST-SAT coupling is not perceptible already under decadal averaging. On the contrary, rainfall occurs more regularly during much of the summer and its annual distribution remains preserved for the long periods. The Prague site represents typical example of the seasonal timing of precipitation. Daily precipitation at Prague has no significant linear long-term trend, but is characterized by

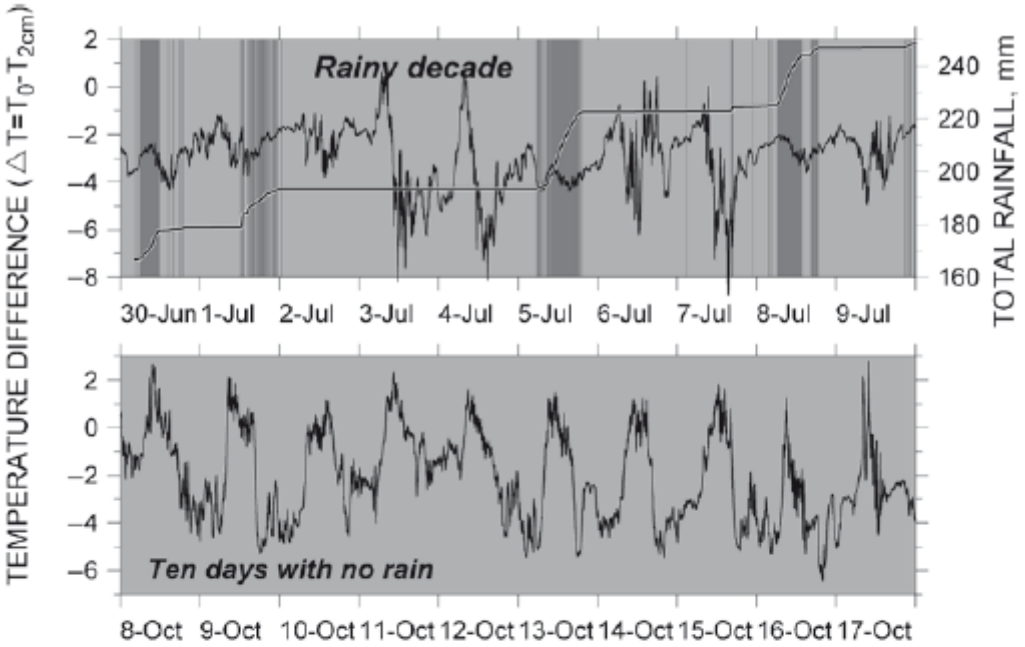

Fig. 11.11 Temperature differences between ground surface and soil temperature at 2 cm depth at Prague-Sporilov station; comparison of the rainy decade with dry period. *Top panel* also shows total rainfall amount

a certain seasonal character (Bodri et al. 2005); the wetter season falls on May–August period and the precipitation minimum occurs in winter. Figure 11.12 shows time series of daily averages of SAT temperature (at 5 cm height) and soil temperatures at the depths of 0.05, 1, 2 and 5 m measured at station Prague-Sporilov during the "rainy" year 2000. The amount of precipitation is shown by the histogram below. Detectable high-frequency oscillations of the soil temperature record in summer are caused mainly by the rains that change the moisture content of the soil and correspondingly affect both latent and sensible heat flow at the ground surface. As seen, rainfall events are accompanied by the corresponding changes of both air and ground temperatures. The main observation fact about summer GST-SAT interrelation is that the rainfall does not cause total decoupling of both temperatures similar to that what occurs in winter due to snow cover and freezing/thawing cycles. The air temperature record at 5 cm height and the GST records at the air-soil interface practically repeat each other. Correlation of both temperatures amounts to 0.96.

Surface temperature oscillations are practically imperceptible at 2 m and at deeper levels. Ground temperatures below 1 m depth are steadily lower than air temperatures from May to September and are higher than the air temperatures from November to February. At shallow depths variations of the GST around SAT are more erratic. At the shallow subsurface soil temperatures remain steadily higher than air temperatures only during November–February). During most of the year shallow GST irregularly oscillates above and below air temperature depending on

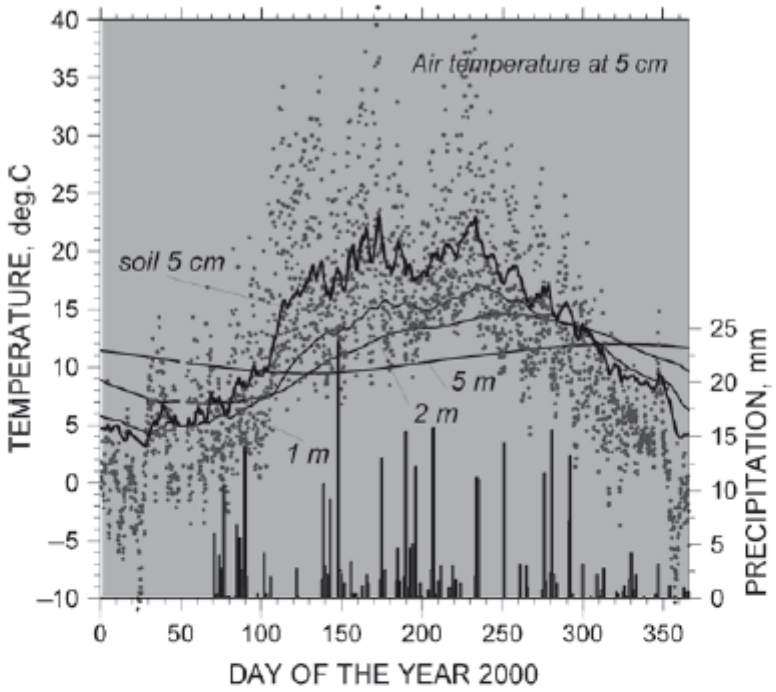

Fig. 11.12 Time series of daily averages of air temperature (5 cm height) and soil temperatures at 5, 100, 200 and 500 cm depth (Prague-Sporilov station). The histogram below shows precipitation amount

the temporal pattern of the rainfall. These oscillations likely will disappear under long scale averaging.

11.6 Meteorological Data and Regional Warming Pattern

Long-term meteorological SAT series from a number of Czech stations were compared with the ground surface temperature evidence obtained by inverting almost one hundred borehole temperature-depth profiles (Bodri and Čermak 1999). Both sets of data showed a certain similarity, which suggested that, the urban and industrial areas with higher population might have recently experienced greater warming than areas predominantly farming. It was presupposed that shallow temperature monitoring may usefully help to assess the potential anthropogenic component of the present (global) warming (Čermak et al. 2000). Now, we have repeated this procedure with the updated SAT data from 32 local meteorological stations for period 1960–2006. Regardless of the nature of the year-to-year fluctuation, all records documented local warming, with a characteristic regional mean of 0.0284 K/year (Fig. 11.13).To void the differences in the recorded local temperatures due to the altitude of the individual station reduced temperatures (relative to the mean of the particular station) are shown. The calculated cross-correlation coefficients between the SAT records from the

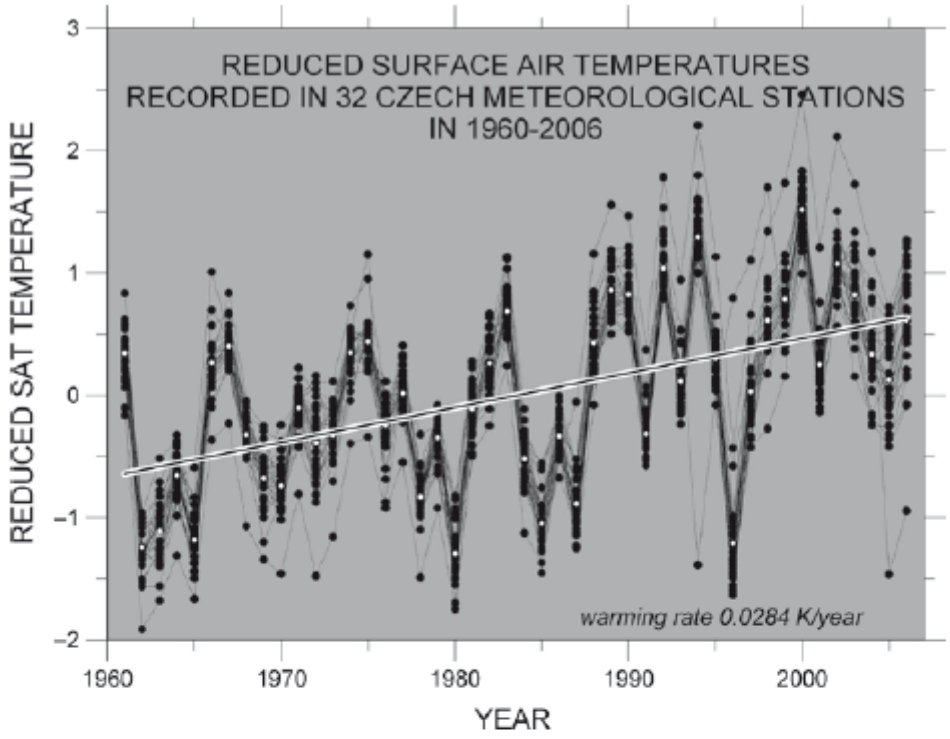

Fig. 11.13 Reduced surface air temperatures recorded in 32 local meteorological stations in the Czech Republic (1960–2006)

individual stations ranges from 0.92 to 0.99, which means that the whole territory of the Czech Republic can be considered as a single homogenous unit and the few existing gaps in data series could have been repaired by using data from the near-by stations with an appropriate datum-offset. All individual warming rates well fitted to the general interval of 0.01–0.04 K/year (Fig. 11.14) (with minimum of 0.0146 K/year at Olomouc station and maximum of 0.0384 K/year at Doksany) with an average value of 0.0284 K/year, which supports the reality of the continuing warming. The previous works (Čermak et al. 2000) focused the attention to decide whether the present warming is just a natural phenomena or there is a certain anthropogenic contribution reflecting the negative consequences of human activities. Figure 11.15 presents a histogram of the warming rates, when the respective sites were subdivided into three categories: (a) sites located in typically farming regions and (c) sites located in the typically industrial regions or near large urban centers. All remaining sites were rated as (b) mixed, when it was difficult to unambiguously affiliate the respective site to one of the above category. Whatever, such subdivision may be a speculative, the predominantly agriculture (rural) regions seem to be characterize by lower warming than industrial regions. Modification of land surface, production of waste heat, pollution and lack of vegetation, that all contribute to the irreversible change in the energy balance. The "urban heat island effect" known in meteorology describing the fact that average temperatures are higher in metropolitan than in rural areas may be thus applicable on the larger regional scale.

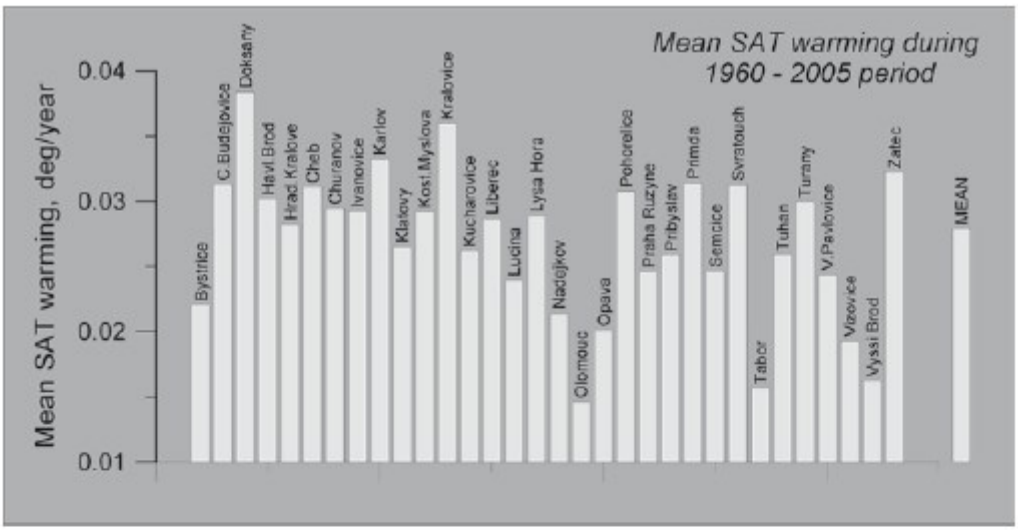

Fig. 11.14 Mean SAT warming recorded in the individual meteorological stations

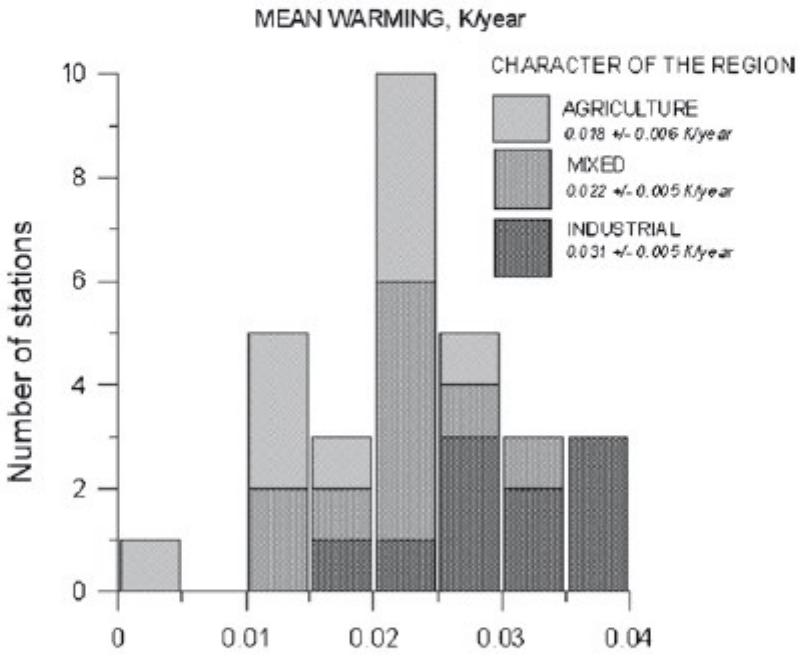

Fig. 11.15 Histogram of observed warming rates (1960–2006) vs dominant character of the region (farming, mixed, industrial)

11.7 Conclusions

Monitoring results have shown that the SAT forcing represents the main cause for the GST changes and this fact supports the use of the GST as an indicator for the climate reconstruction. Differences between the GST and SAT signals are closely

linked to the processes occurring at the ground surface and in the shallow subsurface of upper first few meters.

GST-SAT coupling over short-term timescales (such as single year) is complex. The winter snow cover and freeze/thaw effects may present serious influences causing GST-SAT decoupling. Because snow cover insulates the ground in the cold season, its systematic and persistent variations may distort their relation and hinder the direct comparison of both variables. In regions with short-duration snow cover its random fluctuation tends to vanish in longer averages. The summer rain precipitation and the corresponding moisture transpiration and evaporation have likely weaker effect on the GST-SAT decoupling.

On the daily scale, the GST may be either warmer or cooler than SAT and their difference progressively increases as the seasons become more extreme. However, the mean annual GST is generally always higher than the SAT. For the mid-latitude regions their difference amounts to 1–2 K. This value is higher in the regions of deep, long-duration snow cover or of extreme soil freeze/thaw cycles. The GST-SAT difference may be also much higher under artificial cover-types, such as concrete and asphalt exposed to direct solar radiation. The GST-SAT comparison may also be problematic in regions subjected to significant land use changes. Although snow does decouple SAT and GST on a daily and perhaps monthly basis, ground temperatures still track climate change as long as the characteristics of the snow season (onset and duration) has not changed systematically through time (Bartlett et al. 2004, 2005).

All detected processes that could break the GST-SAT coupling have only short-term effects on the heat transfer in the shallow subsurface, particularly of daily to seasonal timescales. In general, the short-term GST-SAT differences cannot considerably violate the assumption on the tracking of both temperatures on the long timescales.

The shallow-depth temperature monitoring proved to be a useful tool to assess a certain measure proportional to the present-day warming rate. The 12-year (1994–2005) experiment at Sporilov clearly demonstrated a gradual increase of warming rate within the range 0.025–0.040 K/year with a mean value of 0.0296 K/year. Shorter record from Kocelovice revealed lower warming rate of 0.0168–0.0240 K/year. Both values are in good agreement with the observational results of local meteorological SAT series and with the GST histories extracted from the deeper holes. The observed higher warming rate at Sporilov relative to Kocelovice together with the results of the SAT data from a number of local meteorological stations may confirm the assumption of regional character of the present-day (climate) warming and reflects an anthropogenic contribution to warming.

The monitoring technique itself, if applied in an extensive area network of enough measuring sites, may suitably contribute to knowledge of regional aspects of the recent climate evolution.

Acknowledgments The research activities have been supported by projects Nr.IAA300120603 and Nr.KJB300120601 of the Grant Agency of the Academy of Sciences of the Czech Republic. The manuscript was read by an anonymous reviewer who provided a number of useful comments, all of which were thankfully accepted.

References

Backer DG, Ruschy DL (1993) The recent warming in eastern Minnesota shown by ground temperatures. Geophys Res Lett 20:371–374

Bartlett MG, Chapman DS, Harris RN (2004) Snow and the ground temperature record of climate change. J Geophys Res 109:F04008. doi:10.1029/2004JF000224

Bartlett MG, Chapman DS, Harris RN (2005) Snow effect on North American ground temperatures, 1950–2002. J Geophys Res 110:F03008. doi:10.1029/2005JF000293

Bartlett MG, Chapman DS, Harris RN (2006) A decade of ground-air temperature tracking at Emigrant Pass Observatory, Utah. J Climate 19(15):3722–3731

Beltrami H, Mareschal JC (1995) Ground temperature from borehole temperature data: resolution and limitation. Glob Planet Change 11:57–70

Bodri L, Čermak V (1995) Climate change of the last millennium inferred from the borehole temperatures: results from the Czech Republic – Part I. Glob Planet Change 11:111–125

Bodri L, Čermak V (1997) Climate changes of the last two millennia inferred from borehole temperatures. Results from the Czech Republic. Part II. Glob Planet Change 14:163–173

Bodri L, Čermak V (1999) Climate changes of the last millennium inferred from borehole temperatures: regional patterns of climate changes in the Czech Republic – Part III. Glob Planet Change 21:225–235

Bodri L, Čermak V (2007) Borehole climatology – a new method on how to reconstruct climate. Elsevier, Amsterdam

Bodri L, Čermak V, Krešl M (2005) Trends in precipitaion variability: Prague (the czech Republic). Clim change 72:151–170

Brázdil R, Budíková M (1999) An urban bias in air temperature fluctuations at the Klementinum, Prague, the Czech Republic. Atm Environ 33:4211–4217

Camuffo D, Jones P (ed) (2002) Improved understanding of past climate variability from early daily european instrumental sources. Kluwer, Dordrecht

Čermák V (1971) Underground temperature and inferred climatic temperature of the past millennium. Paleogeogr Paleoclimatol Paleoecol 10:1–10

Čermak V, Kukkonen IT, Šafanda J (1993) Temperature logs in deep wells – a useful tool for past climatic reconstruction. Terra Nova 5:134–143

Čermak V, Šafanda J, Kresl M, Dedecek P, Bodri L (2000) Recent climate warming: surface air temperature series and geothermal evidence. Studia Geophys Geod 44:430–441

Čermak V, Bodri L (2001) Climate reconstruction from subsurface temperatures demonstrated on example of Cuba. Phys Earth Planet Inter 126:295–310

CHMI (2007) Green Paper "Adapting to climate change in Europe – options for EU action". http://www.chmi.cz/stanzelkniha.pdf

González-Rouco JF, von Storch H, Zorita E (2003) Deep soil temperature as proxy for surface air-temperature in coupled model simulation of the last thousand years. Geophys Res Lett 30(2116):10.1029/2003GL018264

González-Rouco JF, Beltrami H, Zorita E, von Storch H (2006) Simulation and inversion of borehole temperature profiles in surrogate climates: Spatial distribution and surface coupling. Geophys Res Lett 33:L01703. doi:10.1029/2005GL024693

Gosnold WD, Todhunter PE, Schmidt W (1997) The borehole temperature record of climate warming in the mid-comtinent of North America. Glob Planet Change 15:33–45

Hansen J, Lebedeff S (1987) Global trends of measured surface air temperature. J Geophys Res 92:13345–13372

Harris RN, Chapman DS (1995) Climate change on the Colorado Plateau of Eastern Utah inferred from borehole temperatures. J Geophys Res 100:6367–6381

Harris RH, Chapman DS (1998) Geothermics and climate change: Part 2. Joint analysis of borehole temperature and meteorological data. J Geophys Res 103:7371–7383

Hlaváč V (1937) Die Temperaturverhältnisse der Hauptstadt Prag. Teil I. Prager Geophysikalische Studien VIII. Prague, 111 pp

Huang S, Pollack HN, Shen PY (2000) Temperature trends over the past five centuries reconstructed from borehole temperatures. Nature 403:756–758

IPCC 2001, Houghton JT, Ding Y, Griggs DJ, Noguer M, van der Linden PJ, Dai X, Maskell K, Johnson CA. (eds) (2001) Climate change 2001: the scientific basis. Cambridge University Press, Cambridge

Jones PD, New M, Parker DE, Martin S, Rigor ID (1999) Surface air temperature and its changes over the past 150 years. Rev Geophys 37:173–199

Kalvová J (2001) Projekt VaV/740/1/00 ' Výzkum dopadù klimatické změny vyvolané zesílením skleníkového efektu na Českou republiku'. ZávěreČné zprávy za DP01 'Pravidelné sledování změn klimatu, odhady změn ve variabilitě a Četnosti výskytu extrémních povětmostních jevů a zpřesnění scénářů vývoje klimatu na území ČR', National Climate Program, Praha

Lachenbruch AH, Mareschall BV (1986) Changing climate: geothermal evidence from permafrost in the Alaskan Arctic. Science 234:689–696

Lewis T (ed) (1992) Climatic change inferred from underground temperatures (special issue). Glob Planet Change 2/4(6):71–281

Majorowicz J, Šafanda J, Skinner W (2004) Past surface temperature changes as derived from continental temperature logs. Canadian and some global examples of application of a new tool in climate change studies. In: Dmowska R (ed) Advances in geophysics, vol 47. Elsevier, Amsterdam, pp 113–174

Matsuyama H, Masuda K (1998) Seasonal/interannual variations of soil moisture in the former U.S.S.R. and its relationship to Indian summer monsoon rainfall. J Climate 11:652–658

Možný M, Kott I (2003) Soil temperature and moisture on the territory of the Czech Republic in 2000–2002. In: Functions of energy and water balances in bioclimatological systems. SBS, ČSBS, SAV, 2–4 September 2003, Račkova dolina: 27

NASA (2008) Global land-ocean temperature index. http://data.giss.nasa.gov/gistemp/tabledata/GLB.Ts+dSST.txt.

Pollack HN, Chapman DS (1993) Underground records of changing climate. Sci Am 268(6):44–49

Pollack HN, Huang S (2000) Climate reconstruction from subsurface temperatures. Earth Planet. Sci. 28: 339–365

Putnam SN, Chapman DS (1996) A geothermal climate change observatory: first year results from emigrant pass in Northwest Utah. J Geophys Res 101:21877–21890

Šafanda J (1994) Effects of topography and climatic changes on temperature in borehole GFU-1, Prague. Tectonophysics 239:187–197

Smerdon JE, Pollack HN, Čermak V, Enz JW, Kresl M, Šafanda J, Wehmiller JF (2004) Air-ground temperature coupling and subsurface propagation of annual temperature signals. J Geophys Res 109(D21007), doi:10.1029/2004JD005056

Smerdon JE, Pollack HN, Čermak V, Enz JW, Kresl M, Šafanda J, Wehmiller JF (2006) Daily, seasonal and annual relationships between air and subsurface temperatures. J Geophys Res 111(D07101), doi:10.1029/2004JD005578

Štulc P (1995) Return to thermal equilibrium of an intermittently drilled hole: theory and experiment. Tectonophysics 241:35–45

Tolasz R, et al. (2007) Climate atlas of Czechia. Czech Hydrometerological Institute, Praha and Olomouc

WMO (2005) Statement on the status of the global climate in 2004: global temperature in 2004: Fourth warmest. Data available online from the page of World Meteorological Organization. http://www.wmo.ch/index-en.html

Yasunari T, Kitoh A, Tokioka T (1991) Local and remote responses to excessive snow mass over Eurasia appearing in the northern spring and summer climate – A study with the MRI-GCM. J Meteorol Soc Japan 69:473–487